Peninsula Technikon

Faculty of Science

Department of Physical Sciences
(Chemical Engineering)

TRANSPORT OF GASES ACROSS MEMBRANES

by

Touhami Mokrani

Thesis
Submitted in Fulfilment of Requirements for the Degree of
Master of Technology
in Chemical Engineering

Under Supervision of:

Mr B. A. Hendry (Internal Supervisor)
Dr. E. Jacobs (External Supervisor)

Cape Town, 2000

"Not to care for philosophy is to be the true philosopher"

French Thinker
Blaise Pascal (1623- 1662)

ACKNOWLEDGEMENTS

I would like to express my sincere gratitude to the following people and organization:

My first words of gratitude to my supervisor, Mr B.A.Hendry. Without his guidance and support this thesis would never have materialized. Apart from support on technical issues he has provided an environment conducive to development of research in the area of Chemical Engineering (membrane technology and water treatment) at Peninsula Technikon.

My co-supervisor, Dr. E. Jacobs (Stellenbosch University) who introduced me to membrane technology, and the valuable assistance and guidance he provided me with during this work. His endless patience in discussing the techniques and proof reading has proven invaluable to the successful completion of this thesis.

Ms. A. van der Walt (Stellenbosch University) as a very good collaborator.

Dr. W.Leukes, Prof. P. Rose and Dr. S. Burton (Rhodes University), who introduced me to membrane bio-reactor and bioremediation.

To the Institute for Polymer Science (Stellenbosch University), Mr. D. Koen and Dr. D. Bessarabov.

To Peninsula Tecknikon staff (Dr. D. Gihwala, Mr. J. Farmer, Mr. K. Salo, Dr. E. K. Cairncross).

I would like to express my thanks to Mr. R. O. Dudley for proof reading.

To my two friends Dr. Ammar Bensakhria (UTC, France) and Dr. Ahmed Ould Khaoua (University de Los Andos, Colombia), who encouraged me to start and finish this project.

To my South African friends T. Mogammad, A. Toll, V. Msimang and B. Hendricks.

To Mr. Said Kitouni, Algerian Ambassador in Southern Africa, for his assistance and kindness.

To the Algerian community in Cape Town (Mennad, Dr. Boukarfa, Moustafa, Monji and all the rest).

Special thanks to my family, for the endless support and love. I hope that the result is worthy of their kindness.

The financial support received from ESKOM through the TESP program administered by Rhodes University. The financial support received from Peninsula Technikon.

ABSTRACT

Oxygen transport across biofilms and membranes may be a limiting factor in the operation of a membrane bio-reactor. A Gradostat fungal membrane bio-reactor is one in which fungi are immobilized within the wall of a porous polysulphone capillary membrane. In this study the mass transfer rates of gases (oxygen and carbon dioxide) were investigated in a bare membrane (without a biofilm being present). The work provides a basis for further transport study in membranes where biomass is present.

The diaphragm-cell method can be employed to study mass transfer of gases in flat-sheet membranes. The diaphragm-cell method employs two well-stirred compartments separated by the desired membrane to be tested. The membrane is maintained horizontally. The gas (solute) concentration in the lower compartment is measured versus time, while the concentration in the upper liquid-containing compartment is maintained at a value near zero by a chemical reaction.

The resistances-in-series model can be used to explain the transfer rate in the system. The two compartments are well stirred; this agitation reduces the resistances in the liquid boundary layers. Therefore it can be assumed that in this work the resistance in the membrane will be dominating.

The method was evaluated using oxygen as a test. The following factors were found to influence mass transfer coefficient: i) the agitation in the two compartments; ii) the concentration of the reactive solution and iii) the thickness of the membrane.

The diaphragm-cell method can be adapted to study mass transfer in a biofilm supported by a membrane. However, some modification of the relative technique would be required and are suggested.

More extensive investigations were carried out on capillary membranes, because these are favored for membrane bio-reactors and other applications. Capillary membranes were

used to investigate oxygen removal (deoxygenation), carbon dioxide removal (decarbonation), oxygen absorption (oxygenation or bubble-free aeration) and carbon dioxide absorption (carbonation). The mass transfer rates in capillary membranes were studied in shell and tube modules. The aqueous phase was introduced into the lumen and the gas on the shell side. In such systems theory normally predicts that liquid film resistance would be the most significant and that increased agitation or cross-flow velocity in the liquid phase would increase the rate of mass transfer. The results reported supported this, as well as that the resistance in the gas phase was negligible.

The overall mass transfer coefficient was found to increase with the velocity of the liquid (water) flow in the lumen. The overall mass transfer coefficient reached a maximum and started to decrease as the Reynolds number exceeded 1000. These results are not unexpected because literature suggests that the micro-porous hydrophobic polymer, may be gas filled under low lumen-side velocities and pressures, and liquid filled under higher lumen-side pressures. Thus, as the inlet pressure was increased in the various experiments, there may have been an increasing number of pores that were liquid filled, thus increasing membrane resistance.

For a solution flowing through a narrow bore, it has been suggested that mass transfer can be described by the equation [$Sh = 1.62Pe^{0.33}$, Re<400 (Lévêque, 1928)]. In this thesis, an attempt to extend the Lévêque correlation to higher Reynolds number was made. It was found that the Lévêque equation failed to correspond with the experimental data, agreeing with the finding of Tai et al. (1994) and Malek et al. (1997). This difference is due to the extra-resistance in the membrane (membrane wettability).

The deoxygenation of water can be achieved by using a sweep gas or vacuum in the shell side. The sweep gas was tested both in co-current and counter-current flow to the lumen side flow direction. The counter-current mode resulted in higher mass transfer rates than co-current mode, as expected.

TABLE OF CONTENTS

LIST OF FIGURES

LIST OF TABLES

LIST OF SYMBOLS

a	ratio of membrane surface area to volume	[m^2/m^3]
A	membrane surface area	[m^2]
C	concentration in the bulk solution	[mg/l]
C^*	equilibrium concentration	[mg/l]
$C_{l,lower}$	concentration of the solute in the lower compartment	[mg/l]
$C_{l,upper}$	concentration of the solute in the upper compartment	[mg/l]
C_f	solute concentration in the feed	[mg/l]
C_g	solute concentration in the gas phase	[mg/l]
C_l	solute concentration in the liquid phase	[mg/l]
C_m	solute concentration in the membrane	[mg/l]
C_p	solute concentration in the permeate	[mg/l]
d	diameter	[m]
d_e	characteristic length	[m]
D	diffusion coefficient	[m^2/s]
D_e	effective diffusion coefficient	[m^2/s]
D_j	continuum diffusion coefficient	[m^2/s]
D_k	Knudsen diffusion coefficient	[m^2/s]
D_m	diffusion coefficient of the gas in the polymer	[m^2/s]
f	fugacity	[kPa]
H_c	Henry constant	[-]
H_p	Henry constant	[$kPa.m^3.mol^{-1}$]
H_x	Henry constant	[kPa /mole fraction]
J	flux	[$cm^3.cm^{-2}.s^{-1}$]
K	mass transfer coefficient	[m/s]
K_d	partition coefficient	[-]
K_g	gas film mass transfer coefficient	[m/s]
K_l	liquid film mass transfer coefficient	[m/s]
K_m	membrane mass transfer coefficient	[m/s]
K_{OG}	overall mass transfer coefficient based on the gas phase	[m/s]
K_{OL}	overall mass transfer coefficient based on the liquid phase	[m/s]
L	capillary membrane length	[m]
l	membrane thickness	[m]
M_w	molecular mass	[g/mol]
N	number of capillaries	[-]
n	pore density	[m^2]
P	pressure	[kPa]
q	constant depending in the geometry of the pores	[-]
Q	volumetric flow rate	[m^3/s]
Q_g	volumetric flow rate of the gas	[m^3/s]
Q_l	volumetric flow rate of the liquid	[m^3/s]
r	radius	[m]
R	universal gas constant	[8.314 J / mol. K]

R_t	retention	[-]
S_m	solubility coefficient of the gas in the polymer	[cm^3 (STP) / cm^3 . kPa]
T	absolute temperature	[K]
t	time	[s]
v	velocity	[m/s]
V	volume	[m^3]
V_{lower}	volume of the lower compartment	[m^3]
V_{upper}	volume of the upper compartment	[m^3]
v_s	molar volume of the aqueous solution	[m^3. mol^{-1}]
x	mole fraction	[-]
y	activity coefficient	[-]

Greek symbols:

ν	kinematic viscosity	[kPa.s]
ϕ	packing fraction	[-]
ε	porosity	[-]
α	selectivity factor	[-]
γ	surface tension	[N/m]
λ	the mean free path of gas molecules	[m]
τ	tortuosity	[-]

Subscripts:

f	feed
g	gas
l	liquid
$lower$	lower compartment
m	membrane
p	permeate
$upper$	upper compartment

Superscripts:

0	initial
*	equilibrium

Sh Sherwood number, $Sh = \frac{Kd_e}{D}$ [-]

Pe modified Peclet number (Greatz number), $Gr = Pe = \frac{d_e^2 v_l}{DL}$ [-]

Re Reynolds number, $\mathrm{Re} = \frac{d_e v_l}{\upsilon}$ [-]

Sc Schmidt number, $Sc = \frac{\upsilon}{D}$ [-]

CHAPTER 1
INTRODUCTION

1.1 INTRODUCTION

The development of novel bio-reactors flourished in the early 1980s as efforts to produce more efficient and economical systems continue. Bio-reactors are used for the production of many different compounds from plant, microbial and animal cells, as well as from isolated enzyme systems. Conventionally, bio-reactors were either batch or continuous flow reactors. To improve the performance of these reactors, designs have focused to increase productivity per unit volume and reducing the amount of expensive downstream processing. Immobilization of cells onto various types of barriers or supports can satisfy both criteria (Frank and Sirkar, 1986).

The problems usually associated with batch suspension cultures are: the varying intensity of fluid shear stresses; microbial and mycoplasma contamination; and unsteady culture environments (as the nutrients are consumed the metabolic products accumulate, effecting a continuously changing environment (Belfort, 1989)).

Membrane bio-reactors have the advantage over completely mixed reactors in that high cell densities can be achieved and, hence, high volume productivities, as well as steady and sustained output resulting from a stabilized *in vitro* environment.

Immobilized membrane bio-reactors are particularly attractive for culturing animal and plant cells, and for the production of complex biological molecules. These membrane systems retain the cells in a low shear environment, and allow for the continuous supply of nutrients and co-factors as well as the removal of metabolic products (Belfort, 1989).

Membrane bio-reactors do have some limitations. In general, membrane bio-reactors require a greater number of aseptic connections and more elaborate monitoring and control of the cell culture parameters than do batch processes (Tolbert and Srigley, 1987). Because of the high cell densities the transport of nutrients, including oxygen, and products to and away from the cells can be limited resulting in necrotic regions and the possible demise of the system (Heath and Belfort, 1987; Schonberg and Belfort, 1987). In general, immobilization of whole cells (microbial, animal or plant) creates an environment in which oxygen transfer to the cells becomes more difficult than in free cell suspension cultures where the oxygen transfer is often limited by a gas-liquid interface (Chang and Moo-Young, 1988). The use of hollow fibre reactors for mammalian cell culture has been limited. Most of the drawbacks are associated with the problem of satisfying the oxygen requirement of the cell (Inloes et al., 1983; Adema and Sinskey, 1987).

Bacteria, yeast, mammalian and plant cells have all been immobilized in membrane bio-reactors to produce products that range from ethanol and lactose to monoclonal antibodies (Belfort, 1989).

1.2 HOLLOW FIBRE MEMBRANE BIO-REACTORS

The successful use of hollow fibre reactors for the cultivation of mammalian cells was first reported by Knazek et al. (1972). Since then, others have reported on the use of hollow fibre reactors for culturing mammalian and plant cells and for growing bacterial and yeast cells (Belfort, 1989; and other references therein).

Many hollow fibre membranes are potted together in unit called a module. The cells are injected outside the membrane (shell side) and the culture medium and oxygen are supplied from the inside of the membrane (lumen side). The transport of culture medium and oxygen is inside-out and usually by diffusion. Webster and Patras (1987) used a whole-cell entrapped hollow fibre bio-reactor for the desulphurization and denitrogenation of heavy oils. Tolbert et al. (1985) used a bio-reactor where oxygen is

supplied through a separate gas permeable membranes, and carbon dioxide is exchanged with the oxygen and is removed through the same membrane. Chang et al. (1986) produced rifamycin B using a hollow fibre bio-reactor for more than 50 days. Chung and Chang (1988) used microporous polypropylene hollow fibres contained within silicone rubber tubes to produce citric acid continuously. Robertson and Kim (1985) used hollow silicone rubber tubes contained within a microporous polypropylene hollow fibre; nutrient was supplied through the polypropylene membrane, and air or oxygen was provided through the silicone rubber tubes. Microporous hollow fibres containing flowing extractant have been used to remove inhibitory products from within a bio-reactor. Frank and Sirkar (1986) continuously removed ethanol from a *S. cerevisiae* fermentation using dibutyl pthalate as an extractant. They also used the same membranes to aerate the broth and remove carbon dioxide.

Hollow fibre membranes are advantageous because of their very high surface area to volume ratios, ability to isolate the cells from shear and contamination, separation characteristics allowing selective nutrients into the shell side while retaining and concentrating the product. Limitations of the membrane systems include fouling and clogging of the fibres, difficulty in gaining access to the cell mass, difficulty in maintaining well-defined intrafibre spacing and possible disruption of fibres due to cell growth or excessive gas production (Belfort, 1989).

1.3 FLAT-SHEET MEMBRANE BIO-REACTORS

Multiple-layer flat-sheet membrane bio-reactors have lower surface area to volume ratios than hollow fibre reactors, but they possess all the other advantages of hollow fibres and overcome additional disadvantages. For example, the cell space between two flat-sheet membranes and hence the distance to the furthest cell from the medium channel can be carefully controlled. Also access to the cell space is possible, allowing the cells to be replaced if necessary. Seaver et al. (1984), Klement et al. (1988) and Rainen (1988) used a flat-sheet membrane bio-reactor to produce monoclonal antibodies. Efthymiou and Shuler (1987) used a multiple flat-sheet membrane reactor, where the reactor constituted

four layers, the top layer containing flowing oxygen, the next layer the stationary cells, the next layer the flowing nutrients and the bottom layer the flowing extractant.

1.4 GRADOSTAT FUNGAL BIO-REACTOR

The technology for fungal membrane bio-reactors is in its infancy. The biotechnology group at Rhodes University has developed, in collaboration with the Water Research Commission, the Institute for Polymer Science (University of Stellenbosch) and later ESKOM, a laboratory-scale fungal bio-reactor employing a " white rot fungus" (Leukes, 1999) and have shown that it successfully converts polychlorinated biphenyls (PCBs) to carbon dioxide (Aust, 1990). Enzymes of the " white rot fungi" have the ability to destroy the PCBs, whereas the PCBs are toxic to other microorganisms (bacteria) used in water treatment (Nissen, 1973; Moein et al., 1976). PCBs are therefore not easily bio-degradable (Moein et al., 1976). Literature indicates that complete photochemical degradation does not occur (Safe and Hutzinger, 1971; Ruzo et al., 1972) and thermal degradation produces several highly toxic compounds, such as polychlorinated-dibenzofurans, which are released into the atmosphere, as secondary pollutants (Buser and Rappe, 1979).

The Gradostat reactor is one which involves the establishment of a fungus growing in the wall and on the outer surface of a capillary membrane; the membrane is of a specific design to allow the fungus to establish itself within the wall of the membrane. When a fungal biofilm experiences a nutrient gradient(s) across it, differentiated growth occurs and enzymes are expressed. In order to optimize the production of desired enzymes, oxygen and carbon dioxide gradients across the biofilm need to be known, apart from nutrient gradient(s) and composition of the substrate.

In order to make this new technology practically and commercially useful a rational design basis needs to be established and tested in order to scale up the equipment. A major part of this effort requires a clear understanding of the role of the membrane in the transport of oxygen to the active growth region of the fungi and the transport of carbon dioxide away from this region into water or air streams. There are two possibilities to

supply oxygen to the bio-reactor: i) the gas (pure oxygen or air) can be on the outside of the membrane (shell side); or ii) the gas (pure oxygen) can be dissolved in the nutrient (the nutrients are fed into the lumen of the capillary membranes). Carbon dioxide diffusion can be from inside-out or outside-in. Oxygen diffusion in a Gradostat membrane bio-reactor can be accomplished from the outside to the inside (outside-in), when the oxygen is supplied from the shell side (this case is referred to as gas absorption). Diffusion can also occur from the inside to the outside (inside-out) when the oxygen is dissolved in the nutrient. This case is referred to as gas removal.

The work reported in this thesis can be used as a basis for further experimental work on fungal biofilms. The work only attempts to establish techniques for measuring mass transfer rates of gases in bare membrane systems without attached biofilms.

1.5 GAS-LIQUID CONTACTORS

A spin-off of the study of gas transfer presented in this thesis is that the work can be extended to other applications for gas-liquid contactors using the skinless polysulphone membrane that was specially developed for use in the Gradostat bio-reactors. The techniques and theory developed during this study can also be used for other membranes and for a number of other gas/membrane operations.

Gas-liquid contactors or gas/membrane operations find application in a wide variety of fields. The removal of oxygen from water has commercial value in the pretreatment of boiler feed water and in the deaeration of bottled beverages to improve shelf life (Yang and Cussler, 1986). In the power industry corrosion in boilers and steel pipes can be prevented if the dissolved oxygen content of the water is less than 0.5 ppm (Ito et al., 1998). Production of ultrapure water is one of the key services for manufacturing of semi-conductors and pharmaceuticals in biotechnology and food industries. One of the major problems encountered is the presence of dissolved oxygen in the ultrapure water (Tai et al., 1994; Ito et al., 1998). Membranes can be used to transfer large quantities of oxygen to biological reactors (bubble-free aeration). Bubble-free aeration is desirable for

applications in waste water treatment when bubbling of air would result in the stripping of volatile compounds from or in foaming of industrial waste water (Côté et al., 1988, 1989; Ahmed and Semmens, 1992, 1996). Oxygen transport through membranes is also applied in the medical field, membrane blood oxygenation replaces the lung function during cardiopulmonary bypass operation (Tsuji et al., 1981; Alexander and Fleming, 1982; Wickramasinghe et al., 1992 and Wang and Cussler, 1993). Yang and Cussler (1989) have developed several artificial gills for diving. The gills are membrane modules (tube and shell configuration). These modules harvest oxygen dissolved in water and discharge carbon dioxide to the water. Absorption of CO_2 is used as a treatment step in the production of potable water (Loewenthal et al., 1986). Karoor and Sirkar (1993) and Kreulen et al. (1993b) studied carbon dioxide absorption with the goal of replacing a bubble column.

1.6 OBJECTIVES OF THE STUDY

The objectives of studying mass transfer of oxygen and carbon dioxide across membranes are:

- measure mass transfer for gases in membranes for any configuration (flat-sheets and capillaries), and for any purpose;
- investigate which phase (gas boundary layer, membrane, and liquid boundary layer) is rate controlling;
- investigate the influence of the operating conditions (flow rate of the liquid, and the flow rate of the gas) on mass transfer in membranes;
- compare results obtained for polysulphone with the results found in the literature (for other polymers used as gas-liquid contactors) in mass transfer across membranes;
- establish a simple experiment to measure mass transfer of gases in flat-sheet membranes and make recommendation to study mass transfer across a biofilm;

- investigate two parameters (transfer of oxygen and carbon dioxide) in polysulphone bare membranes; and

- develop dimensionless correlations to describe mass transfer through capillary membranes;

1.7 CHAPTERS GUIDE

In Chapter 2, an overview of membranes (Section 2.2) and membrane processes (Section 2.6) is reported. Pressure-driven membrane operations, ultafiltration and microfiltration, are described in Section 2.6.1. Chapter 3 describes membrane bio-reactors. Section 3.4 provides a full description of the Gradostat fungal bio-reactor. The types of membranes used in a Gradostat bio-reactor, the different modules and the functionality of a Gradostat bio-reactor are also reported on.

Chapter 4 covers theoretical aspects of mass transfer in membrane gas-liquid contactors. In Chapter 5, the experimental procedures and the mathematical equations to study mass transfer of gases across membranes are explained. Chapter 5 has two parts, mass transfer in flat-sheet membranes (Section 5.2) and mass transfer in capillary membranes (Section 5.3).

In Chapter 6, the experimental results and discussions are reported. Chapter 7 details the conclusions and includes recommendations for future work. Sample calculations and other information pertinent to this work is given in various appendices.

CHAPTER 2
MEMBRANES AND MEMBRANE PROCESSES

2.1 THE DEFINITION OF MEMBRANES

A membrane may be defined as a film separating two phases, acting as a selective barrier for the transport of matter.

The membrane can be thick or thin and its structure can be homogeneous or heterogeneous.

The transport across the membrane barriers can be driven by differences in pressure, concentration, temperature or electrical potential. Membranes can be made from natural or synthetic materials and can be neutral or charged.

2.2 MEMBRANE MATERIALS

We can divide synthetic membranes into inorganic and organic. The most important class of membrane materials are organic (polymeric). Figure 2.1 lists the main organic polymers used for membrane manufacture.

The choice of a given polymer is not arbitrary, but is based on very specific properties of the material. Theoretically, any polymer can be used, but in practice only a limited number are used because of processing requirements, membrane life and application.

2.2.1 Inorganic Membranes

Inorganic materials generally possess superior chemical, mechanical and thermal stability compared to polymeric membranes.

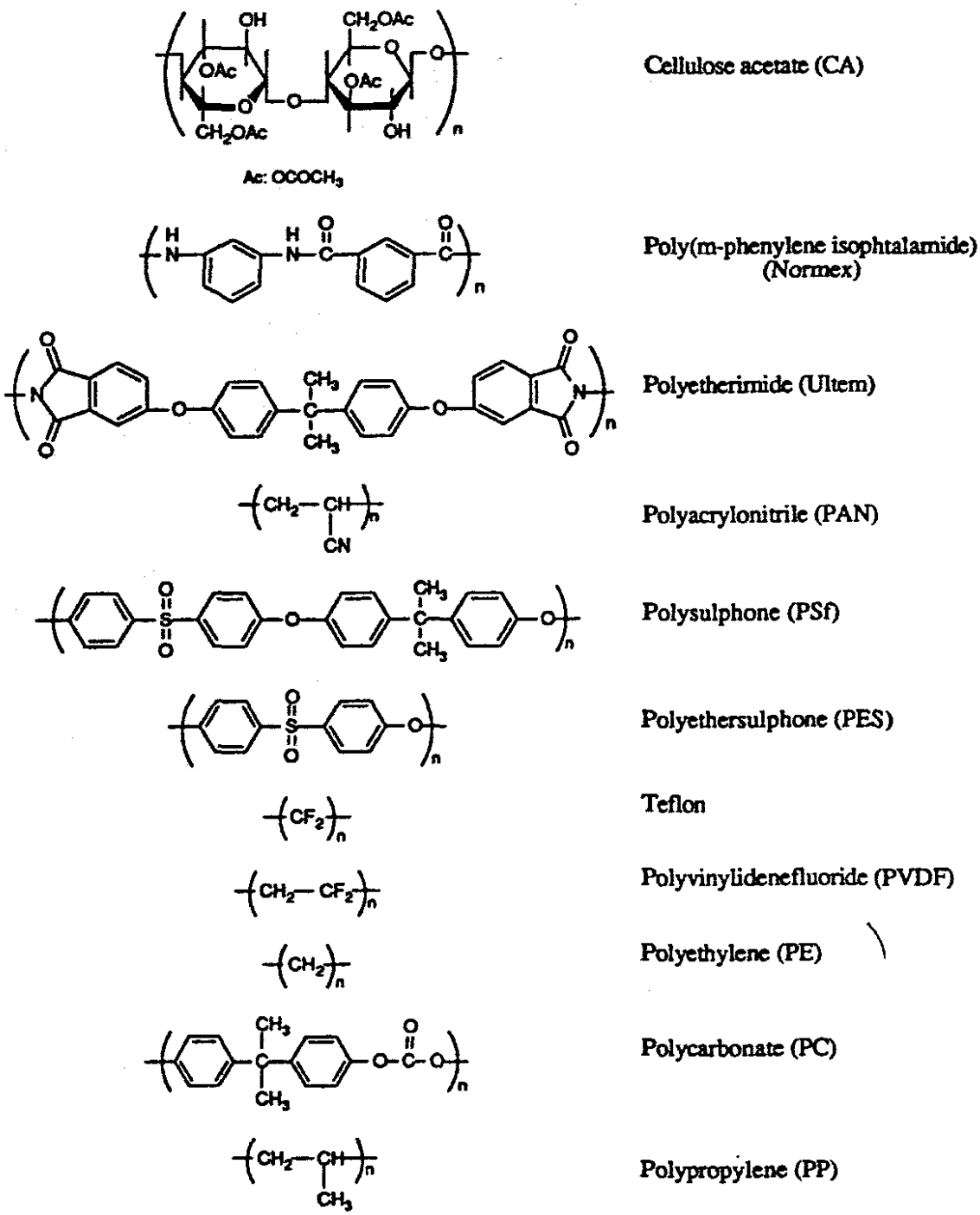

Figure 2.1: The main organic membrane polymers (Aptel and Buckley, 1996).

The disadvantages of these inorganic membranes are that they are more expensive than organic membranes. Ceramic membranes represent the main class of inorganic membranes; these being oxides, nitrides, or carbides of metals.

2.2.2 Organic Membranes

The most widely used polymers are cellulose and its derivatives. These relatively hydrophilic polymers provide low cost implications. The other important class of hydrophilic membrane polymers is polyamides, which are essentially used for desalination.

Another widely used class of polymers is the polysulphone and polyethersulphone. These polymers are hydrophobic and they have very good chemical, mechanical and thermal stability. They are commonly used for ultrafiltration membrane fabrication.

Other hydrophobic polymers are polytetrafluoroethylene, polyvinylidene fluoride, polyethylene and polypropylene. Polypropylene is commonly used for the production of microfiltration membranes.

2.2.2.1 Non-Porous Membranes

Non-porous membranes can be considered as dense media. Diffusion of species takes place in the free volume that is present between the macromolecular chains of the membrane material. The solutes dissolve in the membrane and diffuse through it. Very soluble, mobile solutes pass easily through these membranes, but insoluble, immobile solutes are retained.

The selectivity of these membranes is controlled by adsorption, solubility and desorption. In these types of membranes the performance (permeability and selectivity) is determined by the properties of the material. The choice of material is determined by the type of application.

2.2.2.2 Porous Membranes

Porous membranes contain fixed pores in the size range of 0.1 to 10 μm for microfiltration, and 2 to 100 nm for ultrafiltration. In reverse osmosis membranes the pore size is less than 2nm.

STATEMENT

I, the undersigned, hereby declare that the work contained in this thesis is my own original work, and that I have not previously, in its entirety or in part, submitted it at any other institution for a degree.

Signature: Date:.....

Touhami Mokrani

Using the definition adopted by the IUPAC (1985):

- Macropores are larger than 50 nm;
- Mesopores are in the range of 2 to 50 nm; and
- Micropores are smaller than 2 nm.

When a solution is forced through a porous membrane, small solutes easily pass through the pores but larger solutes are retained. The selectivity of the membrane is controlled by the solute size and the dimensions of the pores. The material only has an effect through phenomena such as adsorption and chemical stability under the conditions of actual application and membrane cleaning.

2.3 CHARACTERISTICS OF MEMBRANES

2.3.1 Selectivity and Permeability

The performance and efficiency of a given membrane is determined by two parameters: its selectivity and permeability (flux through the membrane). The flux is defined as the volume flowing through the membrane per unit area and time.

The selectivity of a membrane towards a mixture is generally expressed by one of two parameters, the retention (R) or the separation factor (α). For dilute aqueous mixtures consisting of a solvent (mostly water) and a solute, it is more convenient to express the selectivity in terms of retention R towards the solute.

The solute is partly or completely retained while the solvent (water) passes freely through the membrane.

In general, retention (R) is given by the following formula (Mulder, 1991):

$$R = \frac{C_f - C_p}{C_f} = 1 - \frac{C_p}{C_f} \tag{2.1}$$

C_f is the solute concentration on the feed side [mg /l]

C_p is the solute concentration on permeate side [mg / l]

Membrane selectivity towards gas mixtures and mixtures of organic liquids is usually expressed in terms of a separation factor α. For a mixture consisting of component A and B, the selectivity factor $\alpha_{A/B}$ is given by:

$$\alpha_{A/B} = \frac{Y_A / Y_B}{X_A / X_B} \tag{2.2}$$

Y_A, Y_B are the concentrations of the components A and B in the permeate [mg / l]

X_A, X_B are the concentration of the components A and B in the feed [mg / l]

The concentration can be expressed either as a mass concentration, or as a molar concentration. The composition of a solution or a mixture can also be described by means of mole fractions and mass fractions.

2.3.2 Hydrophobic and Hydrophilic

Hydrophobic materials are not easily wetted by water; hydrophilic materials are more readily wetted by water. If wetting occurs, the water will penetrate into the pores of the membrane. The wettability is a function of the pore size and the type of material. Water wetting is favoured when the solid polymer has a high surface energy.

The liquid properties have also a role in the wettability. A liquid with high surface tension (i e. water) can wet the hydrophilic porous polymer more easily than a liquid with low surface tension (i e. hexane).

Various hydrophobic and hydrophilic polymers are listed in Section 2.2.2.

Figure 2.2 shows the effect of an increase in hydrophilicity on the contact angle of a water droplet on a solid surface.

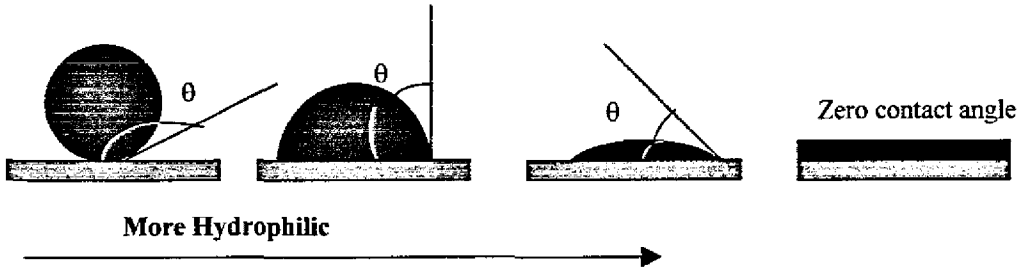

Figure 2.2: Evolution of water drop contact angle as a function of membrane surface hydrophobicity (Anselme and Jacobs, 1996).

2.4 MEMBRANE GEOMETRY

Membranes can be prepared in two configurations: flat and cylindrical.
Flat membranes are prepared by immersion precipitation. Free flat membranes can be obtained by casting the polymer solution upon a metal or a polymer belt. Since flat membranes are relatively simple to prepare, they are very useful for testing on a laboratory scale.

The alternative configuration in which a membrane can be prepared is the cylindrical form. On the basis of differences in dimensions, the following types may be distinguished (with the approximate dimension) (Mulder, 1991):

i) hollow fibre membranes with internal diameter smaller than 0.5 mm;
ii) capillary membranes with internal diameter between 0.5 – 5 mm; and
iii) tubular membranes with diameter greater than 5 mm.

2.5 MEMBRANE MODULES

In order to apply membranes on a technical scale, large membrane areas are normally required. The smallest unit into which membranes are packed for use is called a module. Four major types of modules are found in the market place, plate-and-frame, spiral-wound, tubular and hollow fibre. Plate-and-frame and spiral-wound modules are produced from flat membranes whereas tubular, capillary and hollow fibre modules use the cylindrical membrane configuration.

2.6 MEMBRANE PROCESSES

Every membrane separation process is characterised by the use of a membrane to accomplish a particular separation. The membrane has the ability to transport one component more readily than the other because of differences in physical or chemical properties between the membrane and the permeating components. Transport takes place as a result of a driving force acting on the individual components in the feed.

In many cases the permeability is proportional to the driving force. The flux-force relationship can be described by a linear equation. Proportionality between the flux (J) and the driving force is given by:

$$J = -\beta \frac{dX}{dz} \qquad (2.3)$$

β phenomenological coefficient

The driving force is expressed as the gradient of X (temperature, concentration, pressure) along a coordinate z perpendicular to the transport barrier. Equation (2.3) can be applied for mass transport (Fick's law), heat flux (Fourier's law), momentum flux (Newton's law) and electrical flux (Ohm's law) (Mulder, 1991).

2.6.1 Pressure-Driven Membrane Operations

2.6.1.1 Reverse Osmosis

Reverse osmosis (RO) is a pressure-driven membrane process in which the solvent component of the solution is transferred through a dense membrane tailored to retain salts (Na^+, Cl^-) and low molecular mass solutes. RO uses high operating pressures (e.g. 5 to 8 MPa for sea water).

2.6.1.2 Nanofiltration

Nanofiltration (NF) is also called low-pressure RO and lies between RO and UF in terms of selectivity of the membrane which is designed for the removal of multivalent ions (calcium and magnesium). In nanofiltration the monovalent ions (Na^+, Cl^-) are poorly retained by the membrane. The operating pressure used in NF is much lower than in RO (0.5 to 1.5 MPa).

2.6.1.3 Ultrafiltration (UF)

In water treatment, UF can be defined as a clarification and disinfection membrane operation. UF membranes have pores. This means that separation is accomplished by a sieving mechanism; dissolved ions and low molecular mass organics are therefore not removed, but higher molecular mass species (macromolecules) are retained. The operating pressure is low (50 to 500 kPa).

2.6.1.4 Microfiltration (MF)

The major difference between microfiltration and UF lies in the membrane's pore size, those of MF being 0.1μm diameter or larger and UF being an order of magnitude smaller. The primary application for this operation is in particulate removal (clarification). Typical operating pressure is lower than that of UF, UF being an order of magnitude smaller.

2.6.2 Permeation Operations

Permeation operations are membrane operations where the driving force is activity difference across the membrane.

The solute will diffuse through the membrane from the high concentration side to the low concentration side. The driving force is the concentration (activity) gradient across the membrane.

Gas permeation (GP) is a gas/membrane/gas separation process in which the activity difference is maintained through a pressure difference across a dense membrane.

Gas diffusion is the same as gas permeation, the only difference is the membrane is porous, and the transport takes place by Knudsen flow. This process has been developed for isotope enrichment in the nuclear industries.

Pervaporation (PV) is a liquid/vapour separation operation in which a liquid is partially vapourised through a dense membrane.

2.6.3 Dialysis Operations

Dialysis operations are membrane operations applied to solutions in which the solute is transferred through the membrane. The driving force is an activity or an electrical potential difference in the absence of any transmembrane pressure difference. The driving force in dialysis operations is a transmembrane concentration difference. Selective passage of ions and low molecular mass solutes occurs with the retention of larger colloidal and high molecular mass solutes. Electrodialysis on the other hand is an operation by which ions are driven across ion-selective membranes under the influence of an electrical potential difference across such membranes.

2.6.4 Membrane Bio-Reactor Processes

Membrane bio-reactors involve membranes and microorganisms. The principle of a membrane bio-reactor depends on the way microorganisms are related to membranes. Membranes can be used to aerate a biological tank. They can be used as a filter. Or they can be used as a support for microorganisms used in the process. The next Chapter (Chapter 3) gives more details about membrane bio-reactors.

2.7 APPLICATIONS OF THE TRANSPORT OF GASES ACROSS MEMBRANES

The application of membranes in processes where gas transport occurs is summarized in the following paragraphs.

2.7.1 Bio-Reactors

- Bubble-free aeration (Côté et al., 1988,1989; Ahmed and Semmens, 1992,1996);
- Membrane bio-reactors (Chang and Moo-Young, 1988; Venkatadri and Irvine, 1993).

2.7.2 Petrochemical Industry

- Recovery of hydrocarbon vapours from air streams produced during gasoline loading and unloading operations (tank farm and gasoline stations) (Ohlrogge et al.,1990; Ohlrogge, 1993);
- Hydrogen separation from a syngas / hydrocarbon mixture. Syngas is a mixture of hydrogen and carbon monoxide. It is produced from natural gas, oil or coal and is used for synthesizing various organic chemicals at elevated temperatures.
- Natural gas separation:
    - i) removal of carbon dioxide (McKee et al., 1991; Lee et al., 1995; Meyer and Gamez, 1995; Antari, 1997; Kohl and Nielsen, 1997);
    - ii) removal of hydrogen sulfide (Fournie and Agostini, 1987; Bhide and Stern, 1993); and
    - iii) recovery of helium (Perrin and Stern, 1986; Choe et al., 1988; Kohl and Nielsen, 1997).

2.7.3 Water Treatment

- removal of acid gases (carbon dioxide, hydrogen sulfide and sulfur dioxide) (Qi and Cussler 1985 a,b; Kreulen et al., 1993 a,b; Karoor and Sirkar, 1993); and
- removal of volatile organic contaminants (e.g. trichloroethylene (C_2HCl_3)) (Qi and Cussler, 1985a ; Semmens et al., 1989, 1990).

CHAPTER 3
MEMBRANE BIO-REACTORS

3.1 INTRODUCTION

A membrane bio-reactor is, by definition, a device for simultaneously carrying out a biotransformation and a membrane-based separation in the same physical enclosure (Jacobs, 1997).

There is no adopted definition for membrane bio-reactors. In the literature, the word membrane bio-reactor is used for any process where membranes and microorganisms are involved. Examples are as follows:

- the aeration of activated sludge using a membrane (bubble-free aeration) (Côté et al., 1988, 1989; Ahmed and Semmens, 1992, 1996);
- membranes used to filter the biomass in a biological treatment operation (Ross et al., 1990; Manem and Sanderson, 1996);
- using a membrane to separate a target gas (pollutant) and microorganisms to degrade the pollutant after this separation; and
- a membrane used to support a biofilm in such a way that nutrients are delivered to the biofilm in an efficient manner (Chang and Moo-Young, 1988; Venkatadri and Irvine, 1993; Leukes, 1999).

3.2 BUBBLE-FREE AERATION

Bubble-free aeration is desirable for applications in wastewater treatment when bubbling of air would result in the stripping of volatile compounds or in foaming of industrial waste water. Membranes can be used to transfer large quantities of oxygen (1000 g O_2 /m^3.h) to biological reactors. For conventional activated sludge, the quantity of 100 g O_2 /m^3.h is reported in the literature to be a commonly used transfer rate (Côté et al., 1988, 1989).

Côté et al. (1988, 1989) used silicone rubber membranes assembled in an axial-flow module for bubble-free aeration of a biological tank. Ahmed and Semmens (1992, 1996) used transverse-flow hollow fibres for bubble-free aeration of water; it was successfully demonstrated using sealed-end hollow fibres pressurized with pure oxygen.

3.3 ADUF PROCESS

ADUF (anaerobic digestion ultrafiltration) is a process for the treatment of industrial organic wastes which effectively eliminates the sludge concentration and retention problems associated with conventional systems (Ross et al., 1990). The ADUF process can be defined as the combination of two basic processes, biological degradation and membrane separation, into a single process where suspended solids and microorganisms responsible for biodegradation are separated from the treated water by a membrane filtration unit (Manem and Sanderson, 1996). Figure 3.1 shows a simplified diagram of the ADUF process.

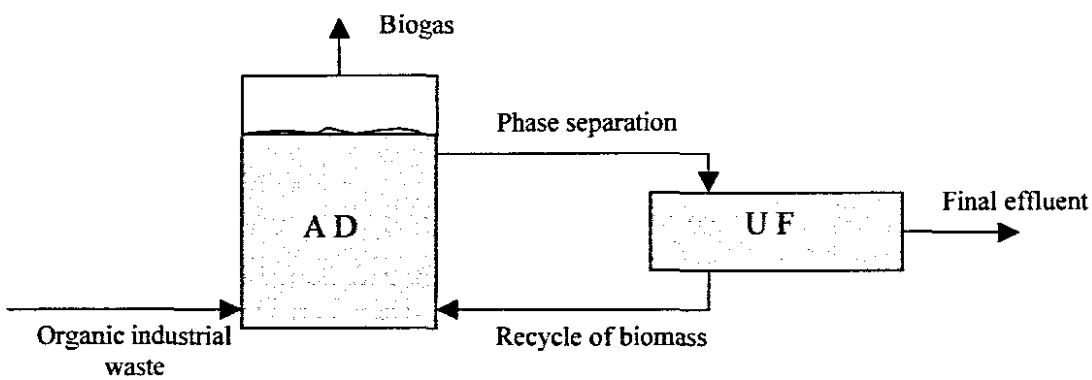

Figure 3.1: Schematic diagram of the ADUF process (Ross et al., 1990).

3.4 GRADOSTAT MEMBRANE BIO-REACTOR

The Gradostat membrane bio-reactor incorporates a process by which enzymes are continuously produced by fungi attached to a membrane. The membrane acts as a support for the microorganism. Bioremediation using the fungus can be in two systems. One uses the whole organism (white rot fungi); the other uses only the enzymes produced.

The Gradostat membrane bio-reactor can be used for both the above systems. For example: i) in water treatment using the whole fungus; and ii) to produce continuously enzymes to be used for biodegradation of aromatic pollutants.

3.4.1 Whole Organism Bioremediation using White Rot Fungi

The Gradostat bio-reactor allows for the continuous production of secondary metabolites, in particular for the bioremediation of waste water containing certain pollutants. It comprises providing a porous substratum which has a biofilm of microorganisms attached thereto, and causing a nutrient solution to flow through the substratum, at a rate which is sufficiently low for a nutrient gradient to be established across the biofilm (Leukes et al., 1997).

In the presence of a nutrient solution of sufficiently high concentration, most microorganisms exhibit exponential growth (primary growth). As the concentration of the nutrient solution falls, the microorganisms, in response to the stress caused by nutrient starvation, switch to a secondary growth phase during which they start to produce secondary metabolites. These include enzymes that are able to degrade less available or more complex food sources (Leukes, 1999).

This degradative ability is due in part to the secretion of a group of H_2O_2 producing oxidases as well as a group of peroxidases called lignin peroxidases (LiP). In whole cell cultures, however, a certain amount of biodegradation of these compounds occurs independently of the secretion of these enzymes (Leukes, 1999).

3.4.2 Advantages Resulting from the Continuous Production of Enzymes

There are two major advantages in the use of enzyme treatments:

- high concentrations of toxic pollutants can be dealt with; and
- certain enzymes are able to function in organic solvents with which several phenolic effluents are associated.

The use of fungal enzyme extracts for degradation, transformation and detoxification of aromatic pollutants has been demonstrated on a laboratory-scale (Leukes, 1999). These enzymes are best suited to applications where they either remove pollutants by depolymerisation, or detoxify them by humification or transformation (transformation of pollutant molecules to less toxic compounds).

Certain secondary metabolites have useful properties. *Phanerochaete Chrysosporium*, is a filamentous fungus capable of degrading a wide range of recalcitrant aromatic pollutants. These compounds include BTEX (benzene, toluene, ethylbenzene and xylene) type compounds, DDT, TCDD (2,3,7,8-tetra-chlorodibenzen-p-dioxin), benzo(a)pyrene, Lindane and certain PCB congeners (Bumpus and Aust, 1987; Gold and Alic, 1993). This organism has thus been considered a candidate for the bioremediation of waste waters containing such pollutants.

3.4.3 White Rot Fungi

The growth of the white rot fungi can be promoted in different ways:

Stationary culture: the fungus grows as a pellicle on the surface of the growth medium in erlenmeyer flasks (Keyser et al., 1978; Kirk and Nakatsubo, 1983).

Agitated culture: the fungus grows in agitated erlenmeyer flasks (Leisola and Fiechter, 1985; Jäger et al., 1985 ; Linko, 1992).

Immobilisation of fungi: the fungus grows on different supports; the most popular matrices for immobilisation of fungi are: nylon web (Linko, 1988), polyurethane foam (Kirkpatrick and Palmer, 1987; Moreira et al., 1997) and silicone rubber (Venkatadri and Irvine, 1993).

The continuous production of ligninolytic enzymes has only recently been reported for white rot fungi (Gradostat membrane bio-reactor) by Leukes (1999).

3.4.4 Oxygen Requirement in Gradostat Fungal Membrane Bio-Reactor

The importance of having a pure oxygen environment for good ligninase production is well documented. The ligninolytic system of white rot fungi has been shown to be particularly active in cultures grown in high oxygen tension (Dosoretz et al., 1990). Lignin degradation was shown to be about 3-fold higher under 100% oxygen than in air (Kirk et al., 1978). Faison and Kirk (1985) reported that both ligninolysis and ligninase activities of *P. Chrysosporium* were increased in cultures initially supplied with air during their growth phase and then shifted to an oxygen atmosphere. Because of this, most laboratory-scale studies as well as scale-up attempts have employed the use of a pure oxygen environment for high productivities (Dosoretz et al., 1993). Dosoretz et al. (1990) also reported that different oxygenation conditions had profound effects on the onset and decay of the peroxidative system, and the production of extra-cellular proteases and polysaccharides.

3.5 MEMBRANE TYPES FOR GRADOSTAT BIO-REACTOR

Capillary membranes have been shown to be geometrically ideal for use in bio-reactors. The morphological properties of the membranes and the materials from which they are manufactured can be modified to suit a variety of biotransformation processes (Belfort, 1989; Jacobs, 1997).

Leukes (1999) identified the shortcomings of commercial capillary ultrafiltration membranes as matrices to support differentiated fungal growth. The most important shortcomings are summarized below:

- conventional ultrafiltration membranes have pore sizes in the range of 2 to 100 nm. This provides little space for the fungal biomass to attach itself and resulted in inconsistencies in the establishment of stable, dense biofilms; and
- the outside skin layer made penetration of the fungal growth into the spongy wall of the membrane very difficult, leading to poor anchorage of the biofilm.

The specification of the type of the membranes that can be used in fungal membrane bio-reactors was made by Jacobs and Sanderson (1996, 1998). This specification is summarized as follows:

" If the biofilm could be firmly entrapped within the macrovoids, sloughing of the biofilm by the above shortcoming could be avoided or reduced. If the macrovoids were not blunt-ended (presence of an external skin), the biofilm would be more firmly attached to a greater available wall surface, which in turn, would be more likely to sustain a differentiated fungal thallus".

Following this specification of a membrane for the Gradostat bio-reactor an ultrafiltration polysulphone capillary membrane with a unique structure was developed (Jacobs and Sanderson 1996, 1998; Jacobs and Leukes, 1996). These membranes are internally skinned, with no skin on the outside. This structure will be referred to us as a "skinless ultrafiltration membrane". The membrane fabrication is described in appendix B.

The membrane that was developed for the Gradostat bio-reactor is a polysulphone ultrafiltration membrane, having a skin on the inside and a micro-void structure which radiates outwardly from below the internal skin. The membranes have an outside diameter of 2 mm, an internal skin thickness of about 1 μm, and a void structure a length of up to 300 μm.

The void structure forms open passages which are many times larger in cross section than the pores in the ultrafiltration skin layer. This allows a relatively thick biofilm of approximately 300 μm to develop on the membrane, the biofilm being firmly anchored to the voids within the membrane (Jacobs and Leukes, 1996).

Figure 3.2 and 3.3 show the structure of the skinless polysulphone capillary membrane.

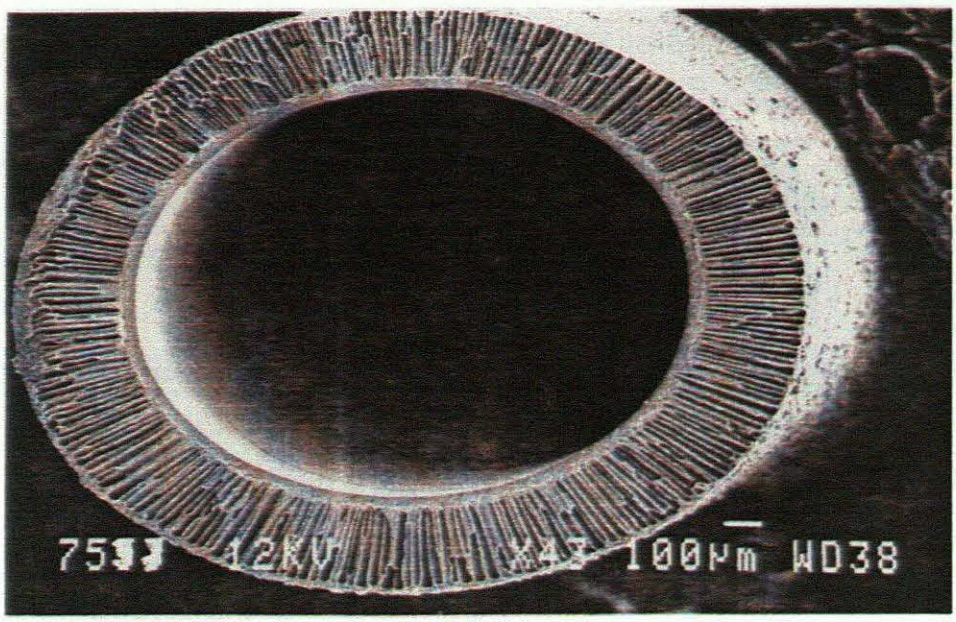

Figure 3.2: Capillary polysulphone membrane, skinless on the outside (Jacobs and Sanderson, 1997)

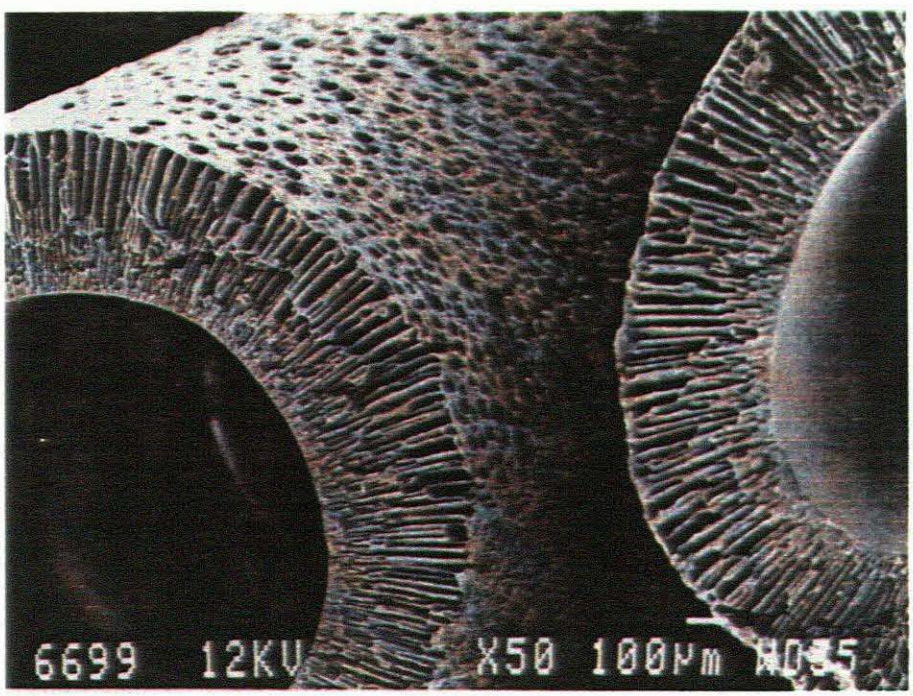

Figure 3.3: Capillary polysulphone membrane, skinless on the outside (Jacobs and Sanderson, 1997)

3.6 GRADOSTAT BIO-REACTOR MODULE DESIGN

With the successful production of a capillary membrane with the required characteristics, it was necessary to develop appropriate reactors.

In membrane technology, the membranes are assembled and associated in a unit. This unit is referred to as a module.

The design and operation of a bio-reactor must complement the biotransformation process under consideration. In this regard capillary and hollow fibre membranes offer much more operational freedom. The flow of the substrate feed may be directed either axially along the length of the membrane fibre or transversely, that is perpendicular to the membrane.

Suitable modules for application of the capillary membrane bio-reactor are:

- axial-flow modules; and
- transverse-flow modules.

3.6.1 Axial-Flow Module

The axial module resembles a tube and shell heat exchanger configuration. In this configuration a bundle of capillaries is potted into a cylindrical vessel. Figure 3.4 depicts the axial-flow module.

The axial modules are the most commonly used in industry, they are easy to construct and operate. Availability is also an important factor; commercially available dialysis and ultrafiltration units can be used as membrane bio-reactors with very little modification (Belfort, 1989).

3.6 GRADOSTAT BIO-REACTOR MODULE DESIGN

With the successful production of a capillary membrane with the required characteristics, it was necessary to develop appropriate reactors.

In membrane technology, the membranes are assembled and associated in a unit. This unit is referred to as a module.

The design and operation of a bio-reactor must complement the biotransformation process under consideration. In this regard capillary and hollow fibre membranes offer much more operational freedom. The flow of the substrate feed may be directed either axially along the length of the membrane fibre or transversely, that is perpendicular to the membrane.

Suitable modules for application of the capillary membrane bio-reactor are:

- axial-flow modules; and
- transverse-flow modules.

3.6.1 Axial-Flow Module

The axial module resembles a tube and shell heat exchanger configuration. In this configuration a bundle of capillaries is potted into a cylindrical vessel. Figure 3.4 depicts the axial-flow module.

The axial modules are the most commonly used in industry, they are easy to construct and operate. Availability is also an important factor; commercially available dialysis and ultrafiltration units can be used as membrane bio-reactors with very little modification (Belfort, 1989).

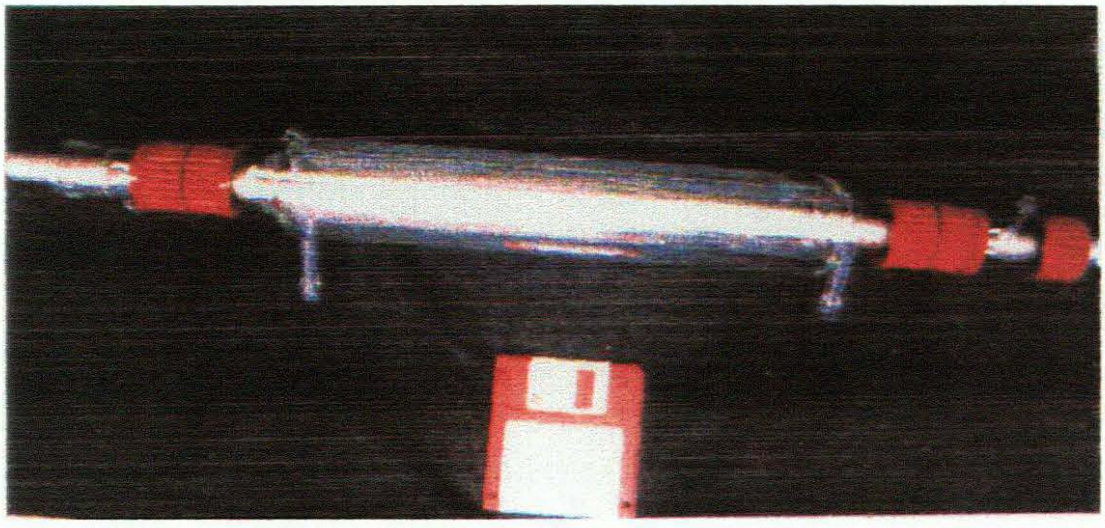

Figure 3.4: Axial module, tube and shell configuration (Leukes, 1999).

3.6.2 Transverse-Flow Module

In transverse-flow modules, the flow is perpendicular to the fibre axis. The term transverse-flow is preferred to cross-flow, the latter has been reserved to indicate feed flow along the membrane axis (Yang and Cussler, 1986; Futselaar et al., 1993a,b).

There are two types of membrane arrangements in transverse-flow modules: parallel-packed and cross-packed. Subsets of these arrangements are: i) randomly-packed and ii) regularly cross-packed.

The randomly packed parallel fibre bundles were investigated by Yang and Cussler (1986,1989), Côté et al. (1989), Lipski and Côté (1990) and Vaslef et al. (1994).

The regularly cross-packed transverse-flow modules are ideal for use in separation processes, such as microfiltration, ultrafiltration and reverse osmosis (Knops et al., 1992; Côté et al., 1992; Futselaar et al., 1993a).

Only a few researchers studied gas transfer in regularly cross-packed transverse-flow (Côté et al., 1992; Wickramasinghe et al., 1992;van der Walt, 1999).

Futselaar et al. (1995) and Smart et al. (1996) used the regularly cross-packed transverse-flow for pervaporation, while Lipski and Côté (1990) investigated pervaporation with a randomly-packed module.

Domröse et al. (1998) summarized the fabrication of one transverse-flow module type as follows:

"A template was designed and produced by injection molding. The material used was high-density polyethylene, propylene or polystyrene. Capillary membranes were cut to the required length and clipped into place on grooves molded into the plastic template. The template (containing the membranes in place) were then stacked with the membranes in alternate plates running perpendicular to those of the adjacent template until a reactor of sufficient size was built. Epoxy resin was then injected under pressure to pot the membranes and to seal the reactor. The extending ends of the membrane capillaries were then trimmed to size when the epoxy had set".

Figure 3.5 and 3.6 show the transverse-flow and the fabrication of the transverse-flow modules, respectively.

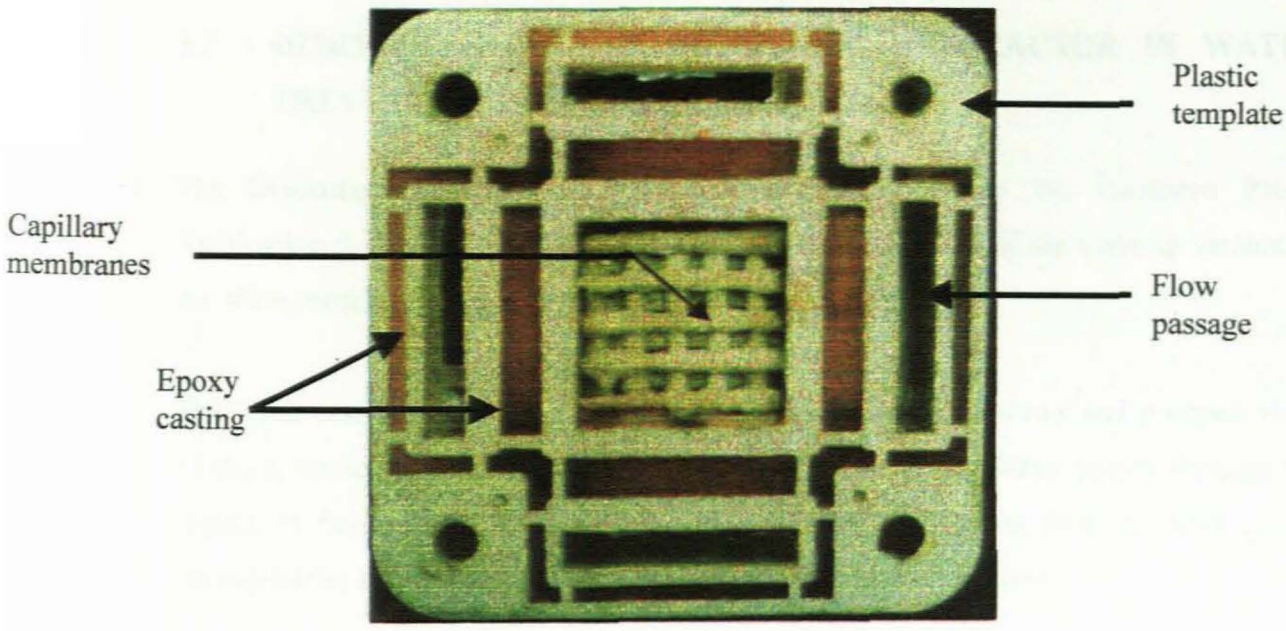

Figure 3.5: Transverse-flow module (Leukes, 1999).

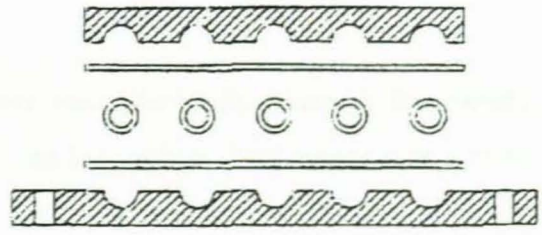

(a)

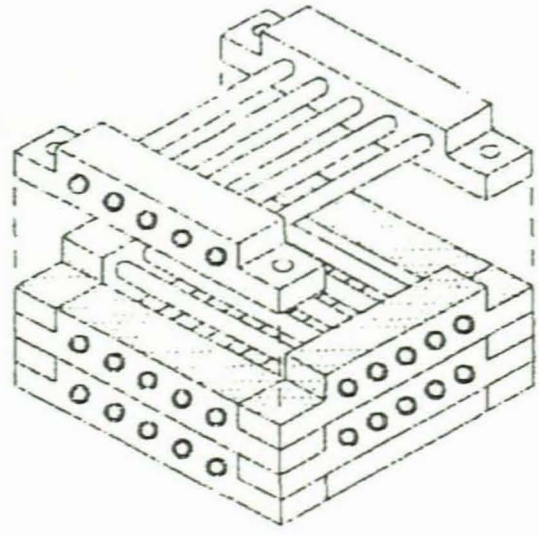

(b)

Figure 3.6: Transverse-flow module fabrication (van der Walt, 1999).
(a) Fibre ends are clamped between two strips to form a fibre segment,
(b) Fibre segment are stacked to form a transverse-flow membrane module.

3.7 DESCRIPTION OF THE MEMBRANE BIO-REACTOR IN WATER TREATMENT

The Gradostat membrane bio-reactor is well described in the European Patent Application (Leukes et al., 1997). What follows is a prediction of the scale up version of the afore-mentioned laboratory-scale apparatus.

The waste water that is to be treated is withdrawn from a reservoir and pumped via a filtration device into the lumen of the capillaries. The waste water passes through the capillaries from one end thereof to the other. Waste water exiting from the other end of the capillaries is returned to the reservoir for recirculation if required.

Nutrients diffuse through the ultrafiltration layer to the fungal biofilm, thus providing the nutrient gradient.

Some of the waste water permeates through the membranes and collects in the extra capillary space of the bio-reactor, from where it is drained through an outwash line. This flow of solution has to be regulated to avoid spoiling the ideal nutrient gradient in the biofilm.

The extra-capillary space of the bio-reactor is ventilated by means of air (oxygen supply) which is blown into the shell via an air inlet, and leaves the shell together with any permeate via the outwash line.

To ready the bio-reactor for production, the capillary membranes are inoculated with a suitable microorganism such as *P. chrysosporium*. This can be done by means of reverse filtration, i.e. by establishing a reverse flow of water through the membrane, the water carrying spores of the microorganism in suspension. A period is then allowed for attachment of the organism to the membranes. Once this has taken place and the spores have germinated, the bio-reactor is ready for use.

Since waste water continuously change character, nutrients can be added to support growth of the microorganism. As a consequence, a biofilm of immobilized microorganism develops on the outside of the membrane. The structure of the membrane was described in Section 3.5 and Appendix B.

The void-structure of the skinless membrane forms open passages, which are many times larger in cross-section than the pores in the ultrafiltration skin. This allows a relatively thick biofilm of approximately 300 μm to develop on and in the membrane, the biofilm being firmly attached to the membrane.

The rate of flow of permeate through the membrane should be low enough so that a nutrient gradient is established across the biofilm. Near the lumen of the membrane the nutrient concentration should be high enough to support primary growth of the biofilm population, whereas, towards the outside of the biofilm, the nutrient concentration should drop to a level which causes the biofilm population to switch to secondary growth, thereby resulting in the production of secondary metabolites.

New biomass would then be produced continuously near the surface of the biofilm where nutrient rich conditions prevail. This biomass would be pushed outward by newly-formed biomass to an area of low nutrient concentration. Here the biomass passes into secondary metabolism activating its enzyme production system at the hyphal tips. The process is stable and steady-state and can thus be operated on a continuous basis. Also, the thickness of the biofilm and immobilization of the organism may contribute to an increased rate of secondary metabolite production.

The air that is blown through the bio-reactor shell serves to supply the oxygen that is required for viability of the biofilm, and also to carry away spores and dead fungi that are shed from the outer surface of the biofilm.

Figure 3.7 and 3.8 shows the laboratory-scale transverse-flow and axial-flow bio-reactors, respectively, as used by Leukes (1999).

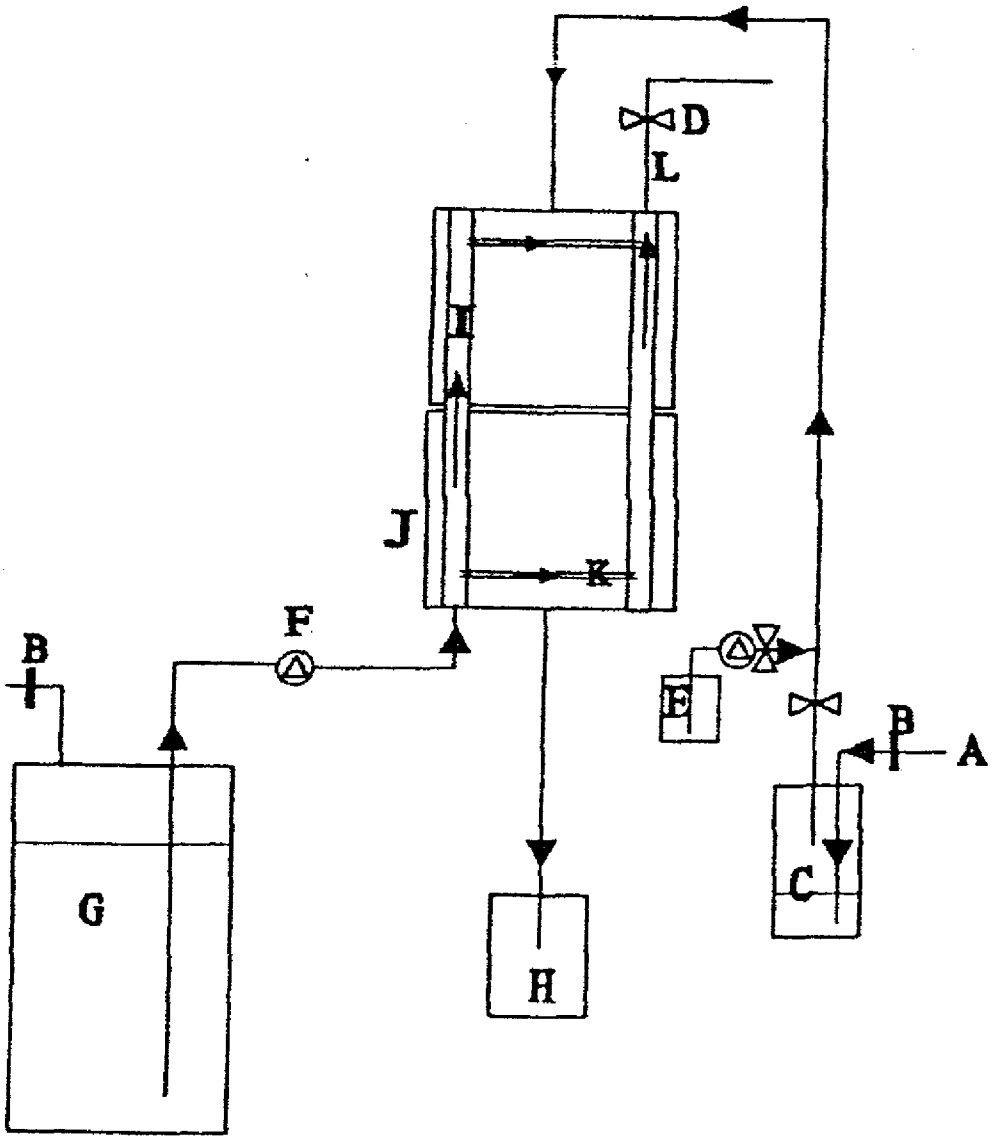

Figure 3.7: Schematic depiction of the transverse-flow membrane bio-reactor reported by Leukes (1999).

A- oxygen supply. Where air was used, an aquarium pump was attached and if pure oxygen was used, an oxygen cylinder was attached. B- air filter. C- humidified vessel- gas was bubbled through distilled water for humidification. D- Hoffmann clamp. E- inoculation vessel. F- peristaltic pump. G- growth medium reservoir vessel. H- permeate collection vessel. The inlet to this vessel was sealed with a cotton wool bung to allow spent air to escape while retaining spores within the vessel. I- growth medium inlet channel within the transverse flow membrane bio-reactor. J- the actual transverse flow membrane bio-reactor. K- represent the membranes. L- prime line. This was used to allow air to be flushed out of the membrane capillaries and to ensure that they were all filled with growth medium. Arrows show direction of flow (Leukes, 1999).

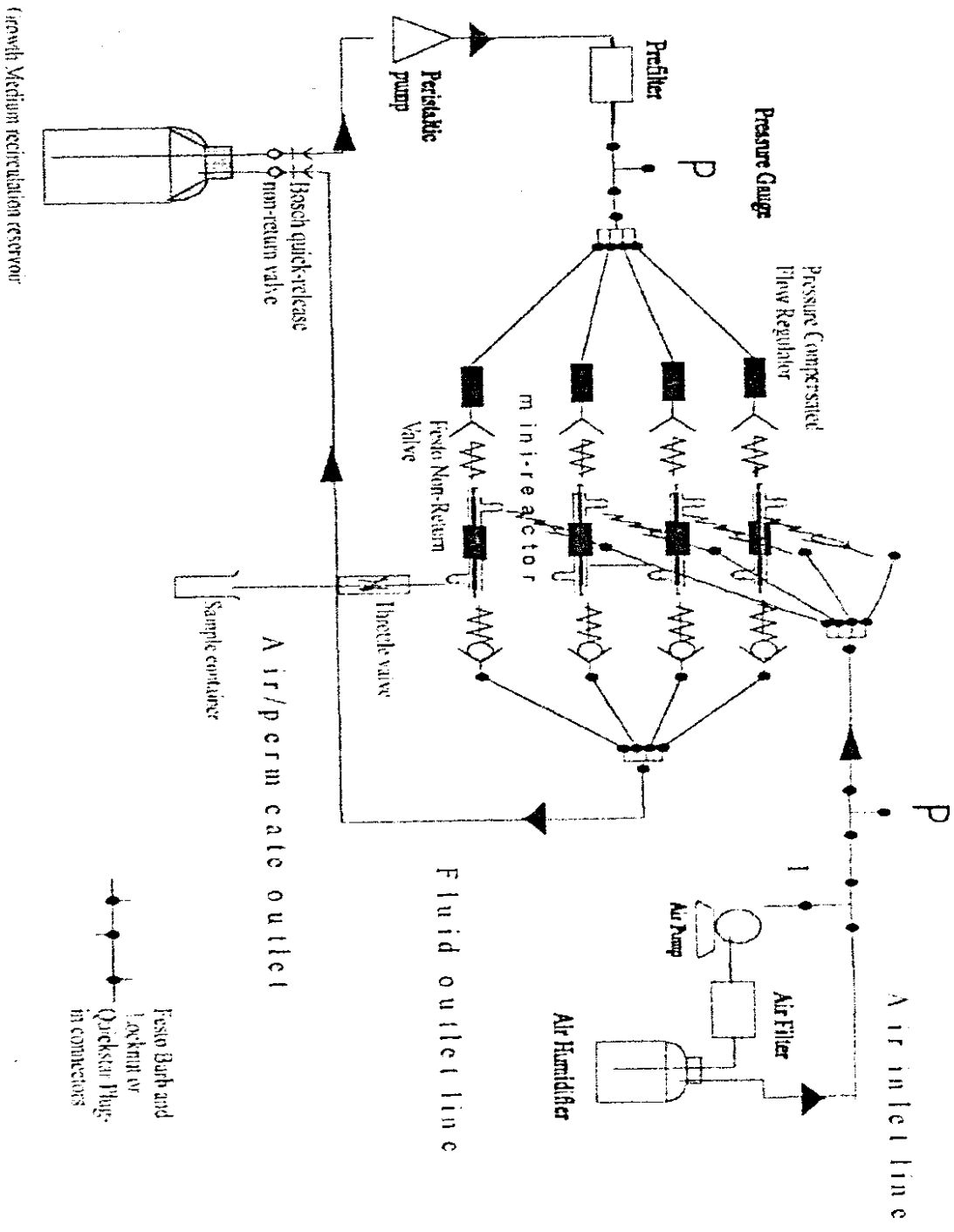

Figure 3.8: Axial-flow membrane bio-reactor (Leukes, 1999).

CHAPTER 4
MASS TRANSFER IN THREE-PHASE MEMBRANE CONTACTORS

4.1 INTRODUCTION

Mass transfer in membranes depends on the membrane type. If the membrane is dense the transport is by solubility in the membrane material; this is well described in the oxygenation of water using silicone rubber membranes. If the membrane is porous, two types of diffusion can be involved (Knudsen diffusion and continuum diffusion). These two types of diffusion depend on the pore size of the membrane and the types of fluid in the pores (gas or water). Knudsen diffusion generally applies in a gas-gas membrane process. In three-phase contactors (gas, membrane and water) the pores of the membrane can be gas or water filled: wetting depends on the size of the pores and the type of polymer. The mechanism of diffusion and the difference between continuum and Knudsen diffusion are reported in this chapter. Full explanations of the mechanism and equations for the different resistances occurring in three-phase contactors are also reported. A literature survey regarding correlations found to predict transport behaviour in different membranes is presented at the end of this Chapter. Some of these correlations were used to evaluate the experimental data.

4.2 DEFINITION OF MASS TRANSFER COEFFICIENT

If we are interested in the transfer of mass from some interface into a well mixed solution, we expect that the rate transfer is proportional to a concentration difference and to the interfacial area (Cussler, 1984):

(mass transferred per unit time) $=K$ * (interfacial area) * (concentration difference)

where the proportionality is summarized by K (the mass transfer coefficient).

If we divide both sides of this equation by the area, we can write the following equation:

$$J = K\ \Delta C \tag{4.1}$$

J flux [$cm^3 . cm^{-2} . s^{-1}$]
K mass transfer coefficient [m/s]
ΔC concentration difference [mg/ l]

In water treatment, it is most common to express mass transfer in terms of the liquid phase (water) concentrations as shown in equation (4.2):

$$J = K_{OL} (C - C^*) \tag{4.2}$$

J the flux (rate / unit area) [$cm^3 . cm^{-2} . s^{-1}$]
C^* equilibrium concentration with the partial pressure in the gas phase [mg/ l]
C concentration in the bulk solution [mg/ l]
K_{OL} overall mass transfer coefficient based on the liquid side [m/s]

4.3 DEFINITION OF THREE-PHASE MEMBRANE PROCESS

In all the membrane processes (UF, MF, RO) cited earlier, water is present on both sides of the membranes. In three-phase membrane processes, the membranes are used to expose the water to a different phase to facilitate the removal of particular contaminants or the transfer of gases. The other phases can be gas, vacuum or a chemically reactive solution. Water may therefore only be in contact with one side of the membrane.

The driving force in three-phase membrane processes is provided by maintaining a concentration gradient across the membrane. This is usually accomplished by exploiting the chemical characteristics of the contaminants that need to be removed (e.g. volatility, polarity, charge, dissociation constant, etc.). Table 4.1 gives an overview of work done by various researchers to study mass transfer in three-phase membrane processes.

Table 4.1: Overview of work done by various researchers to investigate three-phase membrane contactors

Reference	Gas transfer process	Membrane type	Membrane configuration
Yang & Cussler 1986	Removal of O_2	Microporous PP	Hollow fibres (axial & transverse)
Costello et al. 1993	Removal of O_2	Microporous PP	Hollow fibres (axial)
Tai et al. 1994	Removal of O_2	Microporous PP	Hollow fibres (axial)
Ito et al. 1998	Removal of O_2	Dense SiR	Hollow fibres (axial)
Qi & Cussler (1985a)	Removal of VOC	Microporous PP	Hollow fibres (axial) & Flat-sheet
Qi & Cussler (1985c)	Recovery of Br_2	Microporous PP	Hollow fibres (axial) & Flat-sheet
Semmens et al. 1989	Removal of VOC	Microporous PP	Hollow fibres (axial)
Semmens et al. 1990	Removal of NH_3	Microporous PP	Hollow fibres (axial)
Li et al. 1994	Removal of CO_2	Microporous PP	Hollow fibres (axial)
Yang & Cussler 1989	Absorption of O_2 (artificial gills)	Microporous PP	Hollow fibres (axial & transverse)
Côté et al. 1988	Absorption of O_2 (bubble-free aeration)	Dense SiR	Hollow fibres (axial)
Côté et al. 1989	Absorption of O_2 (bubble-free aeration)	Dense SiR	Hollow fibres (axial)
Ahmed & Semmens 1992	Absorption of O_2 (bubble-free aeration)	Microporous PP	Hollow fibres (transverse)
Ahmed & Semmens 1996	Absorption of O_2 (bubble-free aeration)	Microporous PP	Hollow fibres (transverse)
Kreulen et al. (1993b)	Absorption of CO_2	Microporous PP	Hollow fibres (axial)
Kreulen et al. (1993a)	Absorption of CO_2, NH_3	Microporous PP	Flat-sheet
Karoor & Sirkar 1993	Absorption of CO_2, SO_2	Microporous PP	Hollow fibres (axial)
Tsuji et al. 1981	Absorption of O_2 (blood oxygenation)	Microporous PP	Hollow fibres (axial)

Table 4.1: Continued

Wickramasinghe 1992	Absorption of O_2 (blood oxygenation)	Microporous PP	Hollow fibres (axial&transverse)
Wang & Cussler 1993	Absorption of O_2 (blood oxygenation)	Microporous PP	Hollow fibres (axial&transverse)
Alexander & Fleming 1982	Absorption of O_2 (blood oxygenation)	Microporous PP	Hollow fibres (axial)

PP polypropylene
SiR silicone rubber

4.4 MEMBRANE TYPES FOR THREE-PHASE MEMBRANE PROCESS

The different types of membranes that may be used for a three-phase process are: dense membranes, porous hydrophobic membranes, and composite membranes.

The dense membranes are made of a solid non-porous polymer, the common example is silicone rubber which is permeable to volatile low molecular mass organic compounds and gases. Côté et al. (1989) have used these membranes (silicone rubber) to transfer oxygen into water for waste water treatment. Ito et al. (1998) investigated the removal of dissolved oxygen from water through a non-porous (silicone rubber) hollow fiber membrane.

In water treatment applications (ultrafiltration and nanofiltration), when water contacts the membrane, the pores become wet and water can flow through the membrane convectively. For three-phase process applications it is important that the membrane is not hydrophilic and that the pores do not get wet. The membrane is used to create an interface for mass transfer and, as such, the membrane must be hydrophobic and the pores sufficiently small to avoid wetting under the operating conditions.

Polypropylene and polyethylene membranes with pore sizes below 0.1μm are effective for many three-phase processes.

Composite membranes combine the advantage and selectivity of dense polymers with the higher transport kinetics of porous membranes. Composite membranes can be created by coating a very thin dense polymer layer onto the surface of a porous support membrane. This dense layer physically covers and seals the pores of the membrane so that wet-out is impossible even under the most adverse conditions.

4.5 COMPARISON BETWEEN THREE-PHASE MEMBRANE PROCESS AND CONVENTIONAL CONTACTORS

It has been demonstrated that in conventional two-phase contactors, the mass transfer coefficient is higher than that of hollow fibre membrane modules (three-phase). For a system with a membrane at the interface the mass transfer process is determined by three mass transfer resistances in series, that is, resistance in the gas boundary layer, in the membrane layer and in the liquid boundary layer. For gas/liquid interface systems the stagnant gas (the pores gas filled) is not present and therefore only two mass transfer resistances in series have to be considered (Kreulen et al., 1993b).

In the conventional gas-liquid contactors the mass transfer resistance is determined by diffusion and convection, while in membranes the mass transfer resistance only depends on diffusion.

The hydrodynamic state of the gas and liquid flow must be considered. Mass transfer resistances are lower in the turbulent than in the laminar regime. In the hollow fibre membrane contactor the flow is usually laminar because of the small fiber diameters and the small distance between the fibres. In the conventional contactors both the gas and liquid flow are often turbulent (Kreulen et al., 1993a).

Hollow fibre membranes offer some significant advantages compared to conventional absorbers (bubble columns, tray columns or packed beds). In a hollow fibre membrane module the interfacial area between the gas and liquid phase is formed by the membranes, while in the conventional absorbers it is mainly determined by the direct dynamic interaction between gas and liquid flow (Kreulen et al., 1993a).

The amount of interfacial area per unit volume that can be realized in hollow fibre membrane modules is much larger than the values encountered in conventional contactors. For instance, the specific exchange area with a fibre of 10^{-3} m diameter can be about 3000 m^2/m^3 (Kreulen et al., 1993b), while in bubble columns, sieve trays or packed beds this area is around 800 m^2/m^3 at a maximum (Laurent and Charpentier, 1974; Van Landeghem, 1980). For the hollow fibre modules, the ratio of surface area per unit volume can equal up to 8000 m^2/m^3 (Matson et al., 1983).

Mass transferred per equipment volume for gas absorption is about thirty times faster in hollow fibres than in packed towers (Qi and Cussler, 1985b). Liquid extraction is six hundred times faster in fibres than in mixer settlers (Wickramasinghe et al., 1992).

It can be concluded that although the mass transfer coefficients in hollow fibre modules are lower than in conventional contactors, the substantial increase of the interfacial area can result in a more efficient absorber.

For the selection of a gas/liquid contactor the mass transfer rate is not the only property which must be taken into account. Another distinct feature of the hollow fibre module is that the flows of gas and liquid do not influence each other, because the gas and liquid flows are separated by the membrane. This results in a larger operation flexibility than in the conventional absorbers, which are severely limited by phenomena like flooding, loading, weeping, entrainment, etc. (Kim , 1984; Cooney and Jim, 1984; D'elia et al., 1986; Kreulen et al., 1993a).

4.6 MASS TRANSFER IN TRANSVERSE-FLOW AND AXIAL-FLOW MODULES

The mass transfer rate in transverse-flow modules is approximately an order of magnitude higher than that of axial-flow modules (Yang and Cussler, 1986; Ahmed and Semmens, 1996). Some of the reasons are given below.

- The mass transfer rate increases by increasing the shear at the membrane surface. In the transverse-flow module, because the fibres are positioned perpendicular to the feed flow direction, this arrangement results in turbulence promotion by the fibres themselves (Futselaar, 1993a,b).

- Concentration polarization, the deposition of retained material on the membrane surface and clogging of the membrane. This phenomenon decreases the mass transfer rate. The concentration polarization is reduced in transverse-flow, as opposed to that in axial flow (Futselaar, 1993b).

- High packing densities in transverse-flow, and large membrane surface area to volume ratio.

- The small diameter and the long lengths of the capillaries preclude them from being installed into a regular configuration in axial-flow modules. The regular arrangement of the fibers in transverse-flow prevents maldistribution of flow over the cross section of the module on the shell side of the capillaries. This improves flow distribution and ensures the absence of channeling. It therefore ensures the optimal use of all the installed membrane area.

4.7 MECHANISMS OF MASS TRANSFER IN THREE-PHASE MEMBRANE CONTACTORS

The mass transfer of a solute across a membrane can involve many steps.

Case 1: Gas Removal

The steps involved with deoxygenation (oxygen removal) from water, using a dense membrane occurs as five steps (Figure 4.1):

1. diffusion from the bulk water to the surface of the membrane;
2. solution of the gas and selective partitioning into the membrane phase;
3. diffusion through the membrane;

4. desorption from the permeate side of the membrane; and
5. diffusion away from the membrane and into the bulk of the stripping gas.

Oxygenation using a dense membrane follows the same steps, but in reverse to deoxygenation.

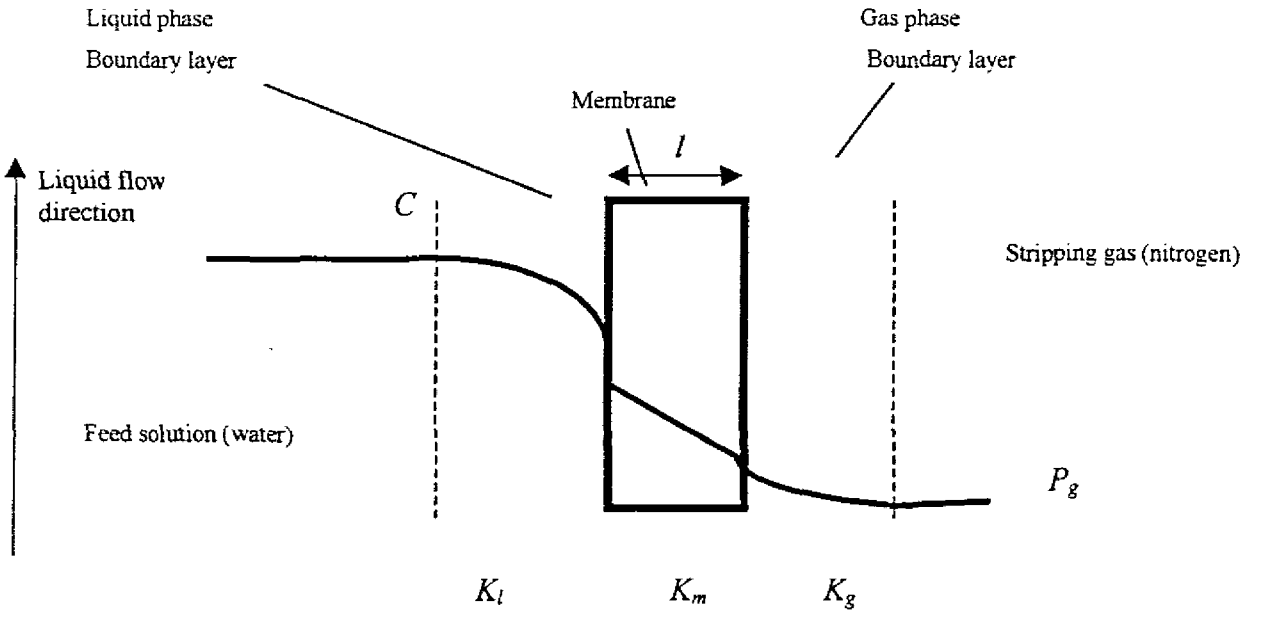

Figure 4. 1: Gas removal across a membrane (simplified representation).

Case 2: Absorption

Physical absorption of a compound from a gas through a porous (gas filled) membrane into water occurs as five steps:

1. transport of gas molecules from the well mixed bulk of the gas phase through the gas phase boundary layer;
2. the transfer from the gas phase boundary layer to the membrane surface;
3. the diffusion through the stagnant gas in the pores of the membrane;
4. desorption in the liquid phase boundary layer; and
5. the transfer from the membrane/liquid interface into the bulk of the water.

Desorption has the same steps, but in reverse (from step 5 to 1).

As with all mass transfer operations, the slowest step will limit the overall rate of mass transfer. In general, the slowest step is determined by the membrane characteristics, the fluid flow regimes that are maintained on each side of the membrane, the properties of the substances being separated and the properties (fluid flow, viscosity) of the phases that are involved.

4.8 DIFFERENT TYPES OF DIFFUSION

Whitman (1923) described the molecular transport and calculated the mass transfer coefficient using equation (4.3):

$$K = \frac{D_e}{d} = D\frac{\varepsilon}{d\tau} \tag{4.3}$$

K mass transfer coefficient [m / s]
D_e effective diffusion coefficient [m^2 / s]
D diffusion coefficient [m^2 / s]
ε porosity, dimensionless [-]
τ tortuosity, dimensionless [-]
d diameter [m]

In the porous structure of a microporous membrane convection can be neglected (Kreulen et al., 1993a).

The types of diffusion that can be distinguished are: i) continuum diffusion; and ii) Knudsen diffusion.

4.8.1 Continuum Diffusion

The continuum diffusion coefficient in a gas phase can be calculated from the kinetic gas theory (Kreulen et al., 1993a). The mass transfer in a hollow fibre is usually described with an overall mass transfer coefficient, which is the reciprocal of the overall mass

transfer resistance. This overall resistance is the sum of three individual resistances (inside the fibre, across the membrane, and outside the fibre). Each individual resistance is in turn proportional to the reciprocal of an individual mass transfer coefficient (Wickramasinghe et al., 1992).

4.8.2 Knudsen Diffusion

The mean free path may be defined as the average distance traversed by a molecule between collisions with other molecules.

If the pores are small and/or when the pressure of the gas is reduced, the mean free path of the diffusing molecules becomes comparable with or larger than the pore size of the membrane. Collisions between the gas molecules are less frequent than collisions with the pore wall: this kind of gas transport is called Knudsen diffusion.

The molecules are very close to each other in a liquid and the mean free path is of the order of a few Angstroms; therefore, Knudsen diffusion can be neglected in liquids.
However, the mean free path of gas molecules will depend on the pressure and temperature. In this case, the mean free path can be written (Mulder, 1991):

$$\lambda = \frac{kT}{\pi d_{gas}^2 p\sqrt{2}} \tag{4.4}$$

- λ the mean free path [m]
- d_{gas} the diameter of the gas molecule [m]
- k constant
- P pressure [kPa]
- T absolute temperature (K)

As the pressure decreases the mean free path increases and at constant pressure the mean free path is proportional to the absolute temperature.

In ultrafiltration membranes, the pore diameter is within the range 20 nm to 0.2 μm, and hence Knudsen diffusion can have a significant effect. At low gas pressures, transport in the membrane is determined completely by Knudsen flow. In this regime the flux is given by (Mulder, 1991):

$$J = \frac{\pi n r^2 D_k}{RT\tau} \frac{\Delta p}{l} \tag{4.5}$$

n pore density [m^{-2}]
τ tortuosity dimensionless [-]
r pore radius [m]
l membrane thickness [m]
R universal gas constant [8.314 J/mol K]
T absolute temperature [K]
D_k the Knudsen diffusion coefficient [m^2 / s]

The Knudsen diffusion coefficient is related to the inverse of the square root of the molecular mass (Mason and Malinauskas, 1983; Mulder, 1991).

$$D_k = \frac{4}{3} q \sqrt{\frac{8RT}{\pi M_w}} \tag{4.6}$$

M_w molecular mass [g / mol]
T absolute temperature [K]
q constant depending on the geometry of the pores
R universal gas constant [8.314 J/mol K]

4.9 RESISTANCES IN SERIES MODEL

The overall mass transfer coefficient may be calculated based on the resistances in series model. A stagnant film is presumed to exist in the fluid phases on either side of a membrane and compound transfer occurs by molecular diffusion through these films and the membrane itself. The thickness of these stagnant films, or fluid phase boundary layers, is determined by the hydrodynamic conditions in each phase, and they will become thinner as the Reynolds number increases.

The mass transfer coefficient for each individual phase (K_l, K_m, K_g) may be estimated by dividing the diffusion coefficient of the compounds in that phase by the distance through which the molecules must diffuse.

In practice, however, the individual mass transfer coefficient cannot be calculated directly since the boundary layer thicknesses are dependent on the local mixing conditions in the liquid and gas. The diffusion path of any contaminant across a membrane is not necessarily equal to the thickness of the membrane. As a result, the individual mass transfer coefficients have to be evaluated empirically.

To measure the interfacial concentrations under different operating conditions, we assume the concentrations in each phase are in equilibrium at an interface. Thus, we need to know the partition coefficient K_d and Henry`s law constant H.

The partition coefficient K_d describes the equilibrium partitioning of the compound between the membrane and the water.

$$K_d = \frac{C_m}{C_l} \tag{4.7}$$

C_m concentration in membrane [mg / l]
C_l concentration in the liquid phase[mg / l]

K_d is dimensionless since it is simply derived from the ratio of the concentrations in the two phases.

Henry`s constant describes the distribution of the compound between the water and air:

$$H_p = \frac{p_g}{C_l} \tag{4.8}$$

p_g gas partial pressure [kPa]

H_p Henry`s constant [kPa.m^3.mol^{-1}]

Sometimes it is convenient to use a dimensionless Henry`s constant H_c, which is defined as the ratio of the gas phase and water phase concentrations at equilibrium:

$$H_c = \frac{C_g}{C_l} \tag{4.9}$$

C_l concentration in the liquid phase [mg / l]

C_g concentration in the gas phase [mg / l]

H_c Henry constant dimensionless [-]

It is most common to express mass transfer in terms of the liquid phase (water) concentration as follows (Aptel and Semmens, 1996):

$$J = K_{OL} (C - C^*) \tag{4.10}$$

J the flux [cm^3 . cm^{-2}.s^{-1}]

K_{OL} the overall liquid phase mass transfer coefficient [m /s]

C^* is assumed to be in equilibrium with the partial pressure in the gas phase [mg / l]

C the concentration in the bulk solution [mg / l]

Equation (4.10) is identical to equation (4.2) on page 35.

Mass transfer in the membrane system can be described with a resistances-in-series model. This means that the overall mass transfer coefficient can be related to the sum of the partial resistance in the gas, the membrane and the liquid phase, respectively.

The relationship of the overall mass transfer coefficient, K_{OL} , to the individual mass transfer coefficients (liquid, membrane, and gas) respectively, will depend on the type of membrane used.

- For a dense membrane (Aptel and Semmens, 1996):

$$\frac{1}{K_{OL}} = \frac{1}{K_l} + \frac{1}{K_m K_d} + \frac{1}{H_c K_g} \tag{4.11}$$

where:

K_{OL}	the overall liquid phase mass transfer coefficient [m / s]
K_l	liquid film mass transfer coefficient [m / s]
K_m	membrane mass transfer coefficient [m / s]
K_g	gas film mass transfer coefficient [m / s]

When the gas solubility in the polymer can be represented by a linear isotherm and the diffusion coefficient in the membrane is constant, Crank and Park (1968) expressed mass transfer resistance through the membrane by equation (4.12):

$$\frac{1}{K_m} = \frac{l}{S_m D_m} \tag{4.12}$$

S_m	solubility coefficient of the gas in the polymer [cm^3 (STP) / cm^3. kPa]
D_m	diffusion coefficient of the gas in the polymer [m^2 / s]
l	membrane thickness [m]

- For a microporous membrane with water occupying pores (Aptel and Semmens, 1996):

$$\frac{1}{K_{OL}} = \frac{1}{K_l} + \frac{1}{K_m} + \frac{1}{H_c K_g} \tag{4.13}$$

- For microporous membrane with gas occupying pores (Aptel and Semmens, 1996):

$$\frac{1}{K_{OL}} = \frac{1}{K_l} + \frac{1}{H_c K_m} + \frac{1}{H_c K_g} \qquad (4.14)$$

The overall mass transfer coefficient can also be calculated where the concentration gradients are expressed as gas-phase concentrations. The flux in this case is expressed by the following equation (Aptel and Semmens, 1996):

$$J = K_{OG}(P^* - P) \qquad (4.15)$$

K_{OG} overall mass transfer coefficient in the gas phase [m / s]

P^* pressure in equilibrium with bulk solution concentration [kPa]

P pressure in the bulk [kPa]

The equation for a microporous membrane with gas occupying pores (system with a non-wetted membrane) (Kreulen et al., 1993a) is given as:

$$\frac{1}{K_{OG}} = \frac{1}{K_g} + \frac{1}{K_m} + \frac{1}{H_c K_l} \qquad (4.16)$$

- For a microporous membrane with water occupying pores (wetted membranes) (Kreulen et al., 1993a):

$$\frac{1}{K_{OG}} = \frac{1}{K_g} + \frac{1}{H_c K_m} + \frac{1}{H_c K_l} \qquad (4.17)$$

In many cases, one of the individual mass transfer coefficients will be much smaller than the others, and hence dominate the overall mass transfer coefficient K. We can often ascertain which one is important by varying the flow rate of gas and liquid. The overall coefficient usually increases with liquid flow rate but is independent of gas flow rate (Qi and Cussler, 1985a,b; Yang and Cussler, 1986; Kreulen et al., 1993a; Tai et al., 1994; Malek et al., 1997).

4.10 MASS TRANSFER CORRELATION

Correlations can be related to the response of the mass transfer coefficients to flow conditions on either side of the membranes. These can be used as design relations and are employed to develop better modules.

Mass transfer correlations are available for a variety of membrane module configurations and for different operating condition ranges (Reynolds numbers). It is important to select a correlation that matches as closely as possible the experimental conditions that prevail in any particular system.

The correlations are based on the dimensionless groups: Sherwood number (*Sh*) as a function of the Reynolds number (Re), Schmidt number (*Sc*) and Peclet number (*Pe*), and generally take the following form:

$$Sh = p.Re^{q}.Sc^{r}.(\frac{d_e}{L})^{s} \qquad (4.18)$$

The values for p, q, r, and s are therefor dependent on the operating conditions and on the design of the membrane contactor, and different values for these constants can be found in the literature (Aptel and Semmens, 1996).

Where:

Sherwood number is expressed by equation (4.19)

$$Sh = \frac{Kd_e}{D} \qquad (4.19)$$

Peclet number is expressed by equation (4.20):

$$Pe = \frac{d_e^2 v_l}{DL} \qquad (4.20)$$

Reynolds number is expressed by equation (4.21):

$$Re = \frac{d_e v_l}{\upsilon} \qquad (4.21)$$

Schmidt number is expressed by equation (4.22):

$$Sc = \frac{\upsilon}{D} \tag{4.22}$$

Where:

K	mass transfer coefficient [m / s]
d_e	characteristic length [m]
D	diffusion coefficient [m^2 / s]
v_l	liquid velocity [m / s]
L	capillary length [m]
υ	kinematic viscosity [kPa. s]

The dimensionless correlations derived by researchers are summarized in Table 4.2; the application and the operating flow regime are also reported.

Table 4.2: Different mass transfer correlations

Authors (References)	Gas transfer process	Correlation	module & mode	Validity range
Yang & Cussler 1986	Removal of O_2 from water	$Sh = 1.64\ Pe^{0.33}$	axial flow, lumen feed	Pe < 1000
Yang & Cussler 1986	Removal of O_2 from water	$Sh = 1.25\ Re^{0.93}\ (de / L)^{0.93}\ Sc^{0.33}$	axial flow, shell feed	$Re.(d_e/L)<1000$
Qi & Cussler 1985c	Removal of Br_2 from water	$Sh = 1.1\ Pe^{0.33}$	axial flow, lumen feed	
Costello et al. 1993	Removal of O_2 from water	$Sh = (0.53\text{-}0.58)\ Re^{0.33} Sc^{0.33}$	axial flow, shell feed	$21<Re<324$
Yang & Cussler 1986, 1989	Removal of O_2 from water	$Sh = 0.9\ Re^{0.4}\ Sc^{0.33}$	transverse flow [a]	$1<Re<20$
		$Sh = 1.38\ Re^{0.34}\ Sc^{0.33}$	transverse flow [b]	$1<Re<20$
Lipski & Côté 1990	Pervaporation	$Sh = 0.9\ Re^{0.4}\ Sc^{0.33}$	transverse flow	$Re<1000$

(a) porosity $\phi = 0.93$
(b) porosity $\phi = 0.3$

The dimensionless correlations derived for liquid flow through the membrane lumens are in close agreement with the analogous equations derived by Seider and Tate (1936) and Lévêque (1928) for heat transfer.

Seider and Tate $$Sh = 1.86Pe^{0.33} \quad (4.23)$$

Lévêque $$Sh = 1.62Pe^{0.33} \quad (4.24)$$

CHAPTER 5
MASS TRANSFER COEFFICIENTS MEMBRANE TEST PROTOCOLS AND MATHEMATICAL EQUATIONS

5.1 INTRODUCTION TO EXPERIMENTAL WORK

The mass transfer of gases across membranes depends on the type of membrane used.

Flat-Sheet: the experiment need two chambers separated by the membrane (e.g. a diaphragm-cell), using the difference in concentration or difference in pressure to determine the mass transfer coefficient.

Capillaries: The experimental procedure to study mass transfer of gases in a capillary membrane system differs completely from procedures for flat-sheet membranes in that different experimental set-ups can be used: liquid can flow in through-mode or in recycle-mode; gas can flow in through-mode or in dead-end mode. In this thesis the liquid and gas are both in through-flow mode. The Gradostat membrane bio-reactor also working in this mode (see Figure 3.7 and 3.8 on page 32, 33 respectively).

5.2 MASS TRANSFER IN FLAT-SHEET MEMBRANES

5.2.1 Description of the Diaphragm-Cell Method

Cussler (1984) stated: "One of the best devices to measure the diffusion coefficient in a solution is the diaphragm-cell". These cells consist of two well-stirred compartments separated by a thin porous barrier or diaphragm (see Figure 5.1).

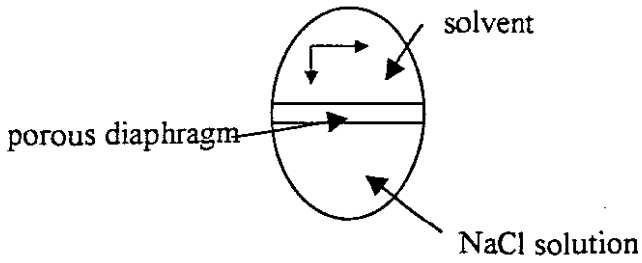

Figure 5.1: Diaphragm-cell

To measure the diffusion coefficient of say NaCl in water with this cell, the lower compartment is filled with a solution of known NaCl concentration and the upper compartment with pure solvent. After a known period, one or both of the upper and lower compartments are sampled and the NaCl concentrations measured. Using equation (5.12) (see page 56) the diffusion coefficient can be calculated.

Qi and Cussler (1985a) and Duffey et al. (1978) adapted the diaphragm-cell to measure the mass transfer coefficient in membranes (K). Previously, Stokes (1950), Mills et al. (1968) and Choy et al. (1974) used a porous membrane instead of a diaphragm (glass frit) to measure the diffusion coefficient (D).

Over the years, there has been much discussion about the best configuration of diaphragm-cells because experiments using a vertical diaphragm can give anomalous results (Cussler, 1984). The most satisfactory experiments most frequently use a horizontal diaphragm with the denser solution (solvent and solute) in the top compartment (Robinson and Stokes, 1960). Many good experiments use a horizontal diaphragm with the denser solution (solvent and solute) in the lower compartment (Cussler, 1984). Figure 5.2 shows different configurations of the diaphragm-cell.

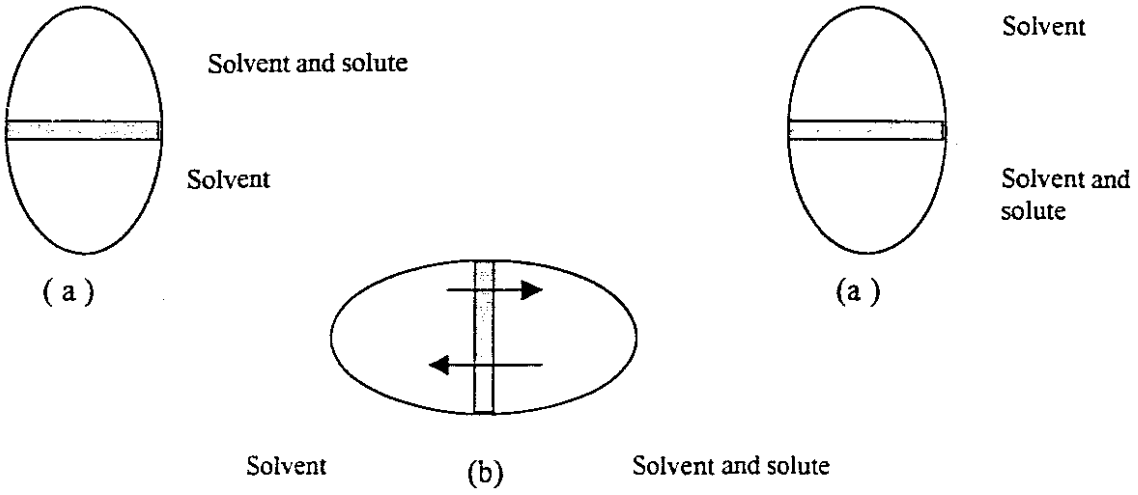

Figure 5.2: Different configurations of the diaphragm-cell with a) horizontally and b) vertically orientated diaphragms.

5.2.2 Derivation of a Theoretical Mass Transfer Equation for Diaphragm-Cell Method

To use the diaphragm-cell, an appropriate equation must be developed. The derivation of this specific equation was developed by Cussler (1984).

The flux across the membrane at any instant is given by equation (5.1):

$$J = \left(\frac{D}{l}\right)\left[C_{1,lower} - C_{1,upper}\right] \qquad (5.1)$$

J the flux [$cm^3 . cm^{-2} . s^{-1}$]
D diffusion coefficient [m^2 / s]
l effective thickness of the membrane [m]
$C_{1,lower}$ concentration of the solute in the lower compartment [mg / l] at any time, t
$C_{1,upper}$ concentration of the solute in the upper compartment [mg / l] at any time, t

The mass balances in each compartments can be written as:

$$V_{lower}\ \frac{dC_{1,lower}}{dt} = -AJ \qquad (5.2)$$

$$V_{upper}\ \frac{dC_{1,upper}}{dt} = +AJ \qquad (5.3)$$

A membrane area available for diffusion [m^2]

V_{lower} volume of the lower compartment [m^3]
V_{upper} volume of the upper compartment [m^3]

Dividing equation (5.2) by V_{lower} :

$$\frac{dC_{1,lower}}{dt} = \frac{-A}{V_{lower}} J \qquad (5.4)$$

Dividing equation (5.3) by V_{upper} :

$$\frac{dC_{1,upper}}{dt} = \frac{A}{V_{upper}} J \qquad (5.5)$$

Equation (5.4) minus equation (5.5):

$$\frac{dC_{1,lower}}{dt} - \frac{dC_{1,upper}}{dt} = \frac{-A}{V_{lower}} J - \frac{A}{V_{upp}} J \qquad (5.6)$$

$$\frac{d}{dt}\left[C_{1,lower} - C_{1,upper}\right] = -A\left[\frac{1}{V_{lower}} + \frac{1}{V_{upper}}\right] J \qquad (5.7)$$

Replacing J in equation (5.7) with equation (5.1):

$$\frac{d}{dt}\left[C_{1,lower} - C_{1,upper}\right] = -A\left[\frac{1}{V_{lower}} + \frac{1}{V_{upper}}\right] \frac{D}{l}\left[C_{1,lower} - C_{1,upper}\right] \qquad (5.8)$$

$$\frac{d}{dt}\left[C_{1,lower} - C_{1,upper}\right] = \frac{-AD}{l}\left[\frac{1}{V_{lower}} + \frac{1}{V_{upper}}\right]\left[C_{1,lower} - C_{1,upper}\right] \qquad (5.9)$$

This differential equation is subject to the initial condition:

t = 0 $\qquad C_{1,lower} - C_{1,upper} = C^0_{1,lower} - C^0_{1,upper}$

$C^0_{1,lower}$ initial concentration in the lower chamber [mg / l]

$C^0_{1,upper}$ initial concentration in the upper chamber [mg / l]

The integration of equation (5.8) with this condition gives:

$$ln\left[C^{0}_{1,lower} - C^{0}_{1,upper}\right] - ln\left[C_{1,lower} - C_{1,upper}\right] = -t\,D\,\frac{A}{l}\left[\frac{1}{V_{lower}} + \frac{1}{V_{upper}}\right] \qquad (5.10)$$

$$ln\,\frac{C^{0}_{1,lower} - C^{0}_{1,upper}}{C_{1,lower} - C_{1,upper}} = -t\,D\,\frac{A}{l}\left[\frac{1}{V_{lower}} + \frac{1}{V_{upper}}\right] \qquad (5.11)$$

$$\frac{D}{l} = \frac{1}{t\,A\left[\frac{1}{V_{lower}} + \frac{1}{V_{upper}}\right]}\,ln\,\frac{C^{0}_{1,lower} - C^{0}_{1,upper}}{C_{1,lower} - C_{1,upper}} \qquad (5.12)$$

$\frac{D}{l}$ the diffusion coefficient divided by the thickness of the diffusion equal to mass transfer coefficient (K)

$$K = \frac{1}{tA}\,\frac{1}{\left[\frac{1}{V_{lower}} + \frac{1}{V_{upper}}\right]}\,ln\frac{C^{0}_{1,lower} - C^{0}_{1,upper}}{C_{1,lower} - C_{1,upper}} \qquad (5.13)$$

If there is in the upper compartment a reactive solution, the concentration of the diffusing solute will equal zero. The left hand side of equation (5.3) becomes zero; this will yield a final equation of the form:

$$K = \frac{V_{lower}}{tA} \ln \frac{C_{1,lower}(t=0)}{C_{1,lower}(t)} \qquad (5.14)$$

Measurements of the time and the various concentrations are made. The membrane area available for transfer and the volume of the lower and the upper compartments are known. Equation (5.14) can be used to calculate the mass transfer coefficient for flat-sheet membranes.

5.3 MASS TRANSFER IN CAPILLARY MEMBRANES

The experimental apparatus consists of a capillary module, a feed reservoir and a gas cylinder. The mass transfer takes place in the capillary module.

5.3.1 Liquid in Recycle Mode and Gas in Flow-Through Mode

5.3.1.1 Description

The feed solution containing the solute (dissolved gas) that has to be removed is pumped from the stirred reservoir through the lumen of the capillary membrane module and returned to the reservoir. Gas is supplied into the shell side of the capillary membrane module, flowing through the module (not dead-end mode) (see Figure5.3). The solute concentration in the feed reservoir is measured as a function of time. This is a non-steady state system. Qi and Cussler (1985 a,b), D'elia et al. (1986), Dahuron and Cussler (1988), Semmens et al. (1990) and Qin and Cabral (1997) used this method to measure mass transfer in hollow fibre membrane modules.

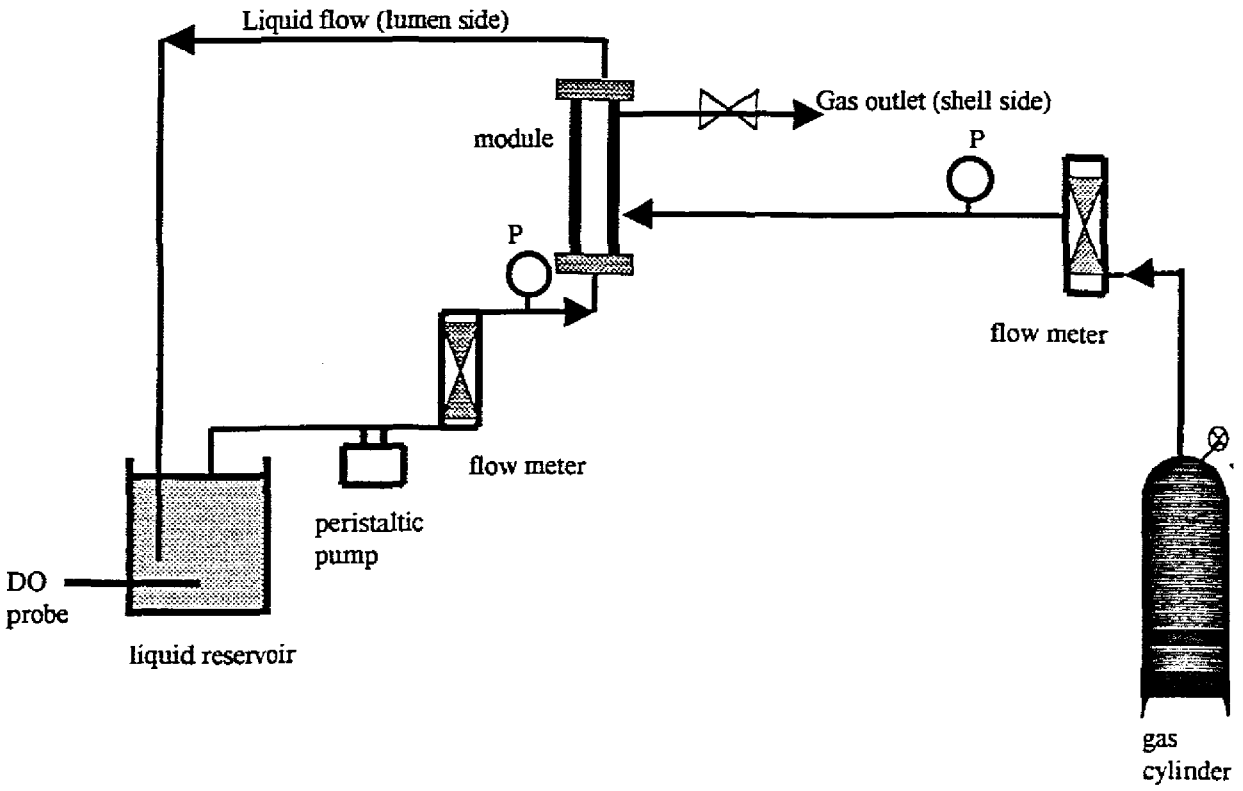

Figure 5.3: Experimental set-up for liquid in recycle mode and gas in flow-through mode.

5.3.1.2 Derivation of a Theoretical Mass Transfer Equation

The solute balance on a single fibre yields the following equation (Qi and Cussler, 1985a): at steady state

$$0 = -v\frac{dC}{dZ} - \frac{4KC}{d} \qquad (5.15)$$

v velocity inside the capillary [m / s]
K overall mass transfer coefficient [m / s]
C total solute concentration [mg / l]
d diameter of capillaries [m]

The initial condition:
$Z = 0 \qquad C = C_0$
C_0 concentration in the capillary membrane mouth [mg / l]
Z the length of the module [m]

$$v\frac{dC}{dZ} = -\frac{4KC}{d} \Rightarrow \frac{dC}{C} = -\frac{4K}{vd}dZ \qquad (5.16)$$

Integration of equation (5.16):

$$\int_{C_0}^{C} \frac{dC}{C} = -\frac{4K}{vd}\int_{0}^{L} dZ \qquad (5.17)$$

$$\frac{C}{C_0} = e^{-\frac{4KL}{vd}} \qquad (5.18)$$

L length of the capillary membrane [m]

The solute balance in the reservoir has the form (Qi and Cussler, 1985a, Semmens et al., 1989):

$$V\frac{dC_0}{dt} = \left(\frac{\pi}{4}d^2v\right)N(C - C_0) \qquad (5.19)$$

V reservoir volume [m^3]
N number of capillaries

The initial condition:
$t = 0 \therefore C_0 = C_0(t = 0)$

Rearranging equation (5.18):

$$C = C_0 e^{\frac{-4KL}{vd}} \qquad (5.20)$$

Replacing C in equation (5.19) with equation (5.20):

$$V\frac{dC_0}{dt}=\left(\frac{\pi}{4}d^2v\right)NC_0\left(e^{\frac{-4KL}{vd}}-1\right) \tag{5.21}$$

Integration of equation (5.21):

$$\int_{C_0(t=0)}^{C(t)}\frac{dC_0}{C_0}=\int_0^t\left(\frac{\pi}{4}d^2v\right)\frac{N}{V}\left(e^{\frac{-4KL}{vd}}-1\right)dt \tag{5.22}$$

$$\ln\frac{C(t)}{C_0(t=0)}=\left(\frac{\pi}{4}d^2v\right)\frac{N}{V}\left(e^{\frac{-4KL}{vd}}-1\right)t \tag{5.23}$$

$$1-e^{\frac{-4KL}{vd}}=\frac{4V}{\pi d^2vNt}\ln\frac{C_0(t=0)}{C(t)} \tag{5.24}$$

$$e^{\frac{-4KL}{vd}}=1-\left[\frac{4V}{\pi d^2vNt}\ln\frac{C_0(t=0)}{C(t)}\right] \tag{5.25}$$

$$\ln e^{\frac{-4KL}{vd}}=\ln\left[1-\frac{4V}{\pi d^2vNt}\ln\frac{C_0(t=0)}{C(t)}\right] \tag{5.26}$$

$$-\frac{4KL}{vd}=\ln\left[1-\frac{4V}{\pi d^2vNt}\ln\frac{C_0(t=0)}{C(t)}\right] \tag{5.27}$$

$$K=\frac{vd}{4L}\ln\left[1-\frac{4V}{\pi d^2vNt}\ln\frac{C_0(t=0)}{C(t)}\right] \tag{5.28}$$

Equation (5.28) can be used to calculate the overall mass transfer coefficient (K) in the module. All the parameters in the equation can be determined experimentally.

5.3.2 Liquid Flow Once-Through Mode and Gas Flow-Through Mode

5.3.2.1 Description

Two types of experiments can be done: i) gas removal, and ii) gas absorption.

For gas removal, the experiments performed to strip dissolved gases from water (water in the lumen) by a stripping gas (N_2) in the shell side.

The other case is gas absorption where a pure gas (O_2, CO_2) is pumped in the shell side (outside) or in the lumen side (inside) of the module, and dissolved in the liquid (water). This method is widely used in bubble-free aeration.

Figure 5.4 shows the experimental set-up when liquid is flowing through the module in the lumen side and gas flow through the module in the shell side.

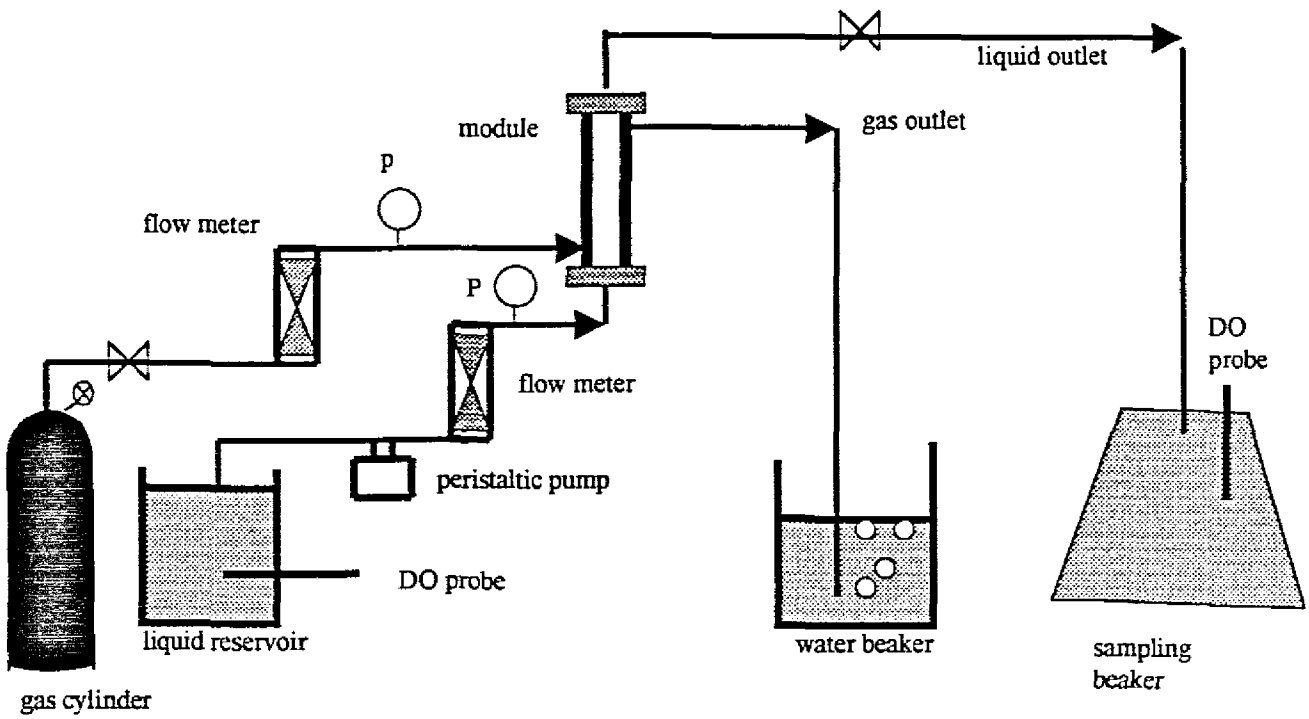

Figure 5.4: Experimental set-up for liquid and gas in flow-through mode.

5.3.2.2 Derivation of Theoretical Mass Transfer Equations

5.3.2.2.1 Removal of Gases, Co-current Flow

Mass transfer (gas removal) of solute across a single capillary can be described by the following equation (Qi and Cussler, 1985a,b; Semmens et al., 1989; Wang and Cussler, 1993):

$$\frac{dC}{dt} = -v\frac{dC}{dZ} - K_{OL}a\left(C - C^*\right) \tag{5.29}$$

K_{OL} overall mass transfer coefficient in the liquid phase [m / s]
v velocity [m / s]
a ratio of surface area to volume [m^2 / m^3]
C solute concentration in water [mg / l]
C^* equilibrium solute concentration in water [mg / l]

At steady state: $\frac{dC}{dt} = 0$

Equation (5.29) becomes:

$$v\frac{dC}{dZ} = -K_{OL}a\left(C - C^*\right) \tag{5.30}$$

The boundary condition:
$C = C_{in}$ at $Z=0$
$C = C_{out}$ at $Z=L$

A mass balance is considered over a module length from the gas input point to any cross section X in the module (see figure 5.5):

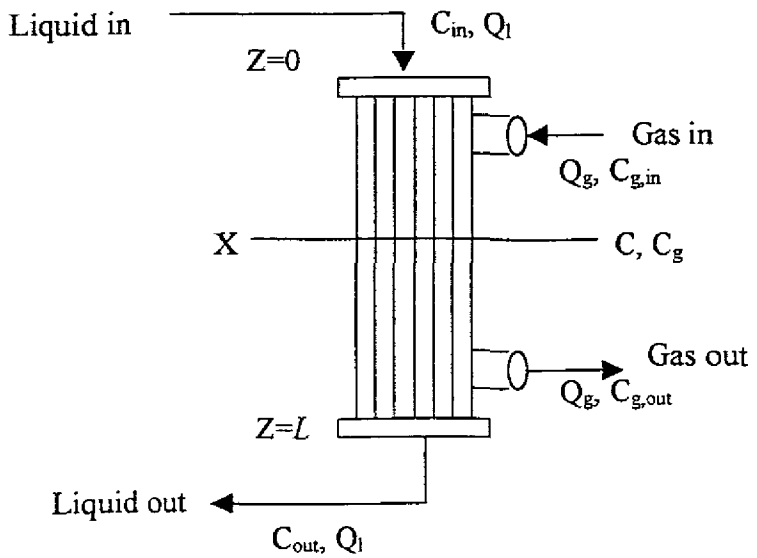

Figure 5.5: Schematic representation of liquid and gas flowing through the module for removal of gases (co-current flow).

Accumulation of solute (dissolved gas) = flow in – flow out

At steady state the accumulation equals zero.

flow in = flow out

$$Q_l C_{in} + Q_g C_{g,in} = Q_l C + Q_g C_g \tag{5.31}$$

Q_l , Q_g flow rate of the liquid and the gas respectively [m^3 / s].
C_{in}, $C_{g,in}$,C_g concentration of the solute in the liquid in, in the gas in and the gas in the section X [mg / l].

It is assumed the sweep gas in the shell side contains a negligible amount of the gas to be removed, $C_{g,in} = 0$.

$$Q_l(C_{in} - C) = Q_g C_g \Rightarrow C_g = \frac{Q_l}{Q_g}(C_{in} - C) \tag{5.32}$$

At equilibrium the concentration in the gas phase (C_g) is related to that in the aqueous phase (C^*) by Henry`s law constant (H_c).

$$H_c = \frac{C_g}{C^*} \Rightarrow C_g = H_c C^* \tag{5.33}$$

Combining equation (5.31) and (5.32):

$$H_c C^* = \frac{Q_l}{Q_g}(C_{in} - C) \Rightarrow C^* = \frac{Q_l}{Q_g H_c}(C_{in} - C) \tag{5.34}$$

Replacing C^* in equation (5.30) with equation (5.34):

$$v\frac{dC}{dZ} = -K_{OL}a\left[C - \frac{Q_l}{Q_g H_c}\left(C_{in} - C\right)\right] \tag{5.35}$$

Rearranging equation (5.35):

$$\frac{dC}{C - \frac{Q_l}{Q_g H_c}(C_{in} - C)} = \frac{-K_{OL}a}{v}dZ \tag{5.36}$$

Where $\frac{Q_l}{Q_g H_c} = R$

Therefore:

$$\frac{dC}{(1+R)C - RC_{in}} = \frac{-K_{OL}a}{v}dZ \tag{5.37}$$

Integrating equation (5.37):

$$\int_{C_{in}}^{C_{out}} \frac{dC}{(1+R)C - RC_{in}} = \frac{-K_{OL}a}{v} \int_{0}^{L} dZ \qquad (5.38)$$

$$\frac{1}{(1+R)} ln\left[(1+R)C - RC_{in}\right]\Big|_{C_{in}}^{C_{out}} = \frac{-K_{OL}aL}{v}$$

$$\frac{1}{(1+R)}\left(ln\left[(1+R)\,C_{out} - RC_{in}\right] - ln\left[(1+R)C_{in} - RC_{in}\right]\right) = \frac{-K_{OL}aL}{v}$$

$$\frac{1}{(1+R)} ln\left[\frac{(1+R)C_{out} - RC_{in}}{C_{in}}\right] = \frac{-K_{OL}aL}{v}$$

$$K_{OL} = \frac{-v}{aL}\frac{1}{(1+R)} ln\left[\frac{(1+R)C_{out} - RC_{in}}{C_{in}}\right] \qquad (5.39)$$

$$A = 2rL\pi = dL\pi \qquad (5.40)$$

A surface area [m^2]
L active length [m]
r radius [m]
d diameter [m]

$$a = \frac{4Ld\pi}{d^2 L\pi} = \frac{4}{d} \qquad (5.41)$$

$$v = \frac{4Q_l}{d^2\pi} \qquad (5.42)$$

Replacing equations (5.41) and (5.42) in equation (5.39):

$$K_{OL} = \frac{-Q_l}{dL\pi}\frac{1}{\left(1+\frac{Q_l}{Q_g H_c}\right)} ln\left[\frac{\left(1+\frac{Q_l}{Q_g H_c}\right)C_{out} - \frac{Q_l}{Q_g H_c}C_{in}}{C_{in}}\right] \qquad (5.43)$$

Equation (5.43) can be used to calculate the overall mass transfer coefficient based on the liquid phase, all variables in equation (5.43) can be determined experimentally.

5.3.2.2.2 Removal of dissolved Gases, Counter-current Flow

An equation was derived for mass transfer (gas removal) when liquid and gas are flowing counter-currently in through-mode.

A mass balance is considered over a module length from the gas input point to any cross section X in the module (see Figure 5.6):

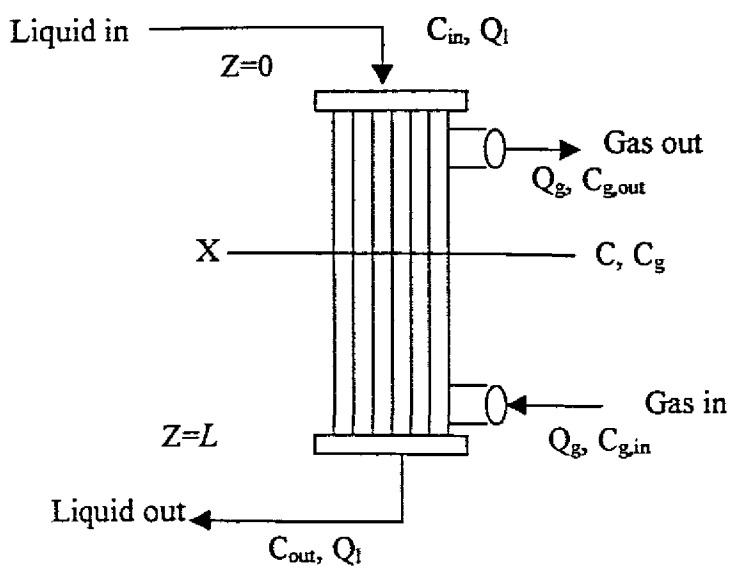

Figure 5.6: Schematic representation of liquid and gas flowing through the module for removal of gases (counter-current flow).

Accumulation of solute (dissolved gas) = flow in – flow out

At steady state the accumulation equals zero.

flow in = flow out

$$Q_l C + Q_g C_{g,in} = Q_l C_{out} + Q_g C_g \tag{5.44}$$

Q_l , Q_g flow rate of the liquid and the gas respectively [m^3 / s].

C_{in}, $C_{g,in}$, C_g concentration of the solute in the liquid in, in the gas in and the gas in the section X [mg / l].

It is assumed the sweep gas on the shell side contains a negligible amount of the gas to be removed, $C_{g,in}$ =0

$$Q_l(C - C_{out}) = Q_g C_g \Rightarrow C_g = \frac{Q_l}{Q_g}(C - C_{out}) \tag{5.45}$$

Henry`s constant H_c:

$$H_c = \frac{C_g}{C^*} \Rightarrow C_g = H_c C^* \tag{5.33}$$

Combining equation (5.45) and (5.33):

$$H_c C^* = \frac{Q_l}{Q_g}(C - C_{out}) \Rightarrow C^* = \frac{Q_l}{Q_g H_c}(C - C_{out}) \tag{5.46}$$

Replacing C^* in equation (5.30) with equation (5.46):

$$v\frac{dC}{dZ} = -K_{OL}a\left[C - \frac{Q_l}{Q_g H_c}(C - C_{out})\right] \tag{5.47}$$

Rearranging equation (5.47):

$$\frac{dC}{C-\frac{Q_l}{Q_g H_c}\left(C-C_{out}\right)}=\frac{-K_{OL}a}{v}dZ \qquad (5.48)$$

Where $\frac{Q_l}{Q_g H_c}=R$

Therefore:

$$\frac{dC}{(1-R)C-RC_{out}}=\frac{-K_{OL}a}{v}dZ \qquad (5.49)$$

Integrating equation (5.49):

$$\int_{C_{in}}^{C_{out}}\frac{dC}{(1-R)C+RC_{out}}=\frac{-K_{OL}a}{v}\int_{0}^{L}dZ \qquad (5.50)$$

$$\frac{1}{(1-R)}\ln\left[(1-R)C+RC_{out}\right]\Big|_{C_{in}}^{C_{out}}=\frac{-K_{OL}aL}{v}$$

$$\frac{1}{(1-R)}\left[\ln\left[(1-R)C_{out}+RC_{out}\right]-\ln\left[(1-R)C_{in}+RC_{out}\right]\right]=\frac{-K_{OL}aL}{v}$$

$$\frac{1}{(1-R)}\left[\ln C_{out}-\ln\left[(1-R)C_{in}+RC_{out}\right]\right]=\frac{-K_{OL}aL}{v}$$

Replacing equations (5.41) and (5.42) in equation (5.51):

$$\frac{1}{(1-R)} ln\left[\frac{C_{out}}{(1-R)C_{in}+RC_{out}}\right] = \frac{-K_{OL}aL}{v}$$

$$K_{OL} = \frac{-v}{aL}\frac{1}{(1-R)} ln\left[\frac{C_{out}}{(1-R)C_{in}+RC_{out}}\right] \qquad (5.51)$$

$$K_{OL} = \frac{-Q_l}{dL\pi}\frac{1}{\left(1-\frac{Q_l}{Q_g H_c}\right)} ln\left[\frac{C_{out}}{\left(1-\frac{Q_l}{Q_g H_c}\right)C_{in}+\frac{Q_l}{Q_g H_c}C_{out}}\right] \qquad (5.52)$$

Equation (5.52) can be used to measure the overall mass transfer coefficient based on the liquid phase; all the variables in equation (5.52) can be measured experimentally.

5.3.2.2.3 Absorption of Gases, Counter-current Flow

The derivation of the mass transfer equation for gas absorption (the gas and liquid are in counter-current mode) is described below.

A mass balance is considered over a module length from the gas input point to any cross section X of the module (see Figure 5.7):

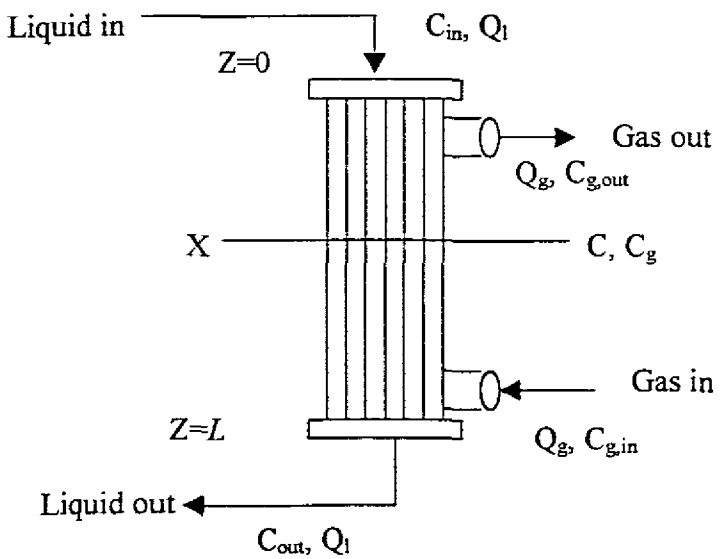

Figure 5.7: Schematic representation of liquid and gas flowing through the module for absorption of gases (counter-current flow).

Accumulation of solute = flow in – flow out

At steady state the accumulation equal zero.

flow in = flow out

$$Q_l C + Q_g C_{g,in} = Q_l C_{out} + Q_g C_g \tag{5.53}$$

$$Q_l (C - C_{out}) = Q_g (C_g - C_{g,in}) \tag{5.54}$$

Henry`s constant H_c:

$$H_c = \frac{C_g}{C^*} \Rightarrow C_g = H_c C^* \tag{5.33}$$

Replacing C_g in equation (5.54) with equation (5.33):

$$H_c C^* - C_{g,in} = \frac{Q_l}{Q_g}(C - C_{out}) \Rightarrow C^* = \frac{Q_l}{Q_g H_c}(C - C_{out}) + \frac{C_{g,in}}{H_c} \tag{5.55}$$

Replacing C^* in equation (5.30) with equation (5.55):

$$v\frac{dC}{dZ} = -K_{OL}a\left[C - \frac{Q_l}{Q_g H_c}(C - C_{out}) - \frac{C_{g,in}}{H_c}\right] \tag{5.56}$$

Rearranging equation (5.56):

$$\frac{dC}{C - \frac{Q_l}{Q_g H_c}(C - C_{out}) - \frac{C_{g,in}}{H_c}} = \frac{-K_{OL}a}{v}dZ \tag{5.57}$$

Where $\frac{Q_l}{Q_g H_c} = R$

Therefore:

$$\frac{dC}{(1-R)C + RC_{out} - \frac{C_{g,in}}{H_c}} = \frac{-K_{OL}a}{v}dZ \tag{5.58}$$

Integrating equation (5.58):

$$\int_{C_{in}}^{C_{out}} \frac{dC}{(1-R)C + RC_{out} - \frac{C_{g,in}}{H_c}} = \frac{-K_{OL}a}{v}\int_0^L dZ \tag{5.59}$$

$$\frac{1}{(1-R)}\ln\left[(1-R)C+RC_{out}-\frac{C_{g,in}}{H_c}\right]\Bigg|_{C_{in}}^{C_{out}}=\frac{-K_{OL}aL}{v}$$

$$\frac{1}{(1-R)}\left[\ln\left[(1-R)C_{out}+RC_{out}-\frac{C_{g,in}}{H_c}\right]-\ln\left[(1-R)C_{in}+RC_{out}-\frac{C_{g,in}}{H_c}\right]\right]=\frac{-K_{OL}aL}{v}$$

$$\frac{1}{(1-R)}\ln\left[\frac{(1-R)C_{out}+RC_{out}-\frac{C_{g,in}}{H_c}}{(1-R)C_{in}+RC_{out}-\frac{C_{g,in}}{H_c}}\right]=\frac{-K_{OL}aL}{v}$$

$$\frac{1}{(1-R)}\ln\left[\frac{C_{out}-\frac{C_{g,in}}{H_c}}{(1-R)C_{in}+RC_{out}-\frac{C_{g,in}}{H_c}}\right]=\frac{-K_{OL}aL}{v}$$

$$\frac{1}{\left(1-\frac{Q_l}{Q_gH_c}\right)}ln\left[\frac{C_{out}-\frac{C_{g,in}}{H_c}}{C_{in}-\frac{1}{H_c}\left[\frac{Q_l}{Q_g}(C_{in}-C_{out})+C_{g,in}\right]}\right]=\frac{-K_{OL}aL}{v}$$

$$\frac{1}{\left(1-\frac{Q_l}{Q_gH_c}\right)}ln\left[\frac{C_{out}-C_2^*}{C_{in}-C_1^*}\right]=\frac{-K_{OL}aL}{v} \qquad (5.60)$$

$$K_{OL}=\frac{-v}{aL}\frac{1}{\left(1-\frac{Q_l}{Q_gH_c}\right)}ln\left[\frac{C_{out}-C_2^*}{C_{in}-C_1^*}\right] \qquad (5.61)$$

Replacing equation (5.41) and (5.42) in equation (5.61):

$$K_{OL} = \frac{-Q_l}{dL\pi} \frac{1}{\left(1 - \frac{Q_l}{Q_g H_c}\right)} ln\left[\frac{C_{out} - C_2^*}{C_{in} - C_1^*}\right] \qquad (5.62)$$

Equation (5.62) can be used to measure the overall mass transfer coefficient based on the liquid phase in the case of absorption in counter-current models. All the parameters in equation (5.62) can be determined experimentally.

CHAPTER 6
MASS TRANSFER COEFFICIENTS MEASUREMENTS, RESULTS AND DISCUSSIONS

6.1 CONTACT AREA BETWEEN GAS AND LIQUID PHASES

In gas-liquid contactors when two phases are involved, the liquid is in direct contact with gas, and it is difficult to define and to measure the contact area. In three-phase membrane contactors, when a porous membrane is used, the question arises as to which area should be taken as the contact area between the gas and liquid phases: the open pore area, or the total membrane surface area.

According to Kreulen et al. (1993b), a very thin liquid layer adjacent to the membrane surface can be considered as having a homogeneous concentration of the gas. Diffusion of the gas into the flowing liquid takes place from this layer. Therefore the total membrane area can be used as the interfacial area through which the transport takes place in both the flat-sheet and capillary configuration.

6.2 MASS TRANSFER IN FLAT-SHEET MEMBRANES

Mass transfer in flat-sheet membranes was investigated using the diaphragm-cell method. The flat-sheet membrane is manufactured by wet-phase inversion whereby a polymer (polysulphone) solution is cast upon a reinforcing fabric, and quenched in water (Malherbe et al., 1995). Figure 6.1 shows a structure of the flat-sheet membrane. The morphology of the flat-sheet polysulphone membrane used in the experiments differs from the internally skinned capillary polysulphone membrane. The internally skinned capillary has a unique structure where there is a skin layer in the inside (lumen) and a microvoid structure in the outside with no skin, as described in Section 3.5. This morphology did not occur when membranes were cast in flat-sheet form, that is, either on a glass plate or on a non-woven fabric carrier (Jacobs and Sanderson, 1997).

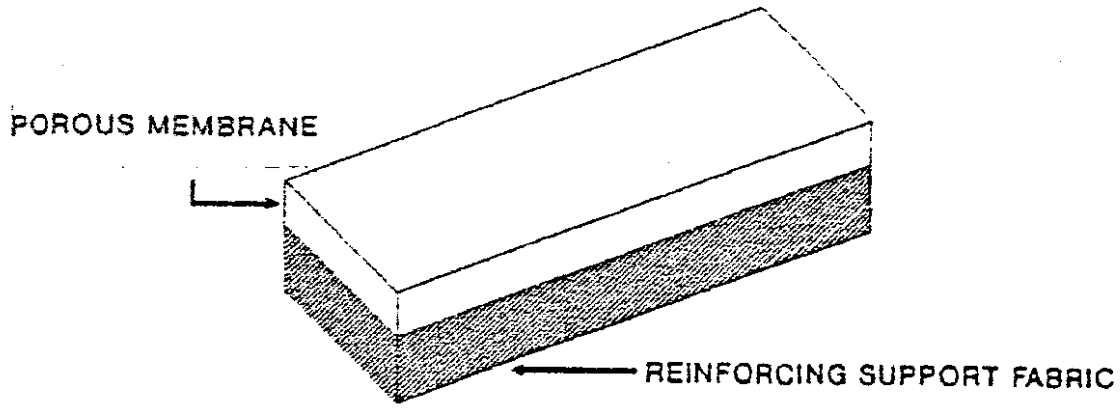

Figure 6.1: Flat sheet polysulphone membrane.

6.2.1 Objectives

The primary objectives of this study are thus:

1) To establish a method to measure mass transfer of gases across a flat-sheet polysulphone membrane.
2) To establish a simple method to test any new polymer with an unknown mass transfer coefficient for gases to be used as gas-liquid contactors, and to test the feasibility before building any module.
3) The flat- sheet configuration is the simplest and is adequate to study mass transfer of gases across membranes and into or out of the biofilm. The advantages of using flat-sheet membranes for mass transfer study on biofilm are:
    i) flat-sheet is easy to fabricate and the cell-test easy to manipulate;
    ii) the growth of the biofilm is simpler on flat-sheets than in capillaries;
    iii) the possibility exists to measure the thickness of the biofilm;
    iv) the study of mass transfer of gases in a membrane bio-reactor can be separated: mass transfer in the bare membrane and mass transfer in the biofilm, specially when the module is complex. In the case of biofilm, we

can use any adequate support. Adequate means high enough permeability to nutrient and oxygen;

v) from the flat-sheet membrane experiments, a correlation between the thickness of the biofilm and oxygen consumption can be found. Using this correlation together with knowledge of the OUR (oxygen utilization rate) we can predict oxygen consumption, knowing the thickness of the biofilm in any module;

vi) if the diffusion rate in a bare membrane is known, its effect on the membrane bio-reactor (membrane + biofilm) can be evaluated.

6.2.2 Experimental Set-Up

The diaphragm-cell used in the experiments has two chambers separated by the membrane to be studied. The lower compartment of the cell was filled with the solvent (water) and the solute (dissolved oxygen). The water was first saturated with oxygen in a beaker outside the cell, after which the saturated water was pumped into the cell. When the lower compartment was full, the appropriate membrane was clamped between the two chambers. Then the upper compartment was filled with the reactive solution. For oxygen scavenging the reactive solution used was sodium sulfite (Na_2SO_3), catalyzed by cobalt nitrate (Co (II) $(NO_3)_2$). The aim of using a reactive solution is to maintain in the upper compartment zero concentration of dissolved oxygen transferred through the membrane from the lower compartment. This arrangement maximises the driving force across the membrane. Table 6.1 gives different reactive solutions for different solutes (gases dissolved in water). The two chambers were well stirred, the lower compartment was stirred magnetically, while the upper compartment was stirred mechanically. The concentration of oxygen in the upper compartment equals zero according to the following reaction (Waters, 1948; Alexander and Fleming, 1981).

$$2\ Na_2SO_3 + O_2 \xrightarrow{Co\ (II)\ (NO_3)_2} 2\ Na_2\ SO_4$$

After a desired period, the contents of the lower compartment were pumped into the sampling cell, and the concentration of dissolved oxygen was measured. The sampling cell was at all times closed to the atmosphere, and before the liquid was transferred, vacuum was applied to remove air from the cell. The concentration of dissolved oxygen before and after the experiment was measured using an oxygen probe (YSI 55 dissolved oxygen). Figure 6.2 shows the experimental set-up.

Table 6.1: Reactive solutions for different solutes in water

Solute	O_2	CO_2	H_2S	SO_2	NH_3
Reactive Solution	$Na_2SO_3/Co(II)(NO_3)_2$ (a)	NaOH (b)	NaOH (c)	NaOH (d)	H_2SO_4 (e)

(a) Waters, 1948; Alexander and Fleming, 1981;
(b) Qi and Cussler, 1985b; Geuzens et al., 1990; Kreulen et al., 1993b;
(c) Qi and Cussler, 1985a; Kreulen et al., 1993b;
(d) Qi and Cussler, 1985a,b; and
(e) Qi and Cussler, 1985b; Kreulen et al., 1993a.

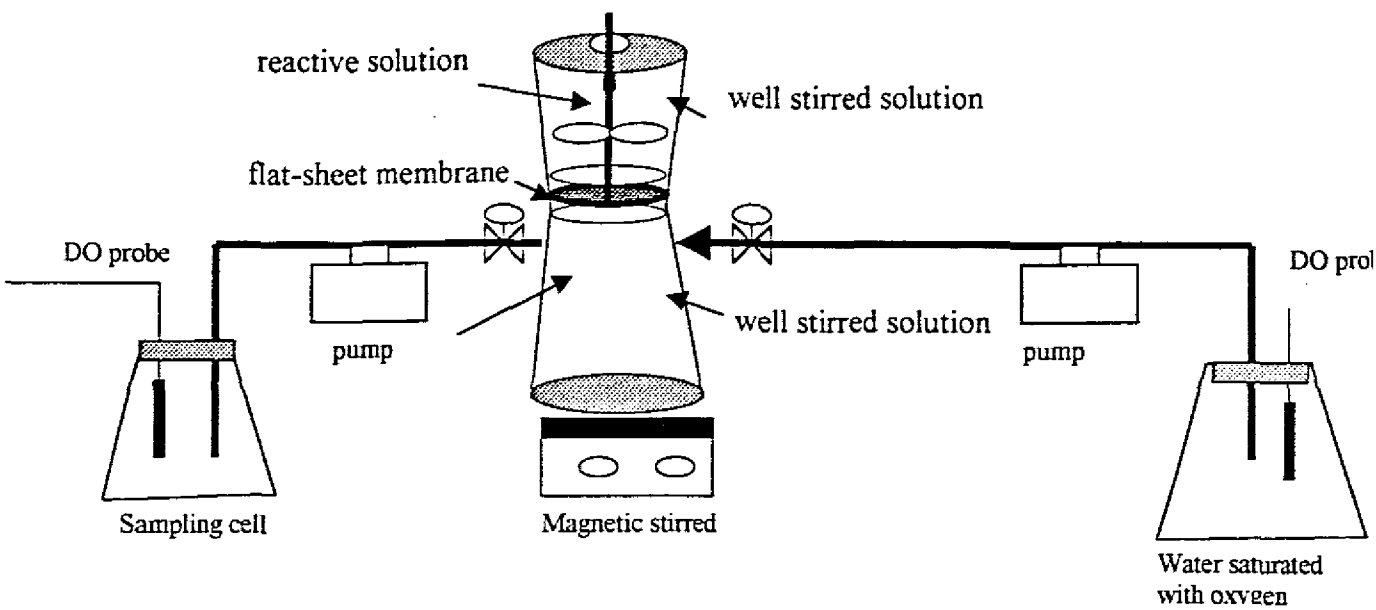

Figure 6.2: Diaphragm-cell experiment.

The characteristics of the cell are summarized in table 6.2.

Table 6.2: Characteristics of the cell

V_{lower} [ml]	V_{upper} [ml]	Reactive solution	ID [mm]
350	250	$Na_2SO_3/Co(II)(NO_3)_2$	39.2

Using equation (5.14) the mass transfer coefficient in flat-sheet membranes was calculated using the data obtained during the experiments.

6.2.3 Alternative Methods to measure residual oxygen in the lower compartment

The above method used a dissolved oxygen probe to measure oxygen concentrations. Two other methods of measuring gas concentrations in studying mass transfer of gases in flat-sheet membranes are: the manometric method and the gas chromatographic method. These methods also employ cells with two compartments, but the difference is that in these methods at least one compartment is gas filled, whereas in the diaphragm-cell both compartments are liquid filled.

6.2.3.1 Manometric Methods

The membrane is mounted between two chambers. One side is pressurized with the test gas and the other side is evacuated. The diffusion rate through the membrane is determined by measuring change in the capillary pressure (ASTM, 1988). This manometric method is also referred to as the Dow cell (McHugh and Krochta, 1994a). There is a similar method called Linde cell, the difference from the Dow cell is the pressure in the lower compartment is maintained near atmospheric pressure and the diffusion of the gas through the membrane is indicated by a change in volume (ASTM, 1988). Kreulen et al. (1993a) used a manometric method, but in their approach the lower compartment was filled with a stripping solution, and the experiments were conducted with batch-operated gas.

6.2.3.2 Gas Chromatography

Several gas chromatographic methods have been established for determining gas permeability (Karel et al., 1963; Gilbert and Pegaz, 1969; Davis and Huntington, 1977; Baner et al., 1986; McHugh and Krochta, 1994b). This method is based on measurement of the amount of gas diffusing through the membrane over time. The test cell consisted of two chambers separated by the membrane to be tested. Both chambers had an inlet and an outlet for gas flushing. The lower test compartment was also equipped with a sampling port. A stream of test gas (O_2, CO_2, etc.) was passed through the upper compartment of the cell, while the lower compartment was sealed. At suitable intervals, gas samples were withdrawn from the lower compartment and analyzed by gas chromatography. To avoid total pressure changes, 1 cm^3 of nitrogen was injected into the lower compartment before each sample was withdrawn.

6.2.3.3 Method of Choice

Clearly the method devised in the equipment illustrated in Figure 6.2 provides a much simpler but also effective method of measuring gas concentrations on either side of the membrane. This was the method of choice. The two alternative methods described in the literature were not considered.

6.2.4 Oxygen Mass Transfer in Flat-Sheet Polysulphone Membrane

To measure the mass transfer coefficient of oxygen in flat-sheet polysulphone the experiment was conducted as cited earlier (Section 6.2.2). The lower compartment was filled with distilled water at a known concentration of oxygen. The upper compartment was filled with the reactive solution (sodium sulfite catalyzed by cobalt nitrate); the concentration of Na_2SO_3 was 0.25 N. The experiment was conducted with an agitation rate of 200 rpm in both chambers. The concentration of oxygen in the lower compartment was measured in 3 separated runs of duration 10 min, 20 min and 30 min . The results are represented in Table 6.3 and Figure 6.3.

Table 6.3: Oxygen mass transfer coefficient in flat-sheet polysulphone

time (min)	*C(0,lower) (mg/l)*	*C(t,lower) (mg/l)*	*K, 10^{-4} (m/s)*
10	9.80	5.19	3.1
15	9.61	3.7	3.1
30	10.00	1.6	3.0

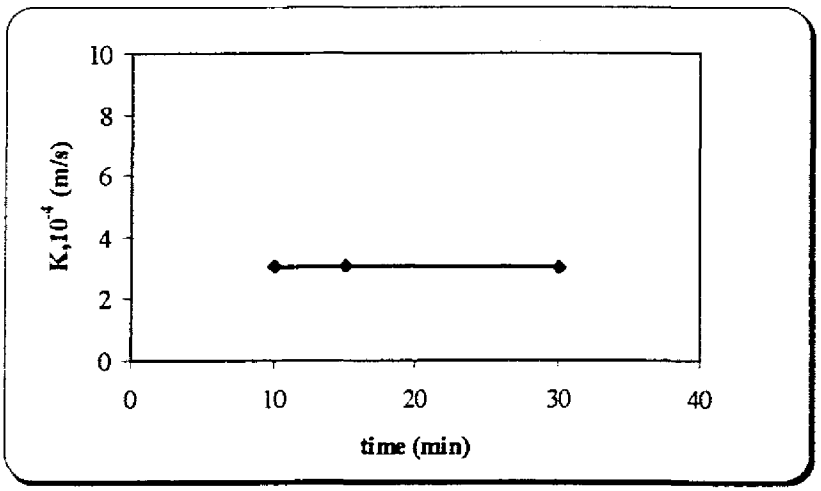

Figure 6.3: Mass transfer coefficient for oxygen in flat-sheet polysulphone.

To analyse these results, the logarithm of concentrations is plotted as a function of time (Ln [C(t=0) / C(t)] vs. time (min)). Equation (5.14) predicts that the logarithm of the measured concentration difference in the cell should vary linearly with time. This prediction is supported by the data in Figure (6.4).

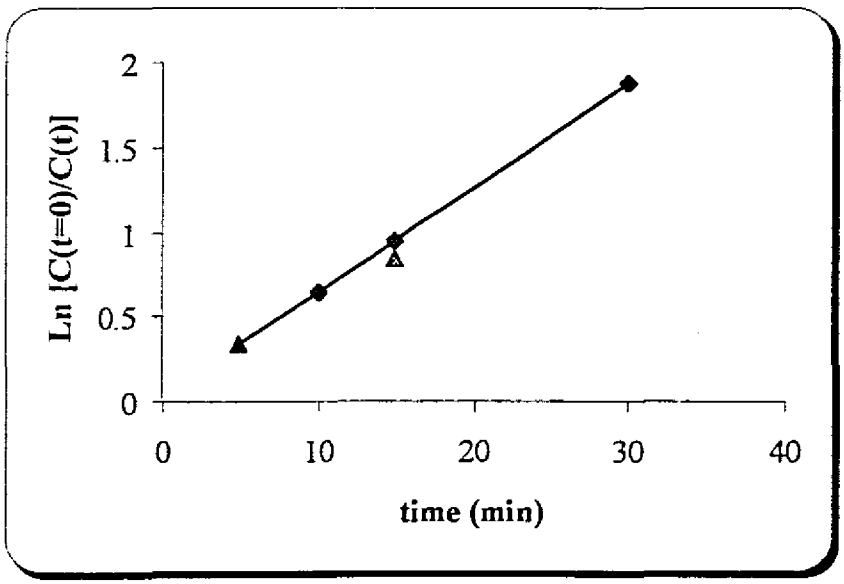

Figure 6.4: Logarithm of the measured concentration difference in the diaphragm-cell method vs. time

◊: the measured concentration difference at duration of 10,15,30 min

Δ: comparison of concentration difference between 3 experiments (10-15 min), (15-30 min)

For 5, 10, 15 and 30 min the variation is linear, but between 15-30 min, it was expected that the calculation would give the same value as for 15 min; it was not the case. We can conclude that the variation in this experiment is about 10%. This variation is due to the sensitivity of the oxygen electrode and also due to the difficulty of measuring the oxygen concentration in the cell. Therefore, for the use of this data, values of mass transfer coefficient rounded off to of 3×10^{-4} (m/s) are recommended.

6.2.5 Effect of Agitation on Mass Transfer

To determine the effect of agitation on mass transfer, it was necessary to repeat the experiments at different agitation rates (0, 200, 300, 600 rpm) in both sides. The duration of the experiments was 10 min, and the concentration of the reactive solution (Na_2SO_3) was 0.25 N, with the catalyst Co(II) $(NO_3)_2$ present. The results are represented in Figure 6.5. Values of the experimental parameters are listed in Appendix A (Table A.12).

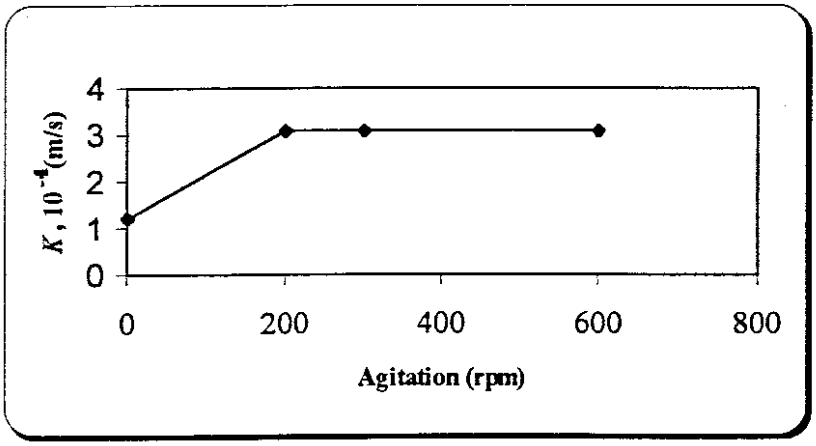

Figure 6.5: Effect of agitation on mass transfer of oxygen in flat-sheet polysulphone.

The mass transfer coefficient was 1.2×10^{-4} (m/s) with no agitation. After an agitation with the speed of 200 rpm, the mass transfer coefficient increased to 3.1×10^{-4} (m/s). That was expected, because with the agitation, the boundary layer in the liquid phase is reduced, this layer became thinner with agitation, so the resistance is reduced, the mass transfer coefficient increased. Above 200 rpm, the variation is very small, and can be neglected. This value of agitation reduces the resistance in the boundary layer, and it is assumed there is no resistance in the liquid phase and the only resistance is in the membrane. Geuzen et al. (1990) studied CO_2 absorption in an aqueous solution of NaOH using a flat porous teflon membrane. They found that the resistance was only in the membrane.

In all our the experiments an agitation rate of 200 rpm was chosen.

6.2.6 Effect of the Concentration of the Reactive Solution on Mass Transfer

The experiments were to determine if the concentration of the reactive solution has an effect on the rate of diffusion or on the reliability of the experimental techniques. The concentration of the reactive solution (Na_2SO_3) was varied from 0.25N to 2N (0.25N, 0.5N, 1N, 2N) in this study, and the stirring speed was kept at 200 rpm in both compartments. The duration of the experiments was 10 min.

The results are represented in Figure 6.6. Values of the experimental parameters are listed in Appendix A (Table A.14).

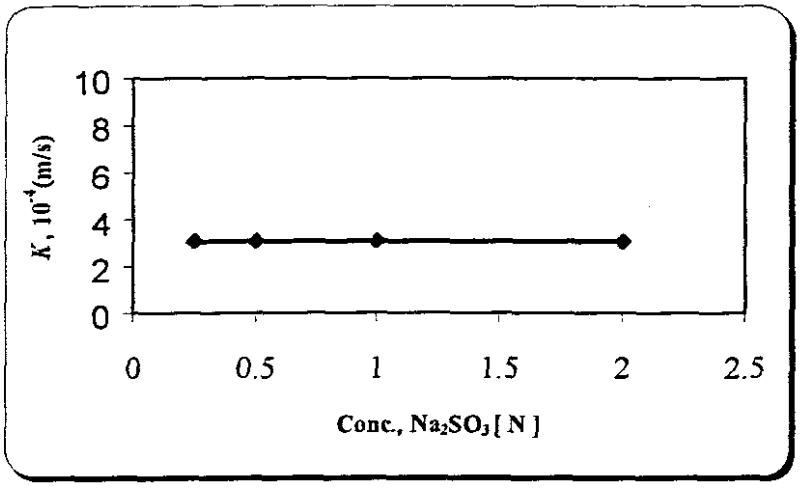

Figure 6.6: Mass transfer coefficients of oxygen vs. reactive solution (Na_2SO_3) concentration.

Figure 6.6 indicates that the mass transfer coefficients fall on a horizontal line. The concentration of the reactive solution (Na_2SO_3) has no effect on mass transfer of oxygen. This means that a concentration of Na_2SO_3 equal to 0.25 N is adequate to remove all oxygen present in the upper compartment. Also it indicates that no reverse flow of reactive solution occurred at any point in the experiment.

6.2.7 Effect of the Thickness of the Membrane on Mass Transfer

The effect of the thickness of the membrane on mass transfer was also investigated. The experiment was conducted by clamping several membranes together, the stirring speed was 200 rpm on both sides of the membrane, and the concentration of the reactive solution (Na_2SO_3) was 0.25 N; the duration of the experiment was 10 min.

The results are represented in Figure 6.7. Values of the experimental parameters are listed in Appendix A (Table A.13).

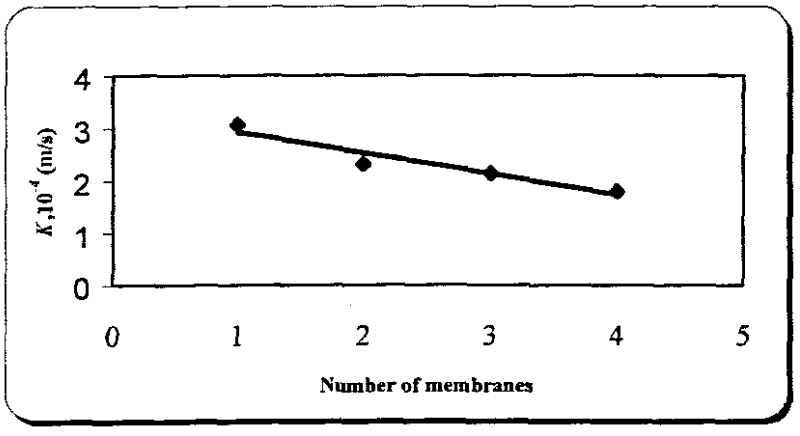

Figure 6.7: *Mass transfer coefficient of oxygen vs. membrane thickness.*

From the above graph it may be deduced that: mass transfer coefficient is inversely proportional to membrane thickness. This further also confirming that the resistance to mass transfer is located only in the membrane. The thicker the membrane, the greater the resistance to mass transfer.

6.3 CAPILLARY MEMBRANE EXPERIMENTS

Mass transfer of oxygen and carbon dioxide was investigated in a skinless polysulphone membrane described in Section 3.5. Oxygenation, deoxygenation, carbonation and decarbonation experiments were conducted in axial-flow module. In all the experiments the liquid (distilled water) was flowing through the capillary lumen without recycle. The gas was flowing through the extra-capillary space of the module. The Gradostat membrane bio-reactor operates in a similar mode, where the substrates (nutrients) were fed into the lumen, and gas (pure oxygen or air) was fed into the shell side (see Chapter 3, Section 3.4).

The axial-flow module resembles a small shell-and-tube type heat exchanger. A bundle of 8 skinless polysulphone capillary membranes, 30 cm long, where potted with epoxy resin into a glass-shroud. The effective membrane length was 22 cm. This module has a surface area of 7.73×10^{-3} m^2. The axial-flow module rather than the transverse-flow module was chosen because the overall mass transfer coefficient is higher in transverse-flow than in an axial-flow modules. The experiments were therefore conducted with a module that has the higher resistance to mass transfer of gases.

In this study, the following was investigated:

1) the difference between using sweep gas and vacuum;
2) the relative rates of diffusion in co-current mode and counter-current mode;
3) determination of which phase (gas, membrane or liquid) is controlling the diffusion;
4) oxygen and carbon dioxide removal;
5) oxygen and carbon dioxide absorption;
6) comparison between oxygen absorption using air or pure oxygen;
7) comparison between oxygenation and carbonation; and
8) determination of dimensionless mass transfer correlation.

6.3.1 Gas Removal

These experiments employed a stripping gas (N_2) to remove dissolved gases from water. The experiments included deoxygenation and decarbonation. Bubbling the specific gas in a distilled water reservoir saturated the water. The saturated water containing oxygen or carbon dioxide, was pumped from a reservoir into the lumen of the capillary membranes (see Figure 5.4). The sweep gas (nitrogen) used as purge gas was introduced into the shell side of the module (on the outside of the capillaries). The water (in the lumen) and gas (in the shell) were flowing through the module in one pass. The flow rate of the liquid was varied using a peristaltic pump. A needle valve controlled the flow rate of the gas. The flow rates of the liquid and the gas were monitored with flow meters. Also the pump used

(type MCP having 4 channels) controlled the flow rate of the liquid by giving a direct reading. The gas outlet was submerged in a water beaker to ensure that the air does not dilute oxygen on the shell side, and the outlet was open to atmosphere, to ensure that the pressure of the gas was held constant at atmospheric pressure.

The concentration of oxygen in the water before entering the module and thereafter was measured using an online oxygen electrode. These measurements were taken only when the module was operating in steady state, and the run times were long enough to ensure that the response time of the oxygen electrode did not influence the data collected. When running the experiment, it was observed that 30 min had to be allowed for the system to equilibrate after changes were made to the liquid flow rate.

The concentration of carbon dioxide in water was measured by back titration. Samples were also taken before the water entered into the module and thereafter. Back titration was conducted by mixing the sample with a known concentration of NaOH solution, then titrating the remaining base (NaOH) with standard HCl solution, using phenolphthalein as indicator (Snell and Hilton, 1966; Yang and Cussler, 1986).

The concentrations of dissolved gas in and out of the module were then used to calculate the overall mass transfer coefficient using equation (5. 43) and (5.52) for co-current and counter-current modes of flow, respectively.

6.3.2 Gas Absorption

Oxygenation and carbonation are processes where gases are added to water. The experiment set-up is the same as was used for gas removal (Figure 5.4). The pure gas to be absorbed (oxygen or carbon dioxide) is introduced into the shell side of the module. The gas was supplied from a gas cylinder, a control valve was used to control the flow rate of the gas. The outlet of the gas was submerged in a water beaker. Distilled water was fed into the lumen of the module by a peristaltic pump, the flow rate of the water was controlled by the same pump, and the flow rate of the gas was monitored with a variable

area flow meter. The distilled water was used as is. The concentration of the desired gas in water was measured before entering the module and after the module. Equation (5.62) was used to calculate the overall mass transfer coefficient.

6.3.3 Comparison Between using Sweep Gas and Vacuum

Gas removal with hollow fibre membranes can be achieved by flowing the liquid, which contains the target dissolved gas, along the lumen of the module, and a stripping gas (nitrogen) along the shell side. Yang and Cussler (1986), Bessarabov et al. (1996) and Ito et al. (1998) applied a vacuum to the shell side to purge the gas. An experiment was conducted to investigate the difference between using nitrogen or vacuum on the shell side.

Deoxygenation: First, a solution of distilled water with a known oxygen concentration was pumped into the lumen of the module, and sweep gas nitrogen was introduced into the shell side. In this experiment oxygen is diffusing from the liquid bulk (distilled water) to the surface of the membrane, then through the membrane into the shell side, where the sweep gas (nitrogen) entrains it. The concentration of dissolved oxygen in the liquid upstream and downstream of the module was measured for different liquid flow rates.

A vacuum was applied to the shell side instead of the sweep gas (nitrogen), and the concentration of dissolved oxygen in the liquid upstream and downstream of the module was measured at different liquid flow rates. The results are plotted as the ratio of the oxygen concentration in the liquid into and out of the module versus the liquid flow rate in Figure 6.8.

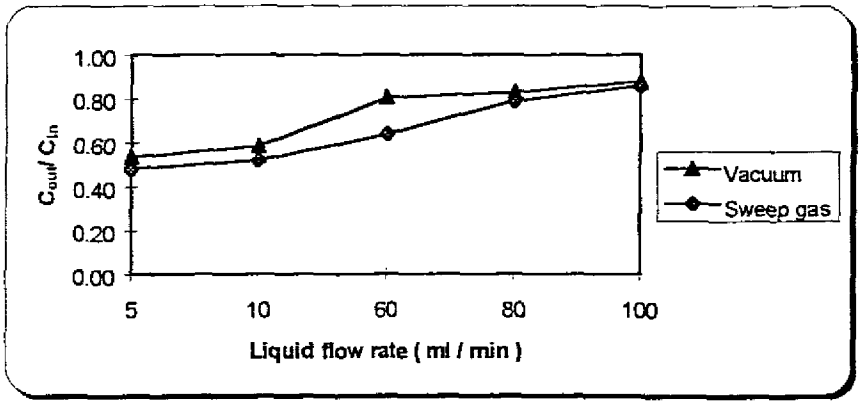

Figure 6.8: Comparison between sweep gas or vacuum in the shell side during deoxygenation.

From Figure 6.8, we can see that applying sweep gas (nitrogen) gave almost the same results as applying vacuum in the shell side. The objective is to remove the dissolved oxygen from water and to avoid concentration polarization on the outside of the membrane; the results show that either sweep gas or vacuum can achieve that. This indicates that the assumption of negligible gas phase resistance is valid.

6.3.4 Phase Controlling Mass Transfer

The resistances to mass transfer in three-phase contactors are in the gas boundary layer, membrane and liquid boundary layer. A deoxygenation of water experiment was conducted to determine which phase is rate controlling. The liquid was fed into the lumen of the module at a constant flow rate of 1.1×10^{-6} (m^3/s). The sweep gas (nitrogen) was fed into the shell side in counter-current mode. The volumetric flow rate of the gas nitrogen was varied between 44.5×10^{-6} and 100×10^{-6} (m^3/s). The concentration of dissolved oxygen was measured upstream and downstream of the module. Using equation (5.52), the overall mass transfer coefficients were calculated. The results are represented by the overall mass transfer coefficients versus the gas flow rates in Figure 6.9.

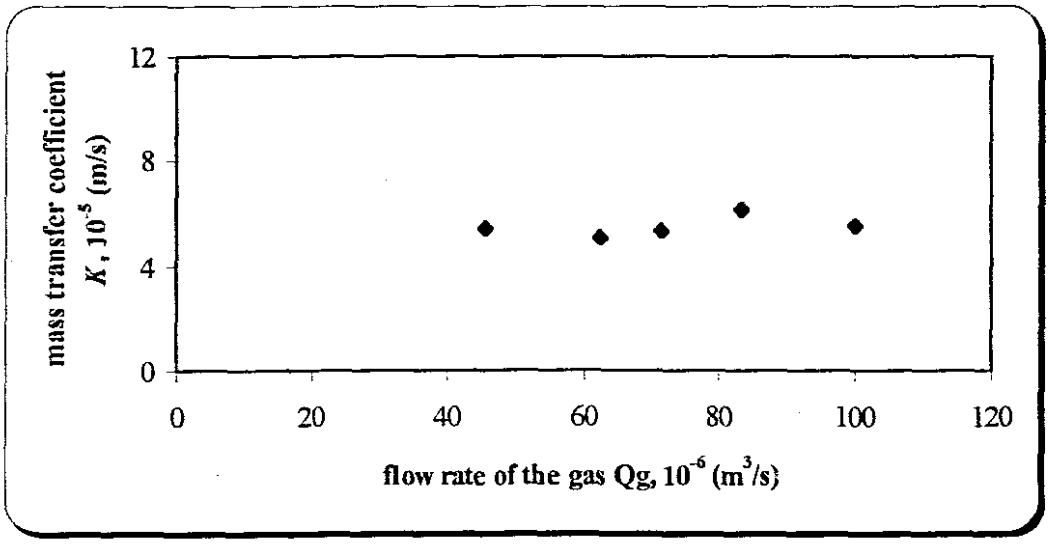

Figure 6.9: The overall mass transfer coefficient vs. Flow rate of the gas (Q_g).

The overall mass transfer coefficient does not vary with the variation of the flow rate of the gas. That means that the resistance in the gas boundary layer is negligible. The gas phase is not rate controlling, and the rate of diffusion is controlled by the two other resistances (membrane and liquid boundary layer).

6.3.5 Comparison between Co-Current and Counter-Current

To compare overall mass transfer coefficient between the liquid and gas when flowing co-currently or counter-currently, an experiment for oxygen removal (see Section 6.3.1) was conducted. Distilled water with a known oxygen concentration was pumped into the lumen at different flow rates between 16.66×10^{-8} (m^3/s) and 166.66×10^{-8} (m^3/s). The sweep gas nitrogen flow rate was kept constant with the value of 48.7×10^{-6} (m^3/s) and 47.6×10^{-6} (m^3/s) for co-current and counter-current, respectively. These two values are in the range tested in Section (6.3.4) where the flow rate of the gas did not influence the overall mass transfer coefficient in this range. The concentration of dissolved oxygen was measured before entering the module and after, using an oxygen electrode. The overall mass transfer coefficient was calculated using equation (5.43) and (5.52) for co-current and counter-current modes, respectively. Figure 6.10 represents the results where the

overall mass transfer coefficient was plotted as Sherwood number (equation 4.19) versus the velocity as Reynolds numbers (equation 4.21).

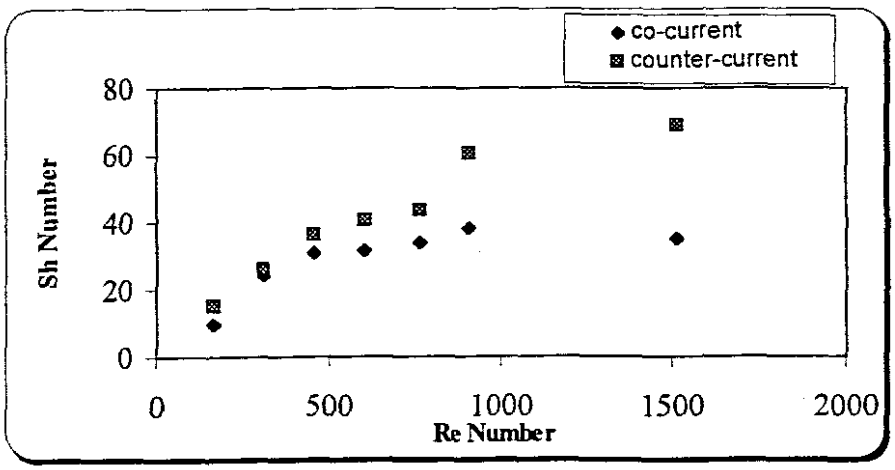

Figure 6.10: Comparison between co-current and counter-current modes for deoxygenation.

The mass transfer rate was found to be higher in counter-current than in co-current mode. These results were expected, because the overall effect in counter-current operations is better than in co-current, as is well known in unit operation processes. The remainder of the experiments were conducted in counter-current mode.

6.3.6 Mass Transfer Coefficient in Skinless Polysulphone Capillary Membranes

Oxygenation, deoxygenation, carbonation and decarbonation experiments were conducted. The oxygenation and carbonation experiments were conducted as in gas absorption (Section 6.3.2). The deoxygenation and decarbonation were conducted as in gas removal (Section 6.3.1). In all these experiments the gas and liquid flows were in counter-current mode. The gas was on the shell side and the liquid on the lumen side. The flow rate of the gas was kept constant, while the flow rate of the liquid was varied. Equation (5.52) was used to calculate the overall mass transfer coefficient for gas removal (deoxygenation and decarbonation). Equation (5.62) was used to calculate the overall mass transfer coefficient for gas absorption (oxygenation and carbonation). The

overall mass transfer coefficient was plotted as a function of velocity. The detailed results are in Appendix A.

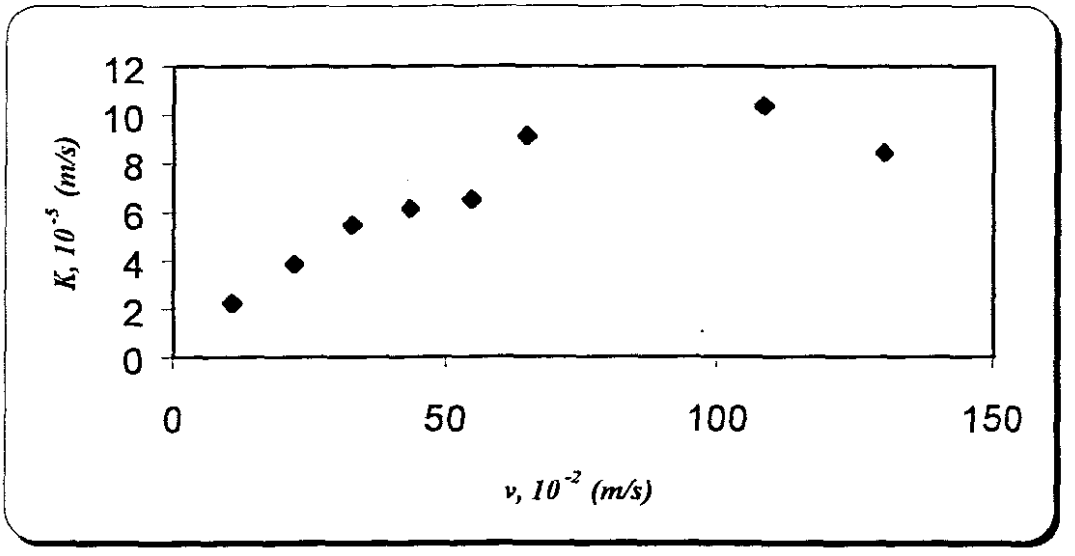

Figure 6.11: The overall mass transfer coefficient as a function of velocity for deoxygenation, using sweep gas (nitrogen) on the shell side.

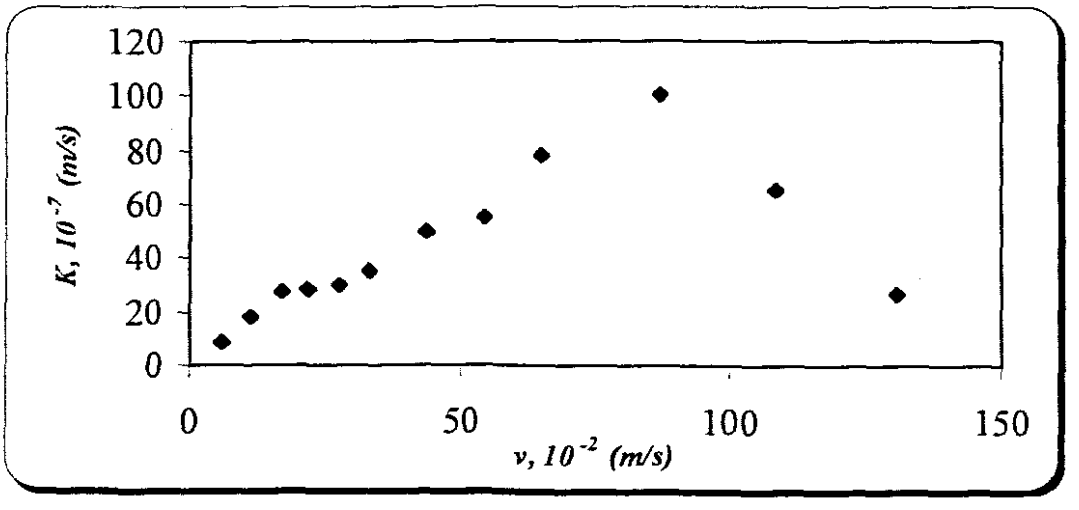

Figure 6.12: *Oxygenation (oxygen absorption) using pure oxygen on the shell side.*

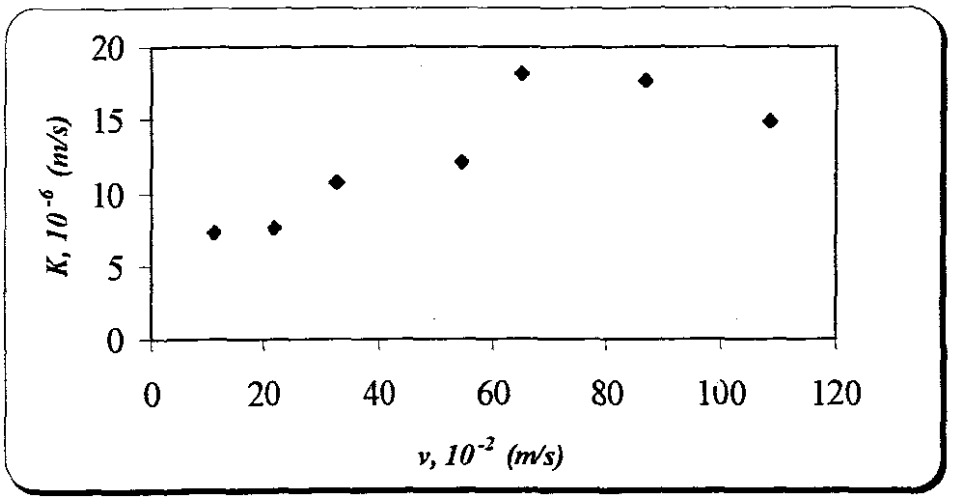

Figure 6.13: The overall mass transfer coefficient as a function of velocity for decarbonation, using sweep gas (nitrogen) on the shell side.

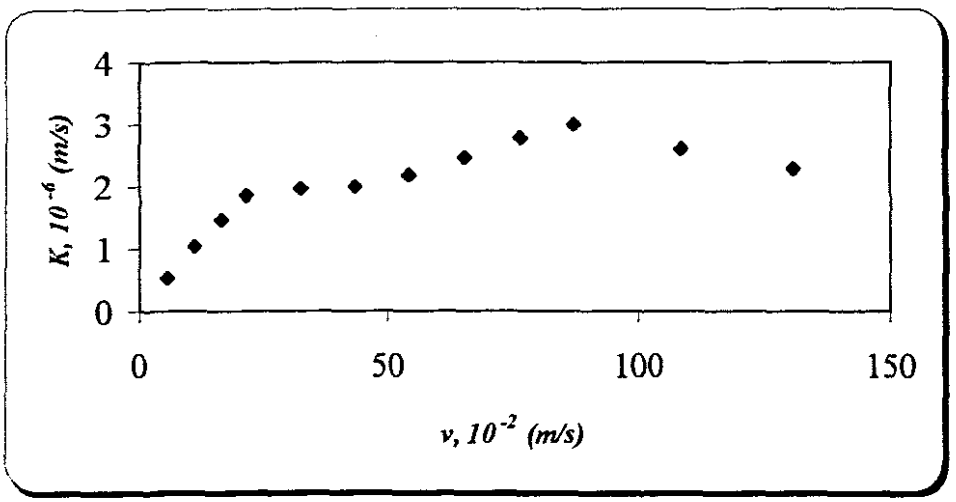

Figure 6.14: Carbonation (carbon dioxide absorption) using carbon dioxide on the shell side.

The phase controlling mass transfer (the liquid boundary layer, membrane and gas boundary layer) was investigated. Figure 6.9 indicated that the overall mass transfer coefficient has no relation to the flow rate of the gas; that indicates that the gas boundary layer resistance was negligible. However, by increasing the flow rate of the liquid, the overall mass transfer coefficient increased, which means there was a strong relation between mass transfer and the velocity of the liquid. The explanation is as follows: by increasing the liquid velocity, the boundary layer resistance decreased, which led to an increase in mass transfer.

Qi and Cussler (1985a,c), Côté et al. (1988), Yang and Cussler (1986), Karoor and Sirkar (1993) and Tai et al. (1994) confirmed the conclusion in their study. Côté et al. (1989) found that the overall rate of transfer with a porous membrane in which liquid water did not penetrate into the pores was comparable with that observed using silicone rubber membrane. The common factor was that the liquid boundary layer was the controlling resistance in both cases.

From Figure 6.11, 6.12, 6.13 and 6.14 it can be seen that the overall mass transfer coefficient increases with increasing velocity to a maximum value and then decreases.

Van der Walt (1999) studied the mass transfer in various capillary membranes gas-liquid contactors and the correlation developed was not applicable at Reynolds numbers greater than 1000. In our experiments, the overall mass transfer coefficient started to decrease at Reynolds numbers greater than 1000. This phenomenon was observed in all our experiments. But such a phenomenon was also observed by Tai et al. (1994) and Malek et al. (1997). The explanation was that the membrane was partially wetted due to the pressure gradient along the fiber lumen. All the investigators studied mass transfer in gas liquid contactors at low flow rate (low Reynolds number) and they concluded that at high flow rate the correlation developed in their studies failed to described the variation of the overall mass transfer coefficient with liquid linear velocity.

6.3.7 Comparison of the effects of using Pure Oxygen and Air in Oxygen Absorption

Since pure oxygen and air were used in Gradostat membrane bio-reactors to supply the microorganisms (fungi) with oxygen, a comparison between oxygenation using pure oxygen and air was investigated. The gas (pure oxygen or air) was fed into the shell side, and distilled water was fed into the membrane lumen. The two experiments were conducted as indicated in Section 6.3.2 (gas absorption). The results are plotted in Figure 6.15. The overall mass transfer coefficient was plotted as Sherwood number (equation 4.19) and the velocity as Reynolds number (equation 4.21).

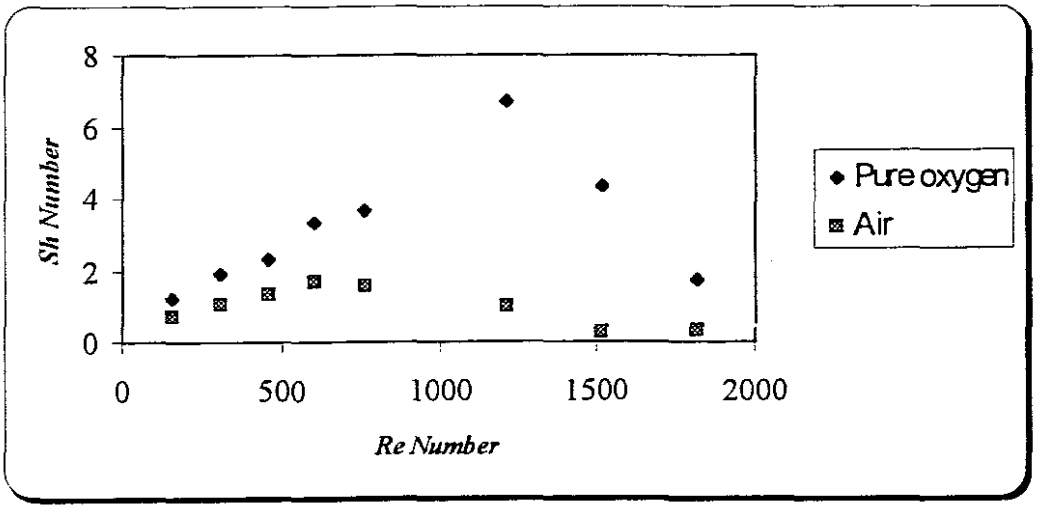

Figure 6.15: Sherwood number as a function of Reynolds number for oxygenation with pure oxygen and air on the shell side.

The absorption using pure oxygen on the shell side has a higher mass transfer coefficient than using air on the shell side. This difference is due to the fact that air contains 21% oxygen; the rest of the air is a mixture of gases, the resistance in the gas phase comprising the mixture was increased. This increased resistance decreases the overall mass transfer coefficient. Karoor and Sirkar (1993) also found that when a gas mixture is used instead of pure gas, there is additional resistance in the gas phase.

Côté et al. (1989) studied oxygen absorption to be used for bubble-free aeration, using pure oxygen and air with silicone rubber membrane. They found mass transfer coefficients values of 22.5×10^{-6} and 18.1×10^{-6} (m/s) when using pure oxygen and air, respectively.

In this study the maximum overall mass transfer coefficients found were 10×10^{-6} and 2.5×10^{-6} (m/s) when using pure oxygen and air, respectively.

Silicone rubber has the highest permeability rate for oxygen compared with other polymers (Côte et al.,1989). In the Côte et al. (1989) experiments the gas was in the

lumen; in this study the gas was on the shell side. In bubble-free aeration it is preferable to use the oxygen in the lumen (Côté et al., 1988, 1989; Ahmed and Semmens, 1992, 1996).

6.3.8 Comparison between Oxygenation and Carbonation

In all aerobic-type membrane bio-reactors, there is the diffusion of two gases (oxygen and carbon dioxide), since the microorganisms require oxygen for growth and at the same time the microorganisms release carbon dioxide.

A comparison between mass transfer coefficients for oxygenation and carbonation was investigated. Figure 6.16 shows the results where the mass transfer coefficient was plotted as Sherwood number (equation 4.19) and the velocity as Reynolds number (equation 4.21).

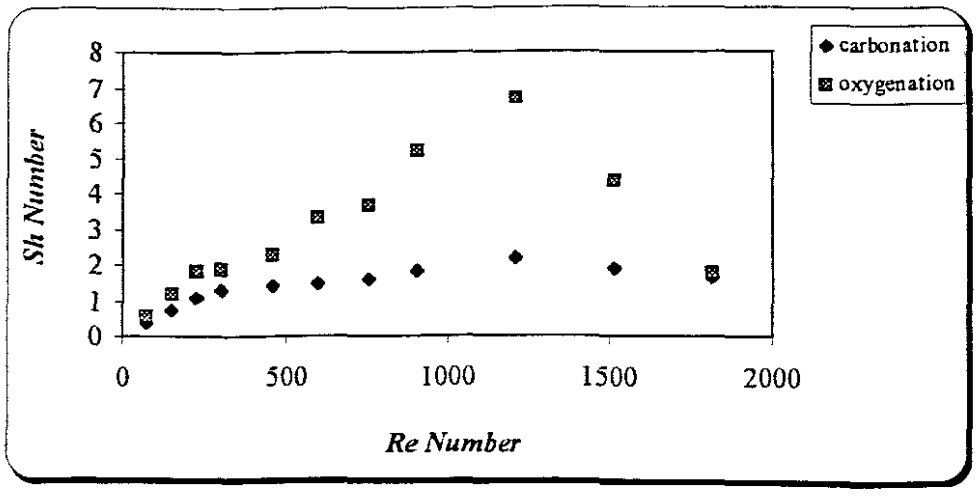

Figure 6.16: Sherwood number as a function of Reynolds number for oxygenation and carbonation.

It can be seen from Figure 6.16 that oxygen transfer rates are higher than those for carbon dioxide. The Henry constant is much smaller for carbon dioxide than for oxygen (H_c for CO_2= 1.063. H_c for O_2= 30.02, see page 125). If a closer inspection of equation (5.62) is

made, the ratio (Q_l / $Q_g H_c$) for the same liquid and gas flow rate is higher for carbon dioxide than for oxygen, and from these values the overall mass transfer coefficient will be higher for oxygen than for carbon dioxide. A possible contributory reason for this difference in mass transfer coefficients is the way the two concentrations were measured. Oxygen concentration was measured online by an oxygen electrode, while the carbon dioxide concentration was measured by back titration. Since samples of carbonated water were taken from the system to the external sampling beaker, and the measurements were not online, there may have been a loss of carbon dioxide between sampling and measurement. Thus, this method may introduce errors.

6.3.9 Comparison of Mass Transfer between Wet and Partially Wetted Membranes

Mass transfer is higher in gases than liquids. This is also true in the three-phase process, where mass transfer of gases is higher in a membrane with gas filled pores than in membranes with liquid filled pores. In Section 6.3.6, it was found that when the membrane was wet, and the pores were water filled, mass transfer was lower. An investigation was conducted to compare mass transfer across wet and partially wetted membranes.

To ensure wet-out of membrane pores, a bundle of membranes was immersed first in an alcohol, and then in water. Because of the low surface tension of alcohol, it can penetrate into the pores of the membrane. When the membrane was immersed in water, the latter would replace the alcohol and the pores would be water filled. Oxygenation with partially wet and wetted membranes was conducted as described earlier (Section 6.3.2). Figure 6.17 shows the results. The overall mass transfer coefficient is a function of velocity.

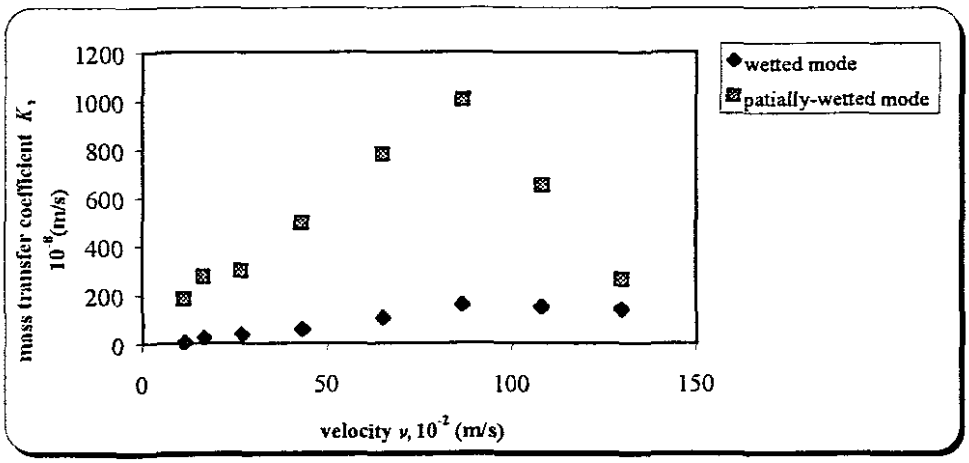

Figure 6.17: Mass transfer coefficient as a function of velocity for wetted and partially wetted membranes.

In the previous experiment (oxygenation, deoxygenation, carbonation and decarbonation) it was found that the mass transfer increases with an increase in the liquid velocity to a certain value, and then starts to decrease. The explanation for this phenomenon was that the pressure gradient along the fibre will allow water to enter the pores.

From Figure 6.17 we can deduce which one of the two factors is dominating. If the phenomenon is due solely to the wettability of the membrane, we expect that when the membrane is wetted the mass transfer coefficient will keep on increasing with the increasing velocity of the liquid, but it was not the case; at high flow rate the mass transfer coefficient remained nearly constant.

Comparing the mass transfer coefficient for the same liquid flow rate for the wetted and the partially wetted membranes, we can see that the wetted membranes have the lower mass transfer. This means they have the higher resistance.

6.3.10 Dimensionless Mass Transfer Correlations

Yang and Cussler (1986) reported a correlation for oxygen removal in an axial-flow hollow fibre module. The feed solution was in the lumen, and nitrogen sweep gas on the outside. The correlation that they obtained was very close to the Lévêque equation.

$$Sh = 1.64\, Pe^{0.33} \quad \text{(Yang and Cussler, 1986)}$$

$$Sh = 1.62\, Pe^{0.33} \quad \text{(Lévêque, 1928)}$$

In this study, least squares regression was used to find correlation equations between Sherwood number and Peclet number for oxygenation and carbonation as show in Figure 6.18.

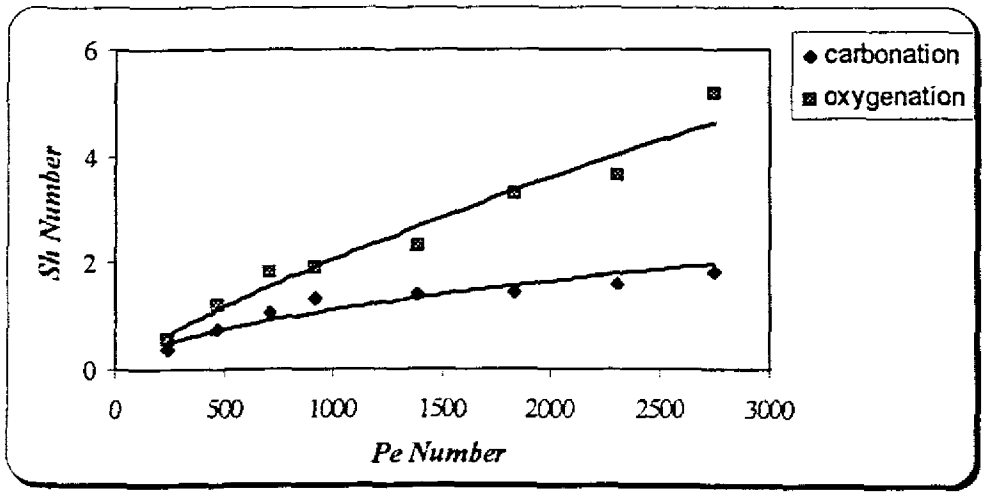

Figure 6.18: Sherwood number as a function of Peclet number for oxygenation and carbonation.

The correlations obtained from Figure 6.18 have the following form:

Carbonation $Sh = 0.021\, Pe^{0.57}$ (regression coefficient: $R^2 = 0.91$)

Oxygenation $Sh = 0.008\, Pe^{0.81}$ (regression coefficient: $R^2 = 0.97$)

The correlations were derived for Reynolds numbers below 1000.

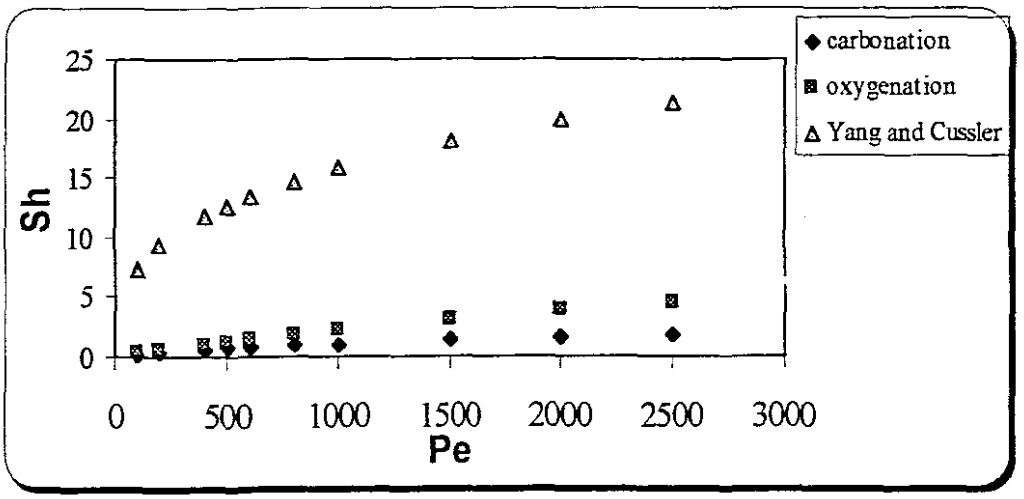

Figure 6.19: Comparison between correlations.

When comparing the correlation derived in this study and the correlation derived by Yang and Cussler (see Figure 6.19), it can be seen that the mass transfer rates which resulted from this study are much lower than those observed by Yang and Cussler. The possible reasons for this difference are:

- Yang and Cussler (1986) used hollow fibre microfiltration polypropylene membranes as gas-liquid contactor. Their pores were gas filled. In this work a polysulphone membrane with an ultrafiltration skin layer and a high voidage wall with a thickness of 300 μm was used. This structure differs completely from the microfiltration polypropylene used in gas-liquid contactors. It was found that the polysulphone membrane during the latter part of the experiment became wet and some of the pores were water filled. If the pores of the ultrafiltration are water filled, the water will fill the void structure, resulting in the formation of a water pellicle of a thickness of 300 μm. In polypropylene membranes it was found that the resistance was in the liquid boundary layer; in polysulphone membrane the resistance to mass transfer was in the liquid boundary and in the membrane. The resistance in the liquid boundary layer can

be reduced by increasing the velocity in the lumen, but the resistance in the membrane is constant where a stagnant liquid film is permanently present in the pores and the void structure. This wettability gives an extra resistance to mass transfer.

- Yang and Cussler derived their correlation for a Reynolds number less than 50. In this study the correlations were developed at Reynolds number less than 1000.

CHAPTER 7
CONCLUSIONS AND RECOMMENDATIONS

7.1 FLAT-SHEET MEMBRANES

7.1.1 Conclusions

- The diaphragm-cell method was found to be the simplest (easy to build and operate) to study mass transfer of gases in flat-sheet membranes.

- The diaphragm-cell was used to study mass transfer of oxygen through polysulphone flat-sheet membranes, and it was found that the following parameters influence mass transfer rate:
  i) the rate of agitation in the two chambers;
  ii) the concentration of the reactive solution in the upper compartment; and
  iii) the thickness of the membrane.

- The diaphragm-cell method can be used to determine mass transfer of gases across membranes to be used as gas-liquid contactors (gas removal and gas absorption). It can also be used to study mass transfer of oxygen across membrane bio-reactors as described by Robertson and Kim (1985), Frank and Sirkar (1986), Chung and Chang (1988).

7.1.2 Recommendations

7.1.2.1 Improvement in Diaphragm-cell technique

- build a dedicated cell so that it will be easy to operate, and provide simple reliable methods of measuring concentration changes; and
- improve solute concentration measurement, e.g. using an electrode inside the lower compartment if technical facilities permit.

7.1.2.2 Proposed Method to Measure Mass Transfer in a Biofilm

A biofilm study requires a special cell. It would consist of two chambers. Between these chambers a support is clamped, the biofilm to be studied would be grown on this support. The support can be any membrane or polymer with high permeability to nutrient and oxygen. The lower compartment is nutrient solution filled and well stirred. The upper compartment is oxygen filled. For oxygen diffusion, first the biofilm will consume a part of the oxygen, and some of the excess oxygen will diffuse through the biofilm into the lower compartment. Oxygen diffusion will be studied in two parts. The oxygen concentration in the upper compartment can be measured by chromatography or by the manometric method. This concentration is as a result of oxygen being consumed by the biofilm and oxygen diffusing through the biofilm. To measure the oxygen consumption by the biofilm, it is necessary to know the oxygen concentration in the lower compartment; this can be measured using an oxygen electrode. These measurements will be repeated for different biofilm thicknesses, and a correlation between oxygen consumption and the thickness of the biofilm can be developed.

7.2 CAPILLARY MEMBRANES

7.2.1 Conclusions

- The overall mass transfer coefficient was found to be independent of gas flow rate in the range between 44.5 and 100 $\times$ 10^{-6} (m^3/s). This means that the gas phase resistance is negligible.

- Mass transfer in membrane gas-liquid contactors is influenced by three resistances in series (the gas phase boundary layer, the membrane and the liquid boundary layer). Since there is negligible resistance in the gas boundary layer, the main resistance was in the membrane and in the liquid boundary layer. It was found that the mass transfer coefficient increased with increasing liquid flow rate. That means the liquid

boundary layer has an important role in mass transfer, and by increasing the flow rate of the liquid, the resistance in the boundary layer is reduced and that gives rise to an increase in the mass transfer rate.

- The calculated mass transfer coefficient was found to be low compared to those obtained in the literature. This difference is believed to be due to the structure of the membrane used (skinless polysulphone membrane). It was found that the membrane was wetted out by the liquid, and since the membrane has a void structure with a thickness of 300 μm, the formation of a water layer inside the membrane will be inevitable. This layer will cause a higher resistance to mass transfer. Therefore the membrane also has a very important role in controlling the rate of mass transfer.

- In all the experiments conducted (oxygenation, deoxygenation, carbonation and decarbonation) it was found that the mass transfer coefficient increased with Reynolds number and reached a maximum. The overall mass transfer coefficient started to decrease as the liquid side Reynolds number approaching 1000. The explanation for this phenomenon lies with the wettability of the membrane.

- When gas and liquid were flowing counter-currently, higher mass transfer rates were achieved than when they were flowing co-currently.

- For gas removal, it was found that the mass transfer coefficient was the same when either a sweep gas (nitrogen) or vacuum was used on the shell side of the module.

- A decrease in mass transfer rates was observed when water was oxygenated using air instead of pure oxygen.

- The mass transfer correlations (for oxygenation and carbonation) obtained in this study were found to be significantly different than those reported by other researchers for other membranes. The reason was that all the researchers in the field used polypropylene hollow fibre membranes, where the pores are always gas filled. In the

latter case the resistance was only in the liquid boundary layer. This contrasted with our case where it was found that the membrane presents a major resistance to mass transfer, as does the liquid boundary layer.

- Two correlations were developed (oxygenation and carbonation). These correlations may be useful in design of Gradostat fungal bio-reactors.

7.2.2 Recommendations

- Mass transfer coefficients were measured for wetted and partially wetted polysulphone membranes. It is recommended that two other cases should be investigated: mass transfer in dry membranes and mass transfer in membranes filled with glycerol. The effects of the wettability of the membrane are unavoidable. To investigate the dry membrane, the experiment should be conducted with a gas-gas contactor (no water involved). To simulate the presence of biomass inside the pores, the membrane can be glycerol filled, because glycerol can give more resistance to transfer nearly as the biomass.

- Mass transfer coefficients in the skinless polysulphone membrane were found to be lower than those reported by others in polypropylene membranes. To improve mass transfer, the membrane should be coated with silicone rubber to avoid water penetration inside the pores to be used as gas-liquid contactor.

- To get higher oxygen transfer in skinless polysulphone, it is preferable to supply oxygen into the lumen of the capillaries, and water on the outside. The actual structure of the membrane does not allow that. If the ultrafiltration layer is outside and the void structure inside (the reverse of the actual structure of the polysulphone membrane), this structure yields better oxygen transfer. Venkatadi and Irvine (1993) found that silicone rubber tubing was an excellent support for fungal growth, where oxygen was fed into the lumen side.

- To improve mass transfer of gases in polysulphone membranes to be used as gas-liquid contactors, a module with an optimally high surface area should be designed.

- In view of the meager data on diffusion coefficient in polymers, consideration should be given to a project to measure such data.

APPENDIX A
DETAILED RESULTS AND CALCULATIONS

A.1 CAPILLARY MEMBRANES

1. Comparison between using vacuum and sweep gas nitrogen in the shell side, liquid flowing into the lumen once-through.

Table A.1: Results using vacuum in the shell side, liquid in once-through mode

Q_l (ml/min)	Q_l 10^{-8} (m^3/s)	C_{in} (mg/l)	C_{out} (mg/l)	C_{out}/C_{in}
4.9	8.16	9.99	5.37	0.54
10.3	17.16	9.92	5.83	0.59
30.2	50.33	9.69	5.89	0.61
50.2	83.66	9.64	6.95	0.72
59.9	99.83	9.42	7.60	0.81
79.9	133.16	10.00	8.30	0.83
99.9	166.50	9.33	8.20	0.88
120.4	200.66	9.00	8.10	0.90

Table A.2: Results using nitrogen as sweep gas on the shell side, liquid in once-through mode

Q_l (ml/min)	Q_l 10^{-8} (m^3/s)	C_{in} (mg/l)	C_{out} (mg/l)	C_{out}/C_{in}
4.9	8.16	8.68	4.19	0.48
10.3	17.16	8.57	4.48	0.52
20.0	33.33	8.32	4.13	0.50
39.9	66.50	8.43	4.89	0.58
50.2	83.66	8.53	5.34	0.63
59.9	99.83	8.42	5.40	0.64
70.2	117.00	8.62	5.68	0.66
79.9	133.16	8.00	6.34	0.79
99.9	166.50	7.69	6.60	0.86

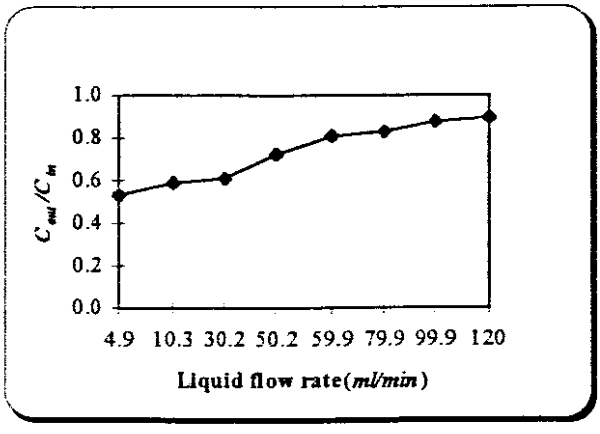

Figure A.1: C_{out}/C_{in} vs. liquid flow rate, using vacuum.

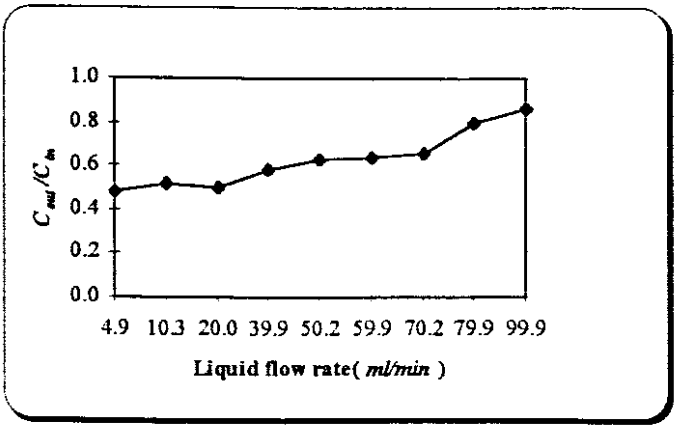

Figure A.2: C_{out}/C_{in} vs. liquid flow rate, using nitrogen as sweep gas.

2. Oxygen removal, liquid in once-through mode, sweep gas nitrogen flowing in the shell side co-currently to the liquid. The volumetric flow rate of the gas was 48.7×10^{-6} (m^3/s).

Table A.3: Results for oxygen removal, co-current flow, calculation of *Re*, *Pe* and *Sh* numbers

v, 10^{-2} (m/s)	*Re*	*Pe*	*K*, 10^{-5} (m/s)	*Sh*
11.17	156	472	1.44	9.59
21.69	302	917	3.68	24.49
32.76	456	1386	4.61	30.67
43.29	603	1831	4.70	31.29
54.46	758	2304	5.08	33.82
64.98	905	2749	5.75	38.28
76.17	1061	3222	6.33	42.13
86.68	1207	3667	5.89	39.23
108.39	1509	4585	5.30	35.27

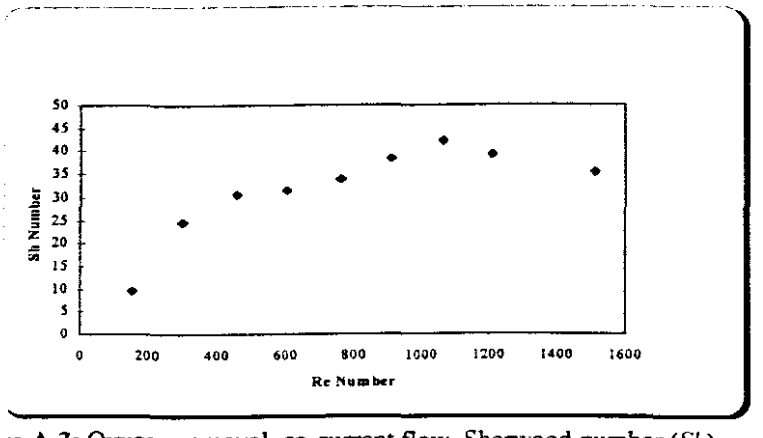

Figure A.3: Oxygen removal, co-current flow. Sherwood number (*Sh*) vs. Reynolds number (*Re*).

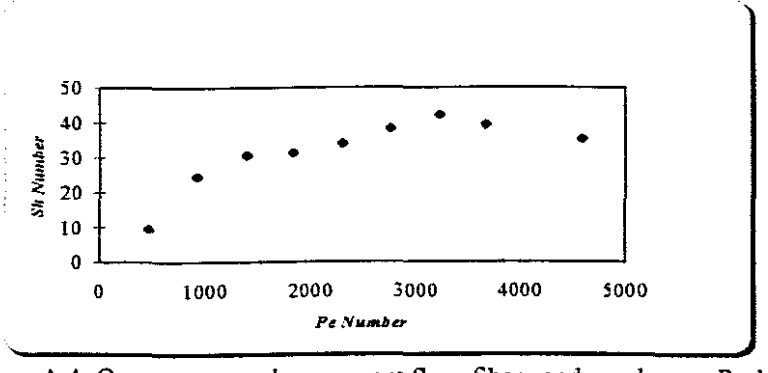

Figure A.4: Oxygen removal, co-current flow. Sherwood number vs. Peclet number.

3. Oxygen removal, liquid in once-through mode, sweep gas nitrogen in the shell side. Flowing counter-currently to liquid. The flow rate of the gas was 47.6×10^{-6} (m^3/s).

Table A.4: Results for oxygen removal, counter-current, calculation of *Re*, *Pe* and *Sh*

$v, 10^{-2}$ (m/s)	*Re*	*Pe*	$K, 10^{5}$ (m/s)	*Sh*
11.06	154	468	2.23	14.85
22.13	308	936	3.87	25.76
32.54	453	1376	5.48	36.48
43.50	606	1840	6.14	40.87
54.56	760	2308	6.51	43.34
64.98	905	2749	9.12	60.71
108.38	1509	4584	10.35	68.90
130.18	1813	5507	8.43	56.12

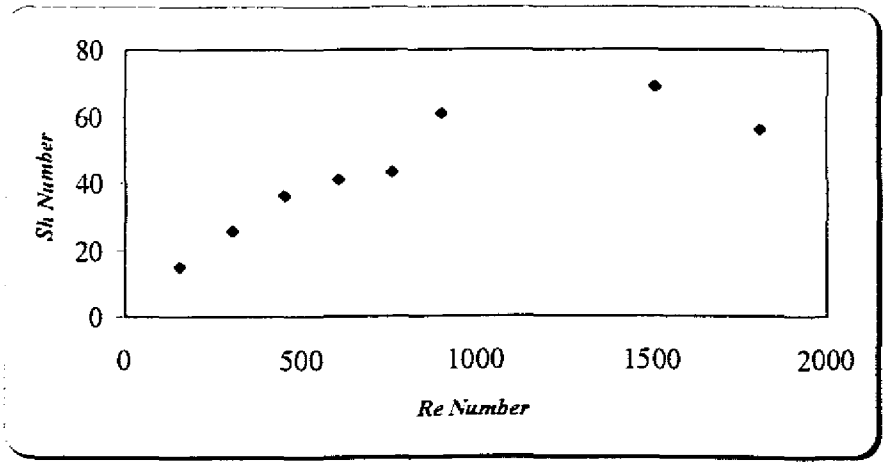

Figure A.5: Oxygen removal, counter-current flow. Sherwood number (*Sh*) vs. Reynolds (*Re*).

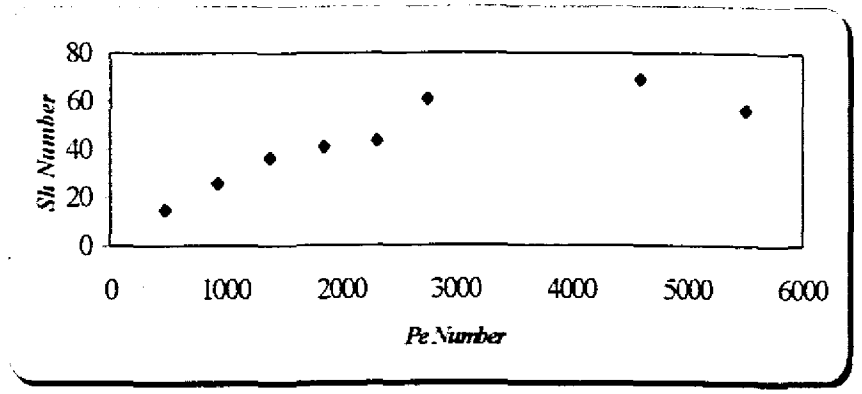

Figure A.6: Oxygen removal, counter-current. Sherwood number vs. Peclet number.

4. Carbon dioxide removal, liquid in once-through mode, sweep gas nitrogen in the shell side flowing counter-currently. The flow rate of the gas was 15.1×10^{-6} (m^3/s).

Table A.5: Results for CO_2 removal, counter-current. *Re*, *Pe* and *Sh* number calculation.

v, 10^{-2} *(m/s)*	*Re*	*Pe*	*K*, 10^{-6} *(m/s)*	*Sh*
11.17	156	516	7.27	5.29
21.69	302	1002	7.60	5.53
32.76	456	1514	10.65	7.75
54.46	758	2516	12.25	8.92
64.98	905	3002	17.94	13.06
86.68	1207	4005	17.41	12.68
108.39	1509	5008	18.99	13.83

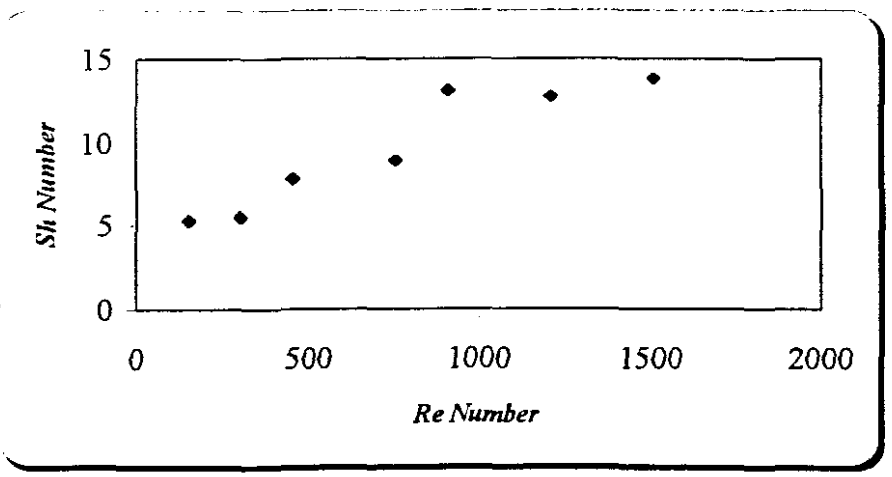

Figure A.7: CO_2 removal, counter-current flow. Sherwood number (*Sh*) vs. Reynolds number (Re).

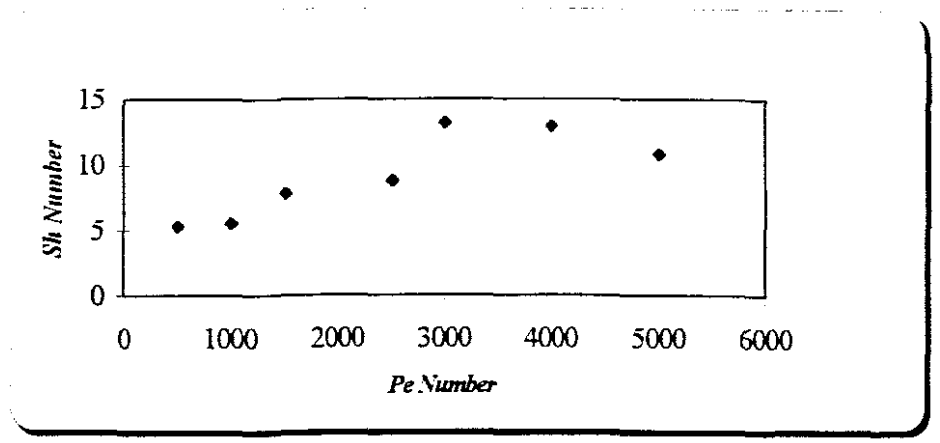

Figure A.8: CO_2 removal, counter-current flow. Sherwood number vs. Peclet number.

5. Carbon dioxide absorption, liquid in once-through mode, pure CO_2 in the shell side flowing counter-currently. The flow rate of the gas was 5.88×10^{-6} (m^3/s).

Table A.6: CO_2 absorption, counter-current flow. *Re*, *Pe* and *Sh* numbers calculation

$v, 10^{-2}$ (m/s)	*Re*	*Pe*	$K, 10^{-6}$ (m/s)	*Sh*
5.53	77	234	0.54	0.39
11.17	156	472	1.03	0.75
16.59	231	702	1.46	1.06
21.69	302	917	1.85	1.34
32.76	456	1386	1.95	1.42
43.29	603	1831	2.01	1.46
54.55	760	2307	2.17	1.58
64.98	905	2749	2.48	1.81
76.47	1065	3235	2.78	2.03
86.98	1211	3679	3.01	2.19
108.39	1509	4585	2.62	1.91
130.52	1817	5521	2.28	1.66

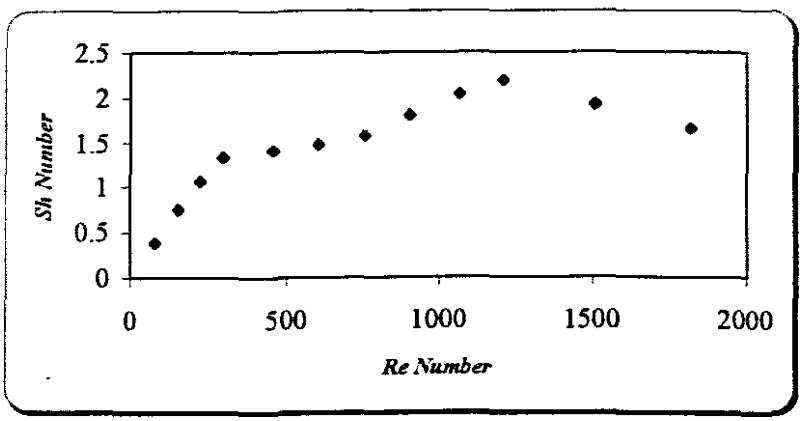

Figure A.9: CO_2 absorption, counter-current flow. Sherwood number (*Sh*) vs. Reynolds number (*Re*).

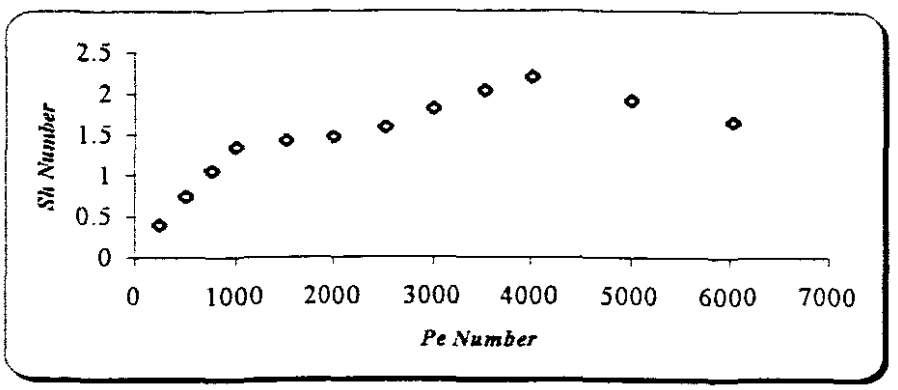

Figure A.10: CO_2 absorption, counter-current flow. Sherwood number vs. Peclet number.

6. Oxygen absorption, liquid in once-through mode, pure oxygen in the shell side flowing counter-currently. The flow rate of the gas was 9.52×10^{-6} (m^3/s).

Table A.7: Results for oxygen absorption, counter-current flow, pure oxygen in the shell side. *Re*, *Pe* and *Sh* numbers calculation

$v, 10^{-2}$ (m/s)	*Re*	*Pe*	$K, 10^{-7}$ (m/s)	*Sh*
5.53	77	234	8.68	0.58
11.17	156	472	18.22	1.21
16.59	231	702	27.31	1.82
21.69	302	917	28.39	1.89
27.00	376	1142	29.88	1.99
32.76	456	1386	34.74	2.31
43.29	603	1831	49.6	3.30
54.55	760	2307	54.94	3.66
64.98	905	2749	78.04	5.20
86.98	1211	3679	100.57	6.69
108.39	1509	4585	65.24	4.34
130.52	1817	5521	26.41	1.76

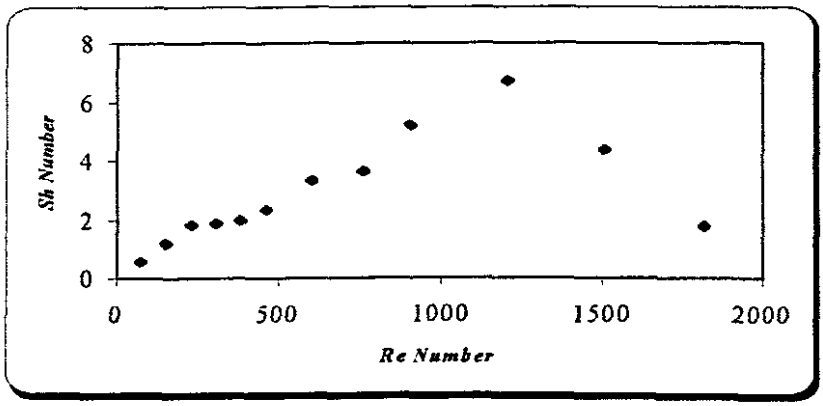

Figure A.11: Oxygen absorption, counter-current flow, pure oxygen on the shell side. Sherwood number (*Sh*) vs. Reynolds number (*Re*)

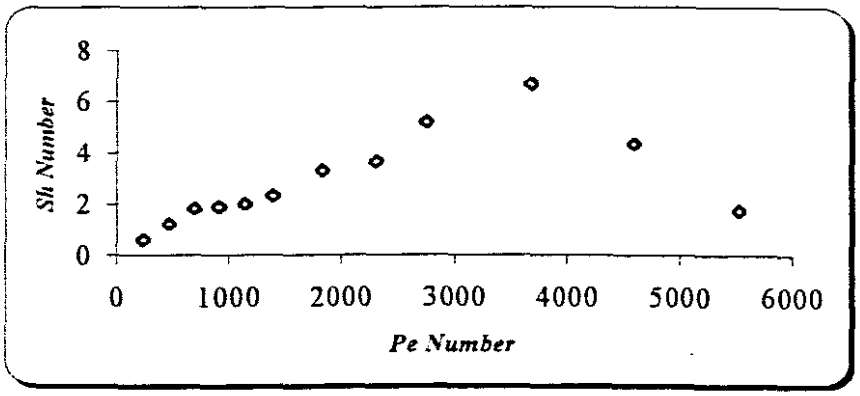

Figure A.12: Oxygen absorption, counter-current flow, pure oxygen on the shell side. Sherwood number (*Sh*) vs. Peclet number (*Pe*)

7. Oxygen absorption, air in the shell side flowing counter-currently to liquid. The flow rate of the gas was 2.63×10^{-6} (m^3/s).

Table A.8: Results for oxygen absorption, counter-current flow, air in the shell side. *Re*, *Pe* and *Sh* numbers calculation

$v, 10^{-2}$ (*m/s*)	*Re*	*Pe*	$K, 10^{-6}$ (*m/s*)	*Sh*
11.17	*156*	*472*	*1.10*	*0.73*
21.69	*302*	*917*	*1.60*	*1.07*
32.76	*456*	*1386*	*2.06*	*1.37*
43.29	*603*	*1831*	*2.50*	*1.66*
54.46	*758*	*2304*	*2.40*	*1.60*
76.17	*1061*	*3222*	*1.80*	*1.20*
86.68	*1207*	*3667*	*1.50*	*1.00*
108.39	*1509*	*4585*	*0.40*	*0.27*
130.52	*1817*	*5521*	*0.50*	*0.33*

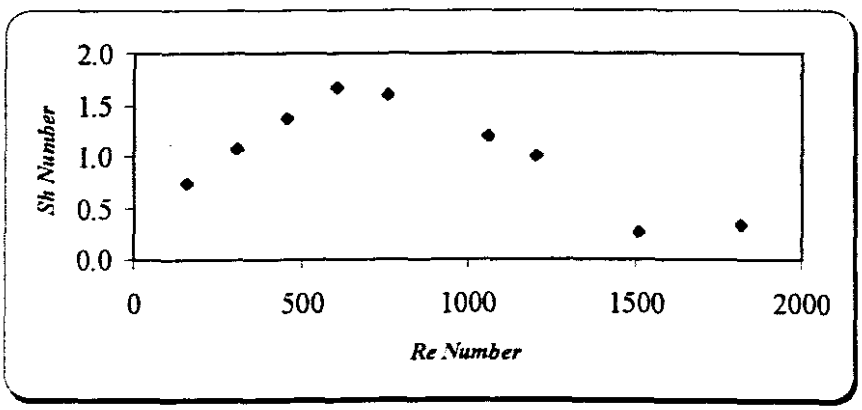

Figure A.13: O_2 absorption, counter-current flow, air on the shell side. Sherwood number (*Sh*) vs. Reynolds number (*Re*).

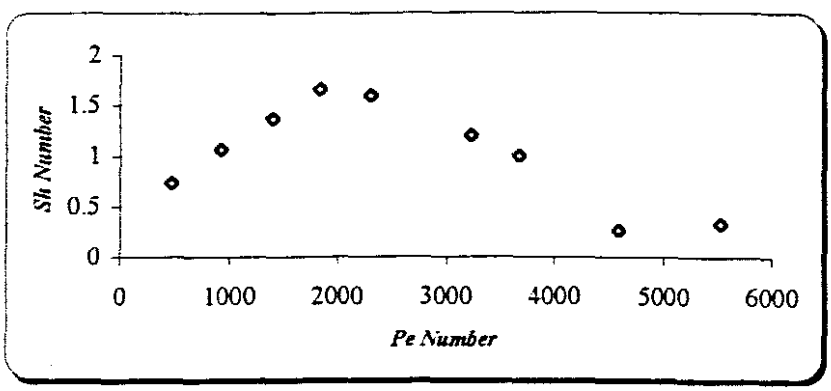

Figure A.14: O_2 absorption, counter-current flow, air on the shell side. Sherwood number (*Sh*) vs. Peclet number (*Pe*).

8. CALCULATIONS:

Oxygen removal, liquid and gas flowing co-currently:

Conditions:

$Q_g = 48.7\times10^{-6}$ (m^3/s)

$A = n\,\pi\,d\,L$

$= 8\,\pi\,(1.398\times10^{-3})\,(0.22)$

$= 7.725\times10^{-3}$ (m^2)

$H_c = 30.02$

We used equation (5.43) to calculate the overall mass transfer coefficient:

$$K_{OL} = \frac{-Q_l}{dL\pi}\frac{1}{\left(1+\dfrac{Q_l}{Q_g H_c}\right)}\ln\left[\frac{\left(1+\dfrac{Q_l}{Q_g H_c}\right)C_{out}-\dfrac{Q_l}{Q_g H_c}C_{in}}{C_{in}}\right] \qquad (5.42)$$

Example of calculation:

$Q_l = 17.16\times10^{-8}$ (m^3/s)

$C_{in} = 8.57$ (mg/l)

$C_{out} = 4.48$ (mg/l)

We replace in equation (5.43):

$$K_{OL} = \frac{-17.16\times10^{-8}}{7.725\times10^{-3}}\frac{1}{\left(1+\dfrac{17.16\times10^{-8}}{48.7\times10^{-6}\times30.02}\right)}ln\left[\frac{\left(1+\dfrac{17.16\times10^{-8}}{48.7\times10^{-6}\times30.02}\right)\times4.48-\left(\dfrac{17.16\times10^{-8}}{48.7\times10^{-6}\times30.02}\right)}{8.57}\right]$$

$K_{OL} = 1.44\times10^{-5}$ (m/s)

Sherwood number:

$D = 2.1\times10^{-5}$ (cm^2/s) $= 2.1\times10^{-9}$ (m^2/s)

From equation (4.19): $Sh = \dfrac{Kd_e}{D}$

$$Sh = \frac{1.44*10^{-5}*1.398*10^{-3}}{2.1*10^{-9}} = 9.59$$

Calculations of *Re* and *Pe* :

$Q_l = 17.16 \times 10^{-8}$ (m^3/s)

$$v = \frac{4Q_l}{d^2\pi}$$

$$v = \frac{4 \times 17.16 \times 10^{-8}}{(1.398)^2 \times 10^{-6} \times \pi} = 11.17 \times 10^{-2} (m/s)$$

Reynolds number:

From equation (4.21): $\mathrm{Re} = \frac{d_e v_l}{\upsilon}$

υ: kinematic viscosity
$\upsilon = 1.004 \times 10^{-6}$ (kPa.s)

$$Re = \frac{1.398 \times 10^{-3} \times 11.17 \times 10^{-2}}{1.004 \times 10^{-6}} = 156$$

Peclet number:

From equation (4.20): $Pe = \frac{d_e^2 v_l}{DL}$

$$Pe = \frac{(1.398)^2 \times 10^{-6} \times 11.17 \times 10^{-2}}{2.1 \times 10^{-9} \times 22 \times 10^{-2}} = 472$$

Table A.9: Detailed results to calculate the overall mass transfer coefficient for oxygen

Q_l (ml/min)	Q_l, 10^{-8} (m^3/s)	C_{in} (mg/L)	C_{out} (mg/L)	K, 10^{-5} (m/s)
10.3	17.16	8.57	4.48	1.441
20.0	33.33	8.46	3.61	3.679
30.2	50.33	8.55	4.22	4.607
39.9	66.50	8.35	4.84	4.701
50.2	83.66	8.53	5.34	5.080
59.9	99.83	8.42	5.40	5.751
70.2	117.00	8.62	5.68	6.329
79.9	133.16	8.68	6.17	5.893
99.9	166.50	8.04	6.29	5.298

Carbon dioxide absorption, counter-current flow, pure CO_2 in the shell side:

Conditions:
$Q_g = 5.88 \times 10^{-6}$ (m^3/s)
$A = n \pi d L$
$= 7.725 \times 10^{-3}$ (m^2)
$H_c = 1.063$

We used equation (5.62) to calculate the overall mass transfer coefficient:

$$K_{OL} = \frac{-Q_l}{dL\pi} \frac{1}{\left(1 - \frac{Q_l}{Q_g H_c}\right)} \ln\left[\frac{C_{out} - C_2^*}{C_{in} - C_1^*}\right] \tag{5.73}$$

The pure gas pressure remained essentially constant along the module length. Therefore C^* remained constant with L (Sujatha Karoor and Sirkar K. K., 1993).

$$C^* = C_1^* = C_2^* = \frac{P_g}{H_p}$$

Example of calculation:
$Q_l = 17.16 \times 10^{-8}$ (m^3/s)
$C_{in} = 30$ (mg/l)
$C_{out} = 104$ (mg/l)

We replace in equation (5.62):

$$K_{OL} = \frac{17.16 \times 10^{-8}}{7.725 \times 10^{-3}} \left(\frac{1}{1 - \frac{17.16 \times 10^{-8}}{5.88 \times 10^{-6} \times 1.063}} \right) ln \frac{104 - \frac{101}{0.0589}}{30 - \frac{101}{0.0589}}$$

$$K_{OL} = 1.03 \times 10^{-6} \text{ (m/s)}$$

Sherwood number:
$D = 1.92 \times 10^{-5}$ (cm^2/s) = 1.92×10^{-9} (m^2/s)
From equation (4.19): $Sh = \frac{K d_e}{D}$

$$Sh = \frac{1.03 \times 10^{-6} \times 1.398 \times 10^{-3}}{1.92 \times 10^{-9}} = 0.75$$

Calculations of *Re* and *Pe*:

Reynolds number:

From equation (4.21): $\mathrm{Re} = \frac{d_e v_l}{\upsilon}$

υ: kinematic viscosity
$\upsilon = 1.004\times10^{-6}$ (kPa.s)

$$Re = \frac{1.398\times10^{-3}\times11.17\times10^{-2}}{1.004\times10^{-6}} = 156$$

Peclet number:

From equation (4.20): $Pe = \frac{d_e^2 v_l}{DL}$

$$Pe = \frac{(1.398)^2\times10^{-6}\times11.17\times10^{-2}}{1.92\times10^{-9}\times22\times10^{-2}} = 516$$

Table A.10: Detailed results to calculate the overall mass transfer coefficient for CO_2

Q_l (ml/min)	Q_l, 10^{-8} (m^3/s)	C_{in} (mg/L)	C_{out} (mg/L)	$K, 10^{-6}$ (m/s)
5.1	8.50	30	110	0.54
10.3	17.16	30	104	1.03
15.3	25.50	30	100	1.46
20.0	33.33	30	97	1.85
30.2	50.33	30	76	1.95
39.9	66.50	30	65	2.01
50.3	83.66	30	59	2.17
59.9	99.83	30	57	2.48
70.2	117.00	30	55	2.78
80.2	133.16	30	53	3.01
99.9	166.50	30	45	2.62
120.4	200.66	30	40	2.28

A.2 FLAT-SHEET RESULTS

- Oxygen mass transfer coefficient for flat-sheet polysulphone:
  Agitation 200 rpm
  Na_2SO_3 = 0.25 N

Table A.11: Oxygen mass transfer coefficient in flat-sheet polysulphone

time (min)	*C(0,lower) (mg/l)*	*C(t,lower) (mg/l)*	*K, 10^{-4} (m/s)*
10	9.80	5.19	3.1
15	9.61	3.7	3.1
30	10.00	1.6	3.0

- Effect of agitation on mass transfer coefficient:
  Concentration of Na_2SO_3 = 0.25 N
  Time t = 10 *min*

Table A.12: Mass transfer coefficient with different agitation rates

agitation (rpm)	*C(0,lower) (mg/l)*	*C(t,lower) (mg/l)*	*K, 10^{-4} (m/s)*
0	6.85	5.32	1.2
200	9.80	5.19	3.1
300	6.38	3.36	3.1
600	6.51	3.45	3.1

- Effect of the thickness of the membrane on mass transfer coefficient:
  Agitation 200 rpm
  Time t = 10 min
  Concentration of Na_2SO_3 = 0.25 N

Table A.13: Mass transfer coefficient with different membrane thicknesses

number of membranes	*C(0,lower) (mg/l)*	*C(t,lower) (mg/l)*	*K, 10^{-4} (m/s)*
1	9.80	5.19	3.1
2	6.79	4.20	2.3
3	6.85	4.4	2.1
4	6.59	4.54	1.8

- Effect of the concentration of the reactive solution on mass transfer coefficient:
  Agitation 200 rpm
  Time t= 10 min

Table A.14: Mass transfer coefficient with different concentration of the reactive solution

Na_2SO_3 (N)	C(0,lower) (mg/l)	C(t,lower) (mg/l)	K, 10^{-4} (m/s)
0.25	9.80	5.19	3.1
0.5	9.82	5.20	3.1
1	9.80	5.17	3.1
2	9.78	5.19	3.1

Example of calculation:

Using equation (5.14), we can calculate the mass transfer coefficient.

$$K = \frac{V_{lower}}{tA} \ln \frac{C_{1,lower}(t=0)}{C_{1,lower}(t)} \qquad (6.2)$$

A= surface area
$A = \pi r^2$
$A = \pi \times (39.2/2)^2 \times 10^{-6}$
$A = 12.06 \times 10^{-4}\ (m^2)$

$V_{lower} = 350 \times 10^{-6}\ (m^3)$
t = 10 min

$$K = \frac{350\times10^{-6}}{\pi\left(\frac{39.2}{2}\right)^2 \times 10^{-6}}\left(\frac{1}{10\times60}\right) ln\frac{9.80}{5.19} = 3.1\times10^{-4}(m/s)$$

APPENDIX B
MEMBRANE FABRICATION PROTOCOL

B.1 INTRODUCTION

The fungal membrane bio-reactor is internally skinned with a substructure containing closely- packed narrow bore macrovoids that extend all the way from just below the skin layer to the membrane periphery.

Integrally skinned refers to the skin layer of the membrane being an integrated part of the membrane structure.

The fungus was growing within the confines of these macrovoids. Furthermore, in order to inoculate the macrovoids with spores, the macrovoids had to be accessible from the outside. This would be possible only if the membrane had no skin layer on the outside.

Integrally skinned membranes are formed by a procedure known as phase inversion. This process requires that a *membrane forming solution* (polymer dissolved in a *solvent(s)* be contacted with a non solvent for the polymer. By a process of solvent / non-solvent exchange, the polymer coagulates and precipitates, leading to the formation of an asymmetric membrane film. By careful manipulation of both the membrane formulation and the coagulation conditions, membranes with different skin and substructure morphologies can be produced.

B.2 CAPILLARY POLYSULPHONE SKINLESS FABRICATION

Capillary membranes are produced by extruding a membrane spinning solution through the annulus of a tube-within-tube spinneret (figure B.1). In the case of a skinless capillary membrane, the fabrication procedure differs from the conventional approach in that the

spinneret was positioned at the bottom of a high concentration solvent tank instead of a high concentration non-solvent tank (Jacobs and Leukes, 1996, Jacobs and Sanderson 1996, 1998). The spinning solution is pumped from a reservoir by a metering pump through a filter to the spinneret.

The spinneret contains a central opening for dispensing the coagulant, which flows under gravitational force from a reservoir, and the membrane was drawn vertically from the spinneret at a linear production rate of 4 $m.min^{-1}$. The bore side coagulant flow rate is monitored and controlled by a rotameter and needle valve.

The lumen fluid prevents the membrane from collapsing before gelation has taken place and also plays a role in the coagulation process to determine the structure of the inside wall.

By adjusting the spinning solution formulation and composition of the internal and external coagulation, internal, external or double skinned membranes with different substructure morphologies, can be produced.

Pure water (strong non-solvent) is used as lumen fluid or internal coagulation to encourage fast coagulation and the formation of thin-skinned membranes.

To obtain an open structure on the outside, solvent exchange across the outside wall was to be prevented. This is effected by a system comprising two coagulation baths. The spinneret is placed at the bottom of the first tank and the membrane is extruded into an aqueous solution containing 94% N-Methyl-2- Pyrrolidone (NMP).

When the membrane leaves this tank, the outside of the nascent membrane was still highly swollen, gel-like and soft, because the external coagulant was high in solvent content. The membrane is then exposed to a non-solvent vapour atmosphere by passing it through a high-humidity chamber (humidified air), to fix the structure once the

membrane had been withdrawn from the first bath and before entering the final rinse bath containing pure water.

The membrane passes over several polypropylene guide-rollers before it reaches the rotating, perforated take-up drum. Water is sprayed onto the take-up drum to rinse the membranes. As the membrane moves through the second tank all excess solvents are also washed out.

Figure B. 1 shows the spinneret for capillary production. Figure B. 2 represent the diagram of a capillary membrane production facility.

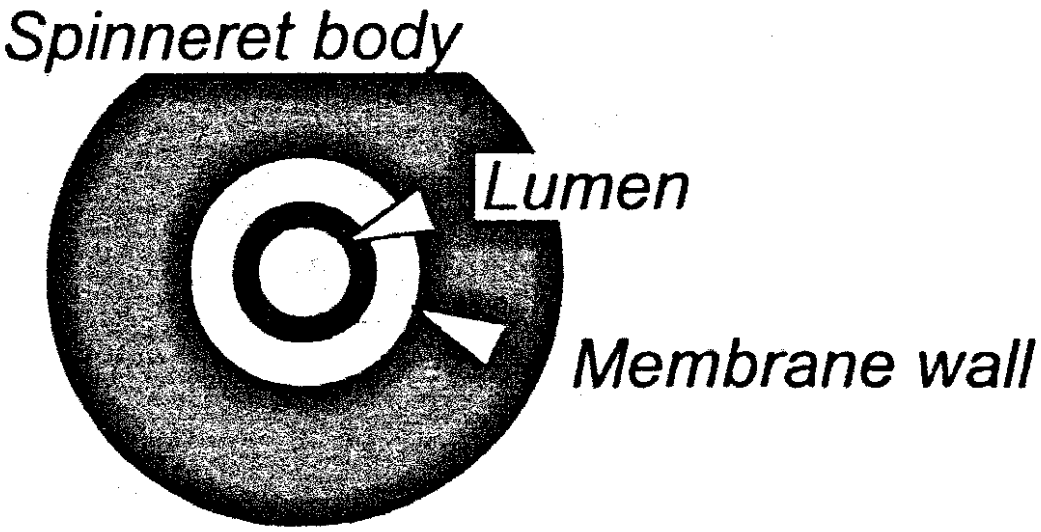

Figure B.1: Spinneret for capillary membrane production (Jacobs and Sanderson, 1997).

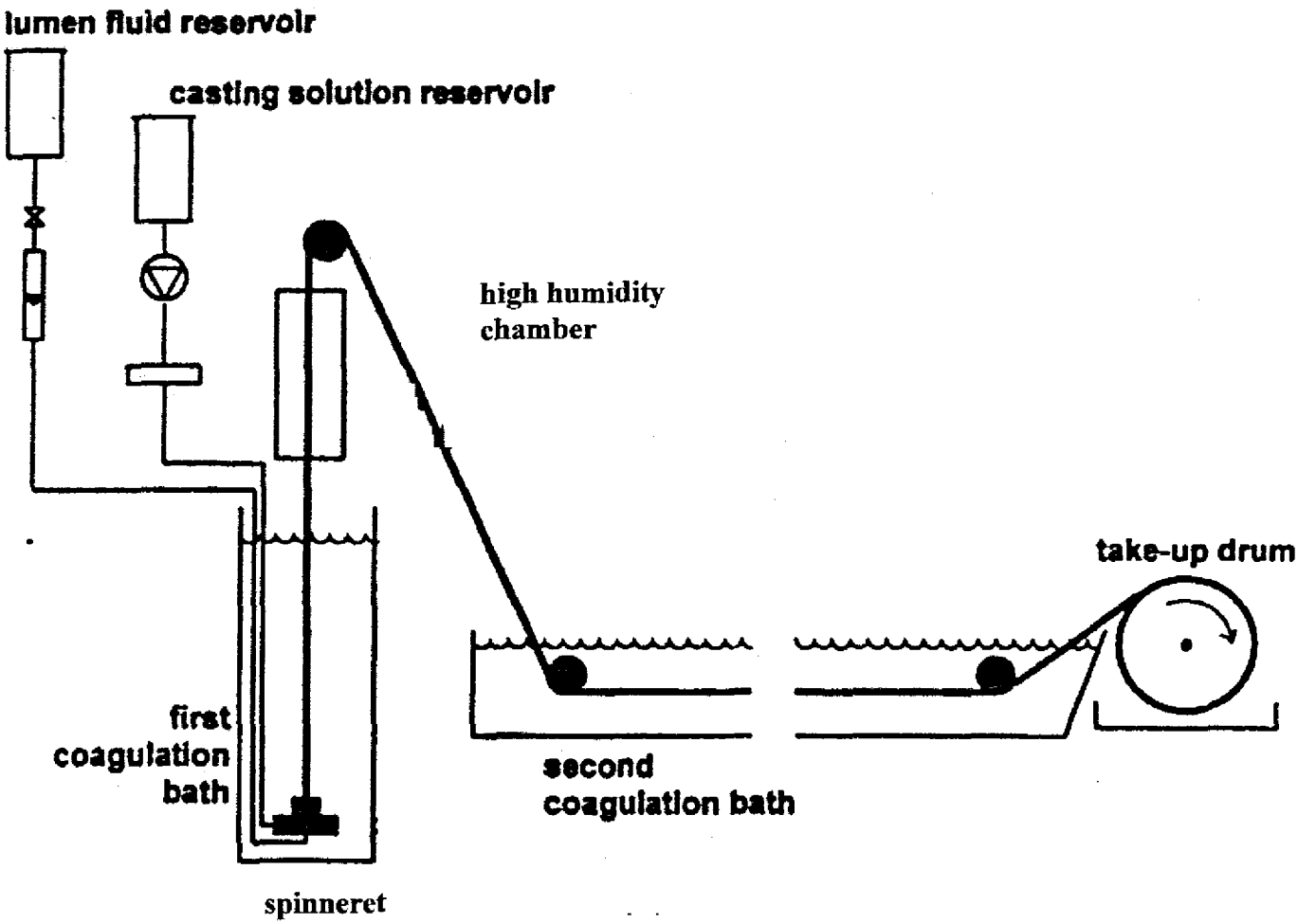

Figure B.2: Diagram of capillary membrane production (van der Walt, 1999).

APPENDIX C
HENRY`S LAW

D.1 DERIVATION OF HENRY`S LAW

For a given solute *i* at constant pressure and temperature, equilibrium exists between two phases when the fugacities (or activities or chemical potentials) in the two phases are equal. Fugacity is a measure of the tendency of a compound to escape from a phase and is defined in units of pressure. At low pressures and ambient temperature, the vapour phase is assumed to behave ideally, such that the partial pressure p is equivalent to the vapor phase fugacity f_i^V (Munz and Roberts, 1987).

The liquid phase fugacity of compound *i* can be expressed in several forms, depending on the reference state chosen (Munz and Roberts, 1987; Carroll, 1999).

$$f_i^L = x_i \cdot y_i \cdot f_{i_R}^0 = x_i \cdot y_i^* \cdot H_x \qquad \text{(D.1)}$$

In which:

x_i mole fraction.

$f_{i_R}^0$ is the pure component reference fugacity in the liquid state at the system temperature T and pressure P.

$y_i ; y_i^*$ are the activity coefficients in the symmetric and asymmetric convention, respectively.

H_x is the Henry`s law constant of compound *i* in a pure solvent or solvent mixture at the system T and P.

It is customary to assume the symmetric convention (Lewis-Randall rule): $y_i \to 1$ as $x_i \to 1$, such that the pure liquid becomes the reference state.

Substituting $y_i^* \to 1$ as $x_i \to 0$ in equation (D.1), the following expression is obtained for the Henry`s constant.

$$H_x = y_i \cdot f_{i_R}^0 \tag{D.2}$$

Further, from liquid-liquid equilibrium considerations; it can be shown that the solubility mole fraction (Munz and Roberts, 1987; Carroll, 1999).

$$x_{i_s} \approx y_i^{-1} = \text{constant} \tag{D.3}$$

Finally, the reference fugacity can be assumed to equal the vapour pressure of the pure liquid i p_i^{vap}.

Substituting back in equation (D.2) yields:

$$H_x = \frac{P_i^{vap}}{x_i} \qquad [\text{ atm / mole fraction }] \tag{D.4}$$

In the literature the values of Henry`s constant is expressed as H_x (atm / mole fraction).

Geankoplis (1993), Faust et al. (1980) and King (1980) gave the value of H_x equal to 4.01×10^{-4} and 0.142×10^{-4} (atm / mole fraction) for oxygen and CO_2 at 20^0C, respectively.

To convert Henry constant from H_x with the unit (atm / mole fraction) to Henry constant unitless H_c. first we convert H_x to H_p using equation (D.5).

$$H_p = \frac{P_i^{vap}}{C_l} = H_x \cdot v_s \qquad [\text{ atm.m}^3\text{.mol}^{-1}\text{ }] \tag{D.5}$$

C_l concentration of the solute in the liquid phase

v_s is the molar volume of the aqueous solution (m^3.mol^{-1})

Then we convert H_p (atm . m^3 . mol^{-1}) to H_c (dimensionless) using equation (D.6) (Munz and Roberts, 1987; Metcalf and Eddy, 1991):

$$H_C = \frac{C_g}{C_l} = H_x \cdot \frac{v_s}{RT} = \frac{H_p}{RT} \qquad \text{[Dimensionless]} \qquad \text{(D.6)}$$

where:

C_g concentrations of the solute in the gas phase [g / m^3].

R universal gas constant equal to $8.206.10^{-5}$ [$atm.m^3.mol^{-1}.k^{-1}$].

T is the absolute temperature [K].

The dimensionless form of equation (D.6), in which H_c is defined as a ratio of mass concentrations per unit volume in two phases, is especially convenient for process engineering calculations.

Conversion from H_x to H_c for oxygen and carbon dioxide:

Oxygen at 20^0C:

$H_x = 4.01\times10^{-4}$ (atm / mole fraction)

$H_p = H_x \times v_s = 4.01\times 10^{-4} \times 1.8\times10^{-5} = 7.218 \times 10^{-9}$ ($atm.m^3.mol^{-1}$)
$= 2.2855$ (KPa.l / mg)

$H_c = H_p / RT = 7.218 \times 10^{-9} / 8.206\ 10^{-5} \times 293 = 30.02$ (dimensionless)

Carbon dioxide at 20^0C:

$H_x = 0.142\times10^{-4}$ (atm / mole fraction)

$H_p = H_x \times v_s = 0.142 \times 10^{-4} \times 1.8\times10^{-5} = 0.255 \times 10^{-9}$ ($atm.m^3.mol^{-1}$)
$= 0.0589$ (KPa.l / mg)

$H_c = H_p / RT = 0.255 \times 10^{-9} / 8.206\ 10^{-5} \times 293 = 1.063$ (dimensionless)

REFERENCES

- Adema, E. and Sinskey, A. J. (1987). An analysis of intra-versus extracapillary growth in hollow fibre reactor, *Biotechnology Progress*, Vol. 3, No. 2, pp 74-79.

- Ahmed, T. and Semmens, M. J. (1992). The use of independently sealed microporous hollow fiber membranes for oxygenation of water: model development, *Journal Memb. Sci.*, 69, pp 11-20.

- Ahmed, T. and Semmens, M. J. (1996). Use of transverse flow hollow fibers for bubbless membrane aeration, *Wat. Res.*, Vol. 30, No. 2, pp 440-446.

- Alexander, B. and Fleming, J. S. (1982). Evaluation of a chemical technique for determining the oxygen permeability of synthetic membranes, *Journal Biomedical Materials Research*, Vol. 16, pp 31-38.

- Anselme, C. E. and Jacobs, E. P. (1996). Chap 10:Ultrafiltration. In Mallevialle, J.; Odendaal, P.E. and Wiesner, M. R. (eds.), *Water Treatment-Membrane Processes*, Mc Graw-Hill.

- Antari, A. (1997). CO_2 removal process for a gas processing plant, *the 20th World Gas Conference*, June, Copenhagen, Denmark.

- Aptel, P. and Buckley, C. A. (1996). Chap 2: Categories of membrane operations. In Mallevialle, J.; Odendaal, P.E. and Wiesner, M. R. (eds.), *Water Treatment-Membrane Processes*, Mc Graw-Hill.

- Aptel, P. and Semmens, M. J. (1996). Chap 8: Multiphase membrane processes. In Mallevialle, J.; Odendaal, P.E. and Wiesner, M. R. (eds.), *Water Treatment-Membrane Processes*, Mc Graw-Hill.

- ASTM (1988). Standard test method for determining gas permeability characteristics of plastic film and sheeting, *ASTM Book of Standards*, D1434-82, pp 255-266.

- Aust, S. D. (1990). Degradation of environmental pollutants by *Phanerochaete chrysosporium. Microbial Ecol.*, 20, pp 197- 209.

- Baner, A. L.; Hernandez, R. J.; Jayaraman, K. and Giacin, J. R. (1986). Isostatic and guasi-isostatic methods for determining the permeability of organic vapor through barrier membranes. In: Troedel, M.L. (ed.), *Current Technologies in Flexible Packaging*, ASTM STP 921,Philadelphia. American Society for Testing and Materials, pp 49-62.

- Belfort, G. (1989). Membranes and bioreactors: A technical challenge in biotechnology, *Biotechnology bioeng.*, 33: pp1047-1066.

- Bessarabov, D. G.; Sanderson; R. D.; Jacobs, E. P. and Beckman, I. N. (1996). Use of nonporous polymeric flat-sheet gas-separation membranes in a membrane-liquid contactor: experimental studies, *Journal Memb. Sci.*, 113, pp 275-284.

- Bhide, B. D. and Stern, S. A. (1993). Membrane processes for the removal of acid gases from natural gas: I: process configurations and optimization of operating conditions. II: effects of operating conditions, economic parameters and membrane properties, *J. Memb. Sci.*, vol 81, part I, pp 209-237, part II, pp 239-252.

- Bumpus, J. A. and Aust S. D. (1987). Biodegradation of environmental pollutants by the white rot fungus *Phanerochaete chrysosporium*: Involvement of the lignin degrading system. *Bioessays* 6: pp 166-170.

- Buser, H. R. and Rappe, C. (1979). Formation of polychlorinated dibenzofurans (PCDF`s) from the perolysis of individual PCB isomers, *Chemosphere*, 3, pp157.

- Carroll, J. J. (1999). Henry`s law revisited, *chemical engineering progress*, January, pp 49-55.

- Chang, H. N.; Chung, B. H. and Kim, I. H. (1986). In Proceedings of the third World Congress of Chemical Engineering, Vol. 1, Tokyo, pp 867.

- Chang, H. N. and Moo-Young, M. (1988). Analysis of oxygen transport in immobilized whole cells. In: Moo-Young, M. (ed.), *Bioreactor Immobilized Enzymes and Cells*: *Fundamentals and Applications*, Elsevier Applied Science, pp 33-51.

- Chung, B. H. and Chang, H. N. (1988). Aerobic fungal cell immobilization in a dual hollow-fiber bioreactor: continuous production of a citric acid, *Biotechnolo. Bioeng.*, Vol. 32, pp 205-212.

- Choe, J. S.; Agrawal, R.; Auvil, S. R. and White, T. R. (1988). Membrane / cryogenic hybrid systems for helium purification, *Proceedings of the 67th Gas Processors Association Annual Convention*, pp 251-255.

- Choy, E. M.; Evans, D. F. and Cussler, E. L. (1974). A selective membrane for transporting sodium ion against its concentration gradient, *Journal of the American Chemical Society*, 96, pp 7085.

- Cooney, D. O. and Jim, C. L. (1984). Solvent extraction of phenol from aqueous solution in a hollow fiber device, *Anaheim AIChE Meet.*

- Costello, M. J.; Fane, A. G.; Hogan, P. A. and Schofield, R. W. (1993). The effect of shell side hydrodynamics on the performance of axial flow hollow fiber modules, *Journal Memb. Sci.*, 80, pp 1-11.

- Côté, P.; Bersillon, J. L.; Huyard, A. and Faup, G. (1988). Bubble-free aeration using membranes: process analysis, *Journal WPCF*, Vol. 60, No.11,pp 1986-1992.

- Côté, P.; Bersillon, J. L. and Huyard, A. (1989). Bubble-free aeration using membranes: mass transfer analysis, *Journal Memb. Sci.*, 47, pp 91-106.
- Côté, P. L.; Maurion, R. P. and Lipski, C. J. (1992). US Patent 5104535.

- Crank, J. and Park, G. S. (eds.) (1968). *Diffusion in Polymers*, Academic Press, London and New York.

- Cussler, E. L. (1984). *Diffusion*, Cambridge Univ. Press, London.

- Dahuron, L. and Cussler, E. L. (1988). Protein extractions with hollow fibers, *AIChE Journal*, Vol. 34, No. 1, pp 130-136.

- Davis, E. G. and Huntington, J. N. (1977). New cell for measuring the permeability of film materials. *CSIRO Food Research Quarterly*, 37, pp 55-59.

- D'elia, N. A.; Dahuron, L. and Cussler, E. L. (1986). Liquid-liquid extraction with microporous hollow fibers, *Journal Memb. Sci.*, 29, pp 309-319.

- Domröse, S. E.; Finch, D. A. and Sanderson, R. D. (1998). Development of transverse-flow capillary-membrane modules of the modular and block types for liquid separation and bioreactors, *Water Research Commission of SA.*

- Dosoretz, C. G.; Chen, H. C. and Grethlein, H. E. (1990). Effect of environmental conditions on extracellular protease activity in ligninolytic cultures of *phanerochaete chrysosporium*, *Appl. Environ. Microbiol.*, 56(2), pp 395-400.

- Dosoretz, C. G.; Rothschild, N. and Hadar, Y. (1993). Overproduction of lignin peroxidase by *Phanerochaete chrysosporium* (BKM-F-1767) under non-limiting nutrient conditions, *Appl. Environ. Microbiol.* 59(6), pp 1919-1926.

- Duffey, M. E.; Evans F. D. and Cussler, E. L. (1978). Simultaneous diffusion of ions and ion pairs across liquid membranes, *Journal Memb. Sci.*, 3, pp 1-14.

- Efthymiou, G. S. and Shuler, M. L. (1987). Elimination of diffusional limitations in a membrane entrapped cell reactor by pressure cycling, *Biotechnology Progress*, Vol. 3, No. 4, pp 259-264.

- Faison, B. D. and Kirk, T. K. (1985). Factors involved in the regulation of a ligninase activity in *Phanerochaete chrysosporium, Appl. Environ. Microbiol.* 49(2), pp 299-304.

- Faust, A. S.; Wenzel, L. A.; Clump, C.W.; Maus, L. and Andersen, L. B.(1980). *Principles of unit operations*, 2nd edition, John Wiley & Sons, New York.

- Fournie, F. J. C. and Agostini, J. P. (1987). Permeation membranes can efficiently replace conventional gas treatment processes, *J. of Pet. Tech.*, June, pp 707-712.

- Frank, G. T. and Sirkar, K. K. (1986). An integrated bioreactor-separator: in situ recovery of fermentation products by a novel membrane-based dispersion-free solvent extraction technique, *Biotechnol. Bioengineering Symp.*, 17, pp 303-316.

- Futselaar, H.; Zoontjes, R. J. C.; Reith, T. and Racz, I. G. (1993a). Economic comparison of transverse and longitudinal flow hollow fibre membrane modules for reverse osmosis and ultrafiltration, *Desalination*, 90, pp 345-361.

- Futselaar, H. (1993b). The transverse flow membrane module (construction, perfermance and applications), *PhD dissertation*, University of Twente, The Netherlands.

- Futselaar, H.; Borges, C. P.; Hapert, A. C. and Nobrega, R. (1995). *Proceedings of Euromembrane` 95,* Bowen, W. R.; Field, R. W.; Howell, J. A. (eds.), Vol 2, Bath, pp 106-111.

- Geankoplis, C. J. (1993). *Transport processes and unit operations*, 3rd edition, Prentice Hall International, Inc.

- Geuzens, P.; Froment, L.; Leysen, R. and Vlasselaar, F. (1990). Gas absorption through membranes. In: Vansant, E. F. and Dewolfs, R. (eds.), *Gas Separation Technology*, pp 405.

- Gilbert, S. G. and Pegaz, D. (1969). Find new way to measure gas permeability, *Package Engineering*, January, pp 66-69.

- Gold, M. H. and Alic, M. (1993). Molecular biology of the lignin-degrading basidiomycete *Phanerochaete chrysosporium. Microbiol. Rev.* 57. Pp 605-622.

- Heath, C. and Belfort, G. (1987). Immobilization of suspended mammalian cells: Analysis of hollow fiber and microcapsule bioreactors, *Adv. Bichem. Eng. / Biotechnol.*, 34, pp 1-31.

- Inlous, D. S.; Taylor, D. P.; Cohen, S. N.; Michaels, A. S. and Robertson C. R. (1983). *Appl. Envir. Microbiol.*, 46, pp 246-278.

- Ito, A.; Yamagiwa, K.; Tamura, M. and Furusawa, M. (1998). Removal of dissolved oxygen using non porous hollow fiber membranes, *Journal Memb. Sci.*, 145, pp 111-117.

- IUPAC (1985).Reporting Physisorption DATA, *Pure Appl. Chem.*, 57, pp 603.

- Jacobs, E. P. and Sanderson, R. D. (1996). *SA Patent Application* 967520, 5 Sep.

- Jacobs, E. and Leukes, W. (1996). Formation of an externally unskinned polysulphone capillary membrane, *Journal Memb. Sci.*, 121, pp 149-157.

- Jacobs, E. P. and Sanderson, R. D. (1997). Capillary membrane production development, *Water Research Commission of South Africa*, pp 10.

- Jacobs, E. (1997). *Biotech SA 97*, Second Grahamstown Conference Biotechnology and Development in Southern Africa, Grahamstown, South Africa.

- Jacobs, E. P. and Sanderson, R. D. (1998). *US Patent Application* 5833896, Nov.

- Jäger, A.; Croan, S. and Kirk, T. K. (1985). Production of ligninase and degradation of lignin in agitated submerged cultures of *Phanerochaete chrysosporium*, Appl. Envi. Microbiol., 50, pp 1274-1278.

- Karel, M.; Issenberg P.; Ronsivalli, L. and Jurin, V. (1963). Application of gas chromatography to the measurement of gas permeability of packaging materials, *Food Technology*, march, pp 91-94.

- Karoor, S. and Sirkar, K. K. (1993). Gas absorption studies in microporous hollow fiber membrane modules, *Ind. Eng. Chem. Res.*, 32, pp 674-684.

- Keyser, P.; Kirk, T. K. and Zeikus, J. G. (1978). Lignolytic enzyme system of *Phanerochaete chrysosporium*: Synthesized in the absence of lignin in response to nitrogen starvation, *J. Bacteriol.*, 135, pp 790-797.

- Kim, B. M. (1984). Membrane based solvent extraction for selective removal and recovery of metals, *Journal Memb. Sci.*, 21, pp 5.

- King, C. J. (1980). *Separation processes*, 2nd edition, McGraw Hill.

- Kirk, T. K. and Nakatsubo, F. (1983). Chemical mechanism of an important cleavage reaction in the fungal degradation of lignin, *Biochim. Biophys. Acta*, 756, pp 376-384.

- Kirk, T. K.; Schultz, E.; Connors, W. J.; Lorenz, L. F. and Zeikus, J. G. (1978). Influence of cultural parameters on lignin metabolism by *Phanerochaete chrysosporium*, *Arch. Microbiol.*, 117, pp 277-285.

- Kirkpatrick, N. and Palmer, J. M. (1987). Semi-continuous ligninase production using foam-immobilised *Phanerochaete chrysosporium*, Appl. Microbiol. Biotechnol., 27, pp 129-133.

- Klement, G.; Scheirer, W. and Katinger, H. W. D. (1988). A large scale membrane reactor system with different compartments for cells, medium and product. In Moo-Young, M. (ed.), *Bioreactor Immobilized Enzymes and Cells: Fundamentals and Applications*, Elsevier Applied Science, pp 53-58.

- Knazek, R. A.; Gullino, P. M.; Kohler, P. O. and Dedrick R. L. (1972). Cell culture on artificial capillaries: An approach to tissue growth in vitro, *Science*, 178, pp 65-66.

- Knops, F. N. M.; Futselaar, H. and Rácz, I. G. (1992). The transversal flow microfiltration module. *Journal Memb. Sci.*, 73, pp 153-161.

- Kohl, A. L. and Nielsen, R. B. (1997). *Gas purification*, fifth edition, Gulf Publishing Company, Houston, Texas.

- Kreulen, H.; Smolders, C. A.; Versteeg, G. F. and Van Swaaij, W. P. M. (1993a). Determination of mass transfer rates in wetted and non-wetted microporous membranes, *Chem. Eng. Sci.*, Vol. 48, No. 11, pp 2093-2102.

- Kreulen, H.; Smolders, C. A.; Versteeg, G. F. and Van Swaaij, W. P. M. (1993b). Microporous hollow fiber membrane modules as gas-liquid contactors,Part I: Physical mass transfer process, Part II: Mass transfer with chemical reaction, *Journal Memb. Sci.*, 78, Part I, pp 197-216, Part II, pp 217-238.

- Laurent, A. and Charpentier, J. C. (1974). Aires interfaciales et coéfficients de transfert de matiére dans les divers types d'absorbeurs et de reacteurs gaz-liquide, *Chem. Eng. Journal*, 8, pp 85-101.

- Lee, A. L.; Feldkirchner, H. L.; Stern, S. A.; Houde, A. Y.; Gamez, J. P. and Meyer, H. S. (1995). Field tests of membrane modules for the separation of carbon dioxide from low-quality natural gas, *Gas. Sep. Purif.*, vol. 9, No.1, pp 35-45.

- Leisola. M. S. A. and Fiechter, A. (1985). Ligninase production in agitated condition by *Phanerochaete chrysosporium*, FEMS Microbiol. Lett., 29, pp 33-36.

- Leukes, W.; Jacobs, E. P.; Rose, P. D.; Sanderson, R. D. and Burton, S. G. (1997). European Patent Application EP 0761 608 A2.

- Leukes, W. (1999). Development and characterisation of a membrane Gradostat bioreactor for the bioremediation of aromatic pollutants using white rot fungi, *PhD dissertation*, Rhodes University, South Africa.

- Lévêque, J. (1928). Les lois de la transmission de chaleur par convection, *Ann. Mines.*,13, pp 201-205, 305-362, 381-405.

- Li, K.; Tai, M. S. L. and Teo, W. K. (1994). Design of CO_2 scrubber for self contained breathing systems using a microporous membrane, *Journal Memb. Sci.*, 86, pp 119-125.

- Linko, S. (1992). Production of *Phanerochraete chrysosporium* lignin peroxidase , Biotechnol. Adv., 10, pp 191-236.

- Linko, S. (1988). Production and characterisation of extracellular lignin peroxidase from immobilised *Phanerochraete chrysosporium* in a 10-1 bioreactor. *Enzyme Microbio. Tech.* 10, pp 410-417.

- Lipski, C. and Côté, P. (1990). *Environmental Progress, 9*, pp 254-261.

- Loewenthal, R. E; Wiechers, H. N. S. and Marais, G. V. R. (1986). Softening and stabilization of municipal waters, *Water Research Commission of SA.*

- Malek, A.; Li, K. and Teo, W. K. (1997). Modeling of microporous hollow fiber membrane modules operated under partially wetted conditions, *Ind. Eng. Chem. Res.*, 36, pp 784-793.

- Malherbe, G. E.; Morkel , C. E.; Bezuidenhout, D.; Jacobs, E. P.; Hurndall, M. J. and Sanderson, R. D. (1995). Industrial applications of membranes, *Water Research Commission of SA*, pp 6-7.

- Manem, J. and Sanderson, R. (1996). Chapter 17, Membrane bioreactors. In: Mallevialle, J.; Odendaal, P.E. and Wiesner, M. R. (eds.), *Water Treatment-Membrane Processes*, Mc Graw-Hill. Sanderson, R. and Manem, J. (1996). Chapter 17, Membrane bioreactors. In: Mallevialle, J.; Odendaal, P.E. and Wiesner, M. R. (eds.), *Water Treatment-Membrane Processes*, Mc Graw-Hill.

- Mason, E. A. and Malinauskas, A. P. (1983). Gas transport in porous media: the dusty gas model, in *Chem. Eng. monograph 17*, Elsevier, Amsterdam.

- Matson, S. L.; Lopez, J. and Quinn, J. A. (1983). Separation of gases with synthetic membranes, *Chem. Eng. Sci.*, 38, pp 503-524.

- McHugh, T. H. and Krochta, J. M. (1994a). Chapter 7, Permeability properties of edible films. In Krochta, J. M.; Baldwin, E. A. and Nisperos-Carriedo, M. (eds.), *Edible Coatings and Films to Improve Food Quality*, Technomic Publishing Company, Inc. Lancaster, Pennsylvania, pp 139-183.

- McHugh, T. H. and Krochta, J. M. (1994b). Sorbitol- vs. glycerol-plasticized whey protein edible films: integrated oxygen permeability and tensile property evaluation, *journal of agricultural and food chemistry*, 42(4).

- McKee, R. L.; Changela, M. K. and Reading, G. J. (1991). CO_2 removal membrane plus amine, *Hydro. Process.*, April, pp 63-65.

- Metcalf and Eddy (1991). *Waste water engineering*, treatment, disposal and reuse, 3rd edition, McGraw Hill, New York.

- Meyer, H. S. and Gamez, J. P. (1995). Gas separation membrane: coming of age for carbon dioxide removal from natural gas, *Proceedings of the 45th annual Laurance Reid Gas Conditioning Conference*. Norman, Ok, Feb. 26- march 1, pp 284-306.

- Mills, R.; Woolf, L. A. and Watts, R. O. (1968). Simplified procedures for diaphragm-cell diffusion studies, *AIChE Journal*, 14, pp 671-673.

- Moein, G. J.; Smith, A. J.; Jr. and Stewart, P. L. (1976). Follow-up study of the distribution and fate of PCB's and benzene in soil, *proc. Natl. conf. On control of hazardous material Spills*, Information Transfer, Rockville, Md., pp 368.

- Moreira, M. T.; Feijoo, G.; Palma, C. and Lema, J. M. (1997). Continuous production of manganese peroxidase by *Phanerochaete chrysosporium* immobilised on polyurethane foam in a pulsed packed-bed bioreactor. Biotechnol. Bioeng., 56 (2), pp 130-137.

- Mulder, M. (1991). *Basic principles of membrane technology*. Kluwer Academic Publishers Dordrecht, Netherlands.

- Munz, C. and Roberts, P. V. (1987). Air-water phase equilibria of volatile organic solutes, *journal AWWA*, 79 (5), pp 62-69.

- Nissen, T. V. (1973). Stability of PCB in the soil, *Tidsskr. Planteavl*, 77, pp 533.

- Ohlrogge, K.; Peinemann, K. V.; Wind, J. and Behling, P. D. (1990). The separation of hydrocarbon vapors with membranes, *Sep. Sci. & Technol.*, 25 (1), pp 375.

- Ohlrogge, K. (1993). Volatile organic compound control technology by means of membranes, *the 1993 eleventh annual membrane technology / separation planing conference*, October 11-13, Newton Massachusetts, USA.

- Perrin, J. E. and Stern, S. A. (1986). Separation of helium-methane mixture in permeators with two types of polymer membranes, *AIChE Journal*, November, vol. 32, No.11, pp 1889-1900.

- Prasad R. and Sirkar K. K. (1988). Dispersion-free solvent extraction with microporous hollow-fiber modules. *AIChE Journal*, Vol. 34, No 2, pp 177-188.

- Qi, Z. and Cussler, E. L. (1985a). Hollow fiber gas membranes, *AIChE Journal*, Vol. 31, No. 9, pp 1548-1553.

- Qi, Z. and Cussler, E. L. (1985b). Microporous hollow fibers for gas absorption, Part I: Mass transfer in the liquid, Part II: mass transfer across the membrane, *Journal Memb. Sci.*, 23, Part I, pp 321-332, Part II, pp 333-345.

- Qi, Z. and Cussler, E. L. (1985c). Bromine recovery with hollow fiber gas membranes, *Journal Memb. Sci.*, 24, pp 43-57.

- Qin, Y. and Cabral J. M. S. (1997). Lumen mass transfer in hollow fiber membrane processes with constant external resistances, *AIChE Journal*, Vol. 43, No. 8, pp 1975-1988.

- Rainen, L. (1988), Am. Biotechnol. Lab., 6(3), pp 20.

- Robertson, C. R. and Kim, I. H. (1985). Dual aerobic hollow-fibre bioreactor for cultivation of streptomyces aureofaciens, *Biotechnolo. Bioeng.*, 27, pp 1012-1020.

- Robinson, R. A. and Stokes, R. H. (1960). *Electrolyte Solutions*. London, Butterworths.

- Ross, W. R.; Barnard, J. P.; le Roux, J. and de Villiers, H. A. (1990). Application of ultrafiltration membranes for solids-liquid separation in anaeribic digestion systems: The ADUF process, *Water SA*, Vol. 16, No. 2, pp 85-91.

- Ruzo, L. O.; Zavik, M. J. and Schuetz, R. D. (1972). Polychlorinated biphenyls: photolysis of 3,4,3`,4`-tetrachlorobiphenyl and 4,4`-dichlorobiphenyl in solution, *Bull. Environ. Contam. Toxicol.*, 8, pp 217.

- Safe, S. and Hutzinger, O. (1971). Polychlorinated biphenyls: photolysis of 2,4,6,2`,4`,6`-hexachloro biphenyl, *Nature* (London), 232, pp 641.

- Schonberg, J. A. and Belfort, G. (1987). Enhanced nutrient transport in hollow fiber perfusion bioreactors: A theoretical analysis, *Biotechnol. Prog.*, 3 (2), pp 80-89.

- Seaver, S.; Rudolph, J. L.; Ducibella, T. and Gabriels, J. E. (1984). Hybridoma cell metabolism/ Antibody secretion in culture, presented at *Biotech `84*, Onine, Pinner, England, pp 325-344.

- Seider, E. N. and Tate, G. E. (1936). Heat transfer and pressure drop of liquids in tubes, *Ind. Eng. Chem.*, 28, pp 1429.

- Semmens, M. J.; Qin, R. and Zander, A. (1989). Using a microporous hollow-fiber membrane to separate VOC's from water, *Journal AWWA* 81 (4), pp 162-167.

- Semmens, M. J.; Foster, D. M. and Cussler, E. L. (1990). Ammonia removal from water using microporous hollow fibers, *Journal Memb. Sci.*, 51, pp 127-140.

- Smart, J. L.; Lloyd, D. R. and Starov, V. M. (1996). *Poster presented at NAMS 8 th annual meeting*, Canada.

- Snell, F. D. and Hilton, C. L. (eds.) (1966). *Encyclopedia of industrial chemical analysis*, Interscience, New York.

- Stokes, R. H. (1950). The diffusion coefficient of eight uni-univalent electrolytes in aqueous solution at 25^0C, *Journal of the American Chemical Society*, 72, 763, pp 2243-2247.

- Tai, M. S. L.; Chua, I.; Li, K.; Ng, W. J. and Teo, W. K. (1994). Removal of dissolved oxygen in ultrapure water production using microporous membrane modules, *Journal Memb. Sci.*, 87, pp 99-105.

- Tolbert, W. R.; Lewis, C.; Jr.; White, P. J. and Feder, J. (1985). Perfusion culture systems for production of mammalian cell biomolecules. In: Feder, J. and Tolbert, W. R. (eds), *Large-Scale Mammalian Cell Culture*, Academic, New York. pp 97-123.

- Tolbert, W. R. and Srigley, W. R. (1987). *BioPharm.*, September, pp 42-48.

- Tsuji, T.; Suma, K.; Tanishita, K.; Furkazawa, Z.; Kanno, M.; Hasegawa, H. and Takahashi, A. (1981). Development and clinical evaluation of hollow fiber membrane oxygenator, *Trans. Am. Soc. Artif. Inter. Organs.* , 27, pp 280-284.

- Van der Walt, A. (1999). Design and characterization of a transverse flow membrane module for gas transfer operations, *M. Eng.*, University of Stellenbosch, South Africa.

- Van Landeghem, H. (1980). Multiphase reactors: mass transfer and modeling, *Chem. Eng. Sci.*, 35, pp 1912-1949.

- Vaslef, S. N.; Mockros, F.; Anderson, R. W. and Leonard, R. J. (1994). *ASAIO Journal*, 40, pp 990-996.

- Venkatadri, R. and Irvine, R. L. (1993). Cultivation of *Phanerochaete chrysosporium* and production of lignin peroxidase in novel biofilm reactor systems: Hollow fibre reactor and silicone membrane reactor. *Water Res.*, 27 (4), pp 591-596.

- Wang K. L. and Cussler, E. L. (1993). Baffled membrane modules made with hollow fiber fabric, *Journal Memb. Sci.*, 85, pp 265-278.

- Waters, W. A. (1948). *The chemistry of free radicals*, Second Edition, Oxford.

- Webster, I. A. and Patras, L. E. (1987). The microbial ugrading of heavy oils, presented at the annual meeting of the AIChE, New York, Nov., pp 15-20.

- Whitman, W. G. (1923). Preliminary experimental confirmation of the two-film theory of gas absorption, *Chem. Met. Eng.*, 29, pp 146-148.

- Wickramasinghe, S. R. ; Semmens, M. J. and Cussler, E. L. (1992). Mass transfer in various hollow fiber geometries, *Journal Memb. Sci.*, 69, pp 235-250.

- Yang, M. C. and Cussler, E. L. (1986). Designing hollow fiber contactors, *AIChE Journal*, Vol. 32, No. 11, pp 1910-1916.

- Yang, M. C. and Cussler, E. L. (1989). Artificial gills, *Journal Memb. Sci.*, 42, pp 273-284.

IN LOVING MEMORY OF MY BROTHER

Kamel Mokrani

(1971-1999)